



**University of  
Nottingham**

UK | CHINA | MALAYSIA

**DEVELOPMENT OF AN INTEGRATED BIO-RURAL  
ENERGY SCHEME IN GHANA**

**By**

**Nii Nelson (MSc)**

A Thesis submitted to the Department of Architecture and Built  
Environment, University of Nottingham in partial fulfilment of the  
requirements for the degree of

**DOCTOR OF PHILOSOPHY**

**In**

**Sustainable Energy Technologies**

**FACULTY OF ENGINEERING**

February, 2023

## **DECLARATION**

I hereby declare that this submission is my own work towards the PhD and that, to the best of my knowledge, it contains no material previously published by another person nor material which has been accepted for the award of any other degree of the university, except where due acknowledgements have been made in the text.

Nii Nelson (14342402)

.....

.....

Signature

Date

## **Dedication**

This thesis is dedicated to my family: Annette, Emma, Dora, and Lisa; and the late Patrick Richard Techie-Mensah (Master Pat) of blessed memory.

## **Acknowledgement**

I want to thank my parents, my siblings, and my entire extended family for their incredible support throughout the difficult times of this research project. I owe my wife and kids a debt of gratitude for staying up late with me during the cold winter nights and also an apology for the many unfulfilled and broken promises I made to them during my period of study.

My supervisors, Prof Jo Darkwa, and Dr John Calautit, provided insightful feedback and were very generous with their support. I am eternally grateful to them. My internal assessor, Prof Yuehong Su, has contributed immensely, for which I am very appreciative.

This research study was supported with a grant from the Global Challenges Research Fund (GCRF) through UK Research and Innovation, and the University of Nottingham, as part of the "Implementation of Bio-Rural Energy Scheme for Ghana (IBRES)" project - GCRF/UoN Grant No H54500.

Dr Mark Worall of the Faculty of Engineering, University of Nottingham, provided me with tremendous assistance as part of the IBRES project.

A section of this study was carried out at Kwame Nkrumah University of Science and Technology, Ghana, during a research visit. . I am therefore grateful to Prof Francis Kemausuor, Dr Eunice Adjei, Mr Roger Banongwie, and Mr Eric Soku for their support.

Lastly, I want to thank my fellow PhD students in SRB, especially Victor Equere, Mohammed Shalak, Abdalrawof Altarog, Shuangyu Wei, Olamide Eso, Lilian Nwachukwu, and all the members of the BEE Research Group.

## Preface

1. 2022 Nelson, N., Darkwa, J., Worall, M., Calautit, J., and Mokaya, R. (2022) Theoretical and Experimental Study of Cocoa Pod Husk Gasification in a Fixed Bed Downdraft Gasifier. The 14<sup>th</sup> International Conference on Applied Energy. August 8 – August 11, 2022. Virtual/Germany. <https://www.energy-proceedings.org/theoretical-and-experimental-study-of-cocoa-pod-husk-gasification-in-a-fixed-bed-downdraft-gasifier/>
2. 2021 Nelson, N., Darkwa, J. and Calautit, J. (2021) Prospects of Bioenergy Production for Sustainable Rural Development in Ghana. Journal of Sustainable Bioenergy Systems, 11, 227-259. <https://doi.org/10.4236/jsbs.2021.114015>
3. 2021 Nelson, N., Darkwa, J., Calautit, J., Worall, M., Mokaya, R., Adjei, E., Kemausuor, F., and Ahiekpor, J. (2021) Potential of Bioenergy in Rural Ghana. Sustainability, 13, 381. <https://doi.org/10.3390/su13010381>
4. 2021 Worall, M., Darkwa, J., Adjei, E., Calautit, J., Kemausuor, F., Ahiekpor, J., Nelson, N. and Mokaya, R. (2021) A Small-scale Gasifier-Generator Fueled by Cocoa Pod Husk for Rural Communities in Ghana. The 12<sup>th</sup> International Conference on Applied Energy. December 1 - December 10, 2020. Virtual/Bangkok, Thailand. <http://www.energy-proceedings.org/wp-content/uploads/enerarxiv/1609412579.pdf>
5. 2020 Nelson, N., Darkwa, J., Calautit, J., and Worall, M. (2020) Future Prospects of Bioenergy in Rural Ghana. 4th South East European Conference on Sustainable Development of Energy, Water and Environmental Systems. June 28-July 02, 2020. Virtual/Sarajevo, Bosnia & Herzegovina

## **Abstract**

Ghana like many sub-Saharan African countries faces significant social issues. Approximately 42% of Ghanaians live in rural areas where agriculture is a predominant livelihood activity. The total population below the poverty line is about 24.2%, with rural poverty almost 4 times as high as urban poverty. Among the many issues confronting Ghana, electricity access is a big concern for rural residents, who currently enjoy less than 30% access. This thesis aimed to develop and evaluate an integrated bio-rural energy scheme in Ghana using cocoa pod husks as feedstock. In order to achieve the aim of this study, biomass materials and their conversion technologies were reviewed. Following this, different varieties of cocoa pod husk materials were characterized using ultimate and proximate analyses. A numerical model for predicting the performance of cocoa pod husk gasification systems was also developed. Eventually, a dedicated rig was used to evaluate the performance of the cocoa pod husk-fed energy generation system. The study revealed that agricultural crop residue and livestock production have a theoretical energy potential of 728.43 PJ and 76.72 PJ, respectively. This is remarkable given that Ghana has a total installed generation capacity of 5134 MW. It was noted that cocoa pod husk has a higher heating value of 14.44-19.21 MJ/kg, which could be useful for power generation through gasification. The moisture content of cocoa pod husk was generally below 15% coupled with low levels of nitrogen and sulphur. There was a fairly good agreement between the results of the numerical model and those of the experiment after a few modifications. A peak carbon conversion efficiency of 75% was observed, although the efficiency of the gasifier system was generally low.

## Table of Contents

1. CHAPTER ONE.....	1
1.0 INTRODUCTION .....	1
1.1 Research background .....	1
1.2 Aim and Objectives .....	4
1.3 Significance of the research .....	5
1.4 Novelty .....	6
1.5 Thesis structure.....	6
1.6 Limitations of Study.....	7
2. CHAPTER TWO.....	8
2.0 LITERATURE REVIEW .....	8
2.1 Introduction .....	8
2.2 General biomass resources .....	8
2.3 Classification of biomass materials .....	10
2.4 Biomass Conversion Technologies .....	11
2.5 Biomass Resources in Ghana .....	32
2.5 Concluding Remarks .....	43
3. CHAPTER THREE.....	45
3.0 CHARACTERIZATION OF COCOA POD HUSKS .....	45
3.1 Introduction .....	45
3.2 Materials and Methods .....	45
3.3 Results and Analysis .....	55

3.4	Concluding Remarks .....	76
4.	CHAPTER FOUR .....	79
4.0	MATHEMATICAL MODELING AND SIMULATION OF CPH GASIFICATION PROCESS .....	79
4.1	CPH Gasification System.....	79
4.2	Mathematical Modelling and Simulation .....	80
4.3	Results and Discussion.....	92
4.4	Concluding Remarks .....	103
5.	CHAPTER FIVE.....	105
5.0	EXPERIMENTAL EVALUATION OF CPH GASIFICATION POWER SYSTEM.....	105
5.1	Experimental setup.....	105
5.2	Materials and methods.....	111
5.3	Test procedure .....	115
5.4	Calculation of the experimental results .....	117
5.5	Results and discussion.....	120
5.6	Model Validation.....	136
5.7	Model Modification.....	138
5.8	Concluding Remarks .....	140
6.	CHAPTER SIX .....	143
6.0	CONCLUSION AND RECOMMENDATIONS .....	143
6.1	Conclusions .....	143

6.2	Recommendations for future work.....	150
7.	REFERENCES.....	151

## List of Figures

FIGURE 2.1: SCHEMATIC OF COMBUSTION PROCESS .....	14
FIGURE 2.2: SCHEMATIC OF GASIFICATION PROCESS .....	16
FIGURE 2.3: PROCESSES INVOLVED IN BIOMASS GASIFICATION .....	17
FIGURE 2.4: SCHEMATIC OF SLOW PYROLYSIS PROCESS.....	21
FIGURE 2.5: SCHEMATIC OF BIOMASS LIQUEFACTION. ....	23
FIGURE 2.6: SCHEMATIC OF SERIAL FERMENTATION USING MICROALGAE. ....	28
FIGURE 2.7: ILLUSTRATION OF BIOGAS PLANT OPERATION. ....	31
FIGURE 2.8: FOREST RESIDUES FROM THE PRODUCTION OF PLYWOOD. ....	40
FIGURE 3.1: REGIONAL DESIGNATION OF CPH SAMPLES .....	46
FIGURE 3.2: RETSCH PLANETARY BALL MILL PM 100.....	48
FIGURE 3.3: RETCH ELECTROMAGNETIC SHAKER AS 200 WITH SIEVE MESH ON THE SIDE .....	48
FIGURE 3.4: MILLED CPH PACKAGED IN SAMPLE BOTTLES AND LABELLED. ....	49
FIGURE 3.5: THERMOGRAVIMETRIC ANALYSER – TGA Q500 SET-UP.....	50
FIGURE 3.6: TYPICAL WEIGHT LOSS AND HEATING PROFILE OF A TG PROXIMATE ANALYSIS TECHNIQUE. ....	52
FIGURE 3.7: (A) LECO, CHN-628 ANALYSER AND (B) LECO SULPHUR ADD-ON MODULE CHN-628S.....	53
FIGURE 3.8: VARIATION IN MOISTURE CONTENT OF CPH SAMPLES .....	58
FIGURE 3.9: DIFFERENCES IN MOISTURE CONTENT BY CPH TYPE.....	59
FIGURE 3.10: MOISTURE CONTENT OF CPH BASED ON REGIONS.....	60
FIGURE 3.11: ASH CONTENT OF CPH TYPES IN THE VARIOUS REGIONS.....	62
FIGURE 3.12: ASH CONTENT OF CPH SAMPLE TYPES .....	63
FIGURE 3.13: ASH CONCENTRATION OF CPH BASED ON REGION .....	64

FIGURE 3.14: VOLATILE MATTER CONTENT OF CPH TYPES IN VARIOUS REGIONS	65
.....	65
FIGURE 3.15: VARIATION IN VOLATILE MATTER OF CPH TYPES	65
FIGURE 3.16: REGION-SPECIFIC VOLATILE MATTER CONTENT OF CPH	66
FIGURE 3.17: FIXED CARBON CONTENT OF CPH TYPES IN THE VARIOUS REGIONS	67
.....	67
FIGURE 3.18: FIXED CARBON CONTENT OF CPH TYPES	68
FIGURE 3.19: REGION-SPECIFIC FIXED CARBON CONTENT OF CPH	68
FIGURE 3.20: COMPARISON OF HIGHER HEATING VALUES OF CPH SAMPLES BY ULTIMATE AND PROXIMATE ANALYSIS.	73
FIGURE 3.21: THE HIGHER HEATING VALUE OF THE CPH TYPES BASED ON PROXIMATE ANALYSIS	74
FIGURE 3.22: THE HIGHER HEATING VALUE OF THE CPH TYPES BASED ON ULTIMATE ANALYSIS	74
FIGURE 3.23: REGION-SPECIFIC HIGHER HEATING VALUE BASED ON ULTIMATE ANALYSIS	75
FIGURE 3.24: REGION-SPECIFIC HIGHER HEATING VALUE BASED ON PROXIMATE ANALYSIS	76
FIGURE 4.1: A SCHEMATIC DIAGRAM OF THE GASIFICATION SYSTEM	79
FIGURE 4.2: SYNGAS COMPOSITION VARIATION WITH EQUIVALENCE RATIO (A1)	97
.....	97
FIGURE 4.3: SYNGAS COMPOSITION VARIATION WITH EQUIVALENCE RATIO (A2)	97
.....	97
FIGURE 4.4: SYNGAS COMPOSITION VARIATION WITH EQUIVALENCE RATIO (A3)	98
.....	98

FIGURE 4.5: EFFECTS OF EQUIVALENC RATIO ON SYNGAS HEATING VALUE AND COLD GAS EFFICIENCY .....	98
FIGURE 4.6: EFFECTS OF MOISTURE ON GAS COMPOSITION .....	100
FIGURE 4.7: EFFECT OF TEMPERATURE ON GAS COMPOSITION (CPH C1) .....	101
FIGURE 4.8: EFFECT OF TEMPERATURE ON GAS COMPOSITION (CPH A1) .....	101
FIGURE 4.9: EFFECT OF TEMPERATURE ON HEATING VALUE AND COLD GAS EFFICIENCY (CPH C1) .....	102
FIGURE 4.10: EFFECT OF TEMPERATURE ON HEATING VALUE AND COLD GAS EFFICIENCY (CPH A1) .....	103
FIGURE 5.1: 5 kW GASIFIER-GENERATOR SET WITH VARIOUS COMPARTMENTS LABELLED.....	105
FIGURE 5.2: TECHNICAL SPECIFICATION OF THE BIOMASS ENGINE GENERATOR .....	107
FIGURE 5.3: GASIFIER FEEDING SYSTEM .....	108
FIGURE 5.4: GASIFIER FILTERS.....	111
FIGURE 5.5: SOLAR DRYER FILLED WITH SOME COCOA POD HUSK.....	112
FIGURE 5.6: BIOMASS CRUSHER .....	113
FIGURE 5.7: SCHEMATIC OF THE CPH GASIFIER SHOWING THE LOCATION OF ALL THERMOCOUPLES.....	116
FIGURE 5.8: SYNGAS ANALYSER FOR GAS SAMPLING.....	117
FIGURE 5.9: VARIATION OF TEMPERATURE ( <sup>0</sup> C) WITH TIME AT DIFFERENT LOADS .....	122
FIGURE 5.10: VARIATION IN GAS COMPOSITION AND POWER GENERATION POTENTIAL OF PRODUCER GAS (Q <sub>CG</sub> ).....	125
FIGURE 5.11: VARIATION IN MASS CONSUMPTION WITH MOISTURE CONTENT..	127

FIGURE 5.12: VARIATION IN CGE, CCE AND VG AT DIFFERENT LOADS .....	129
FIGURE 5.13: VARIATION IN CGE, CCE AND QCG AT DIFFERENT LOADS .....	132
FIGURE 5.14: VARIATION IN ENGINE EFFICIENCY AND OVERALL EFFICIENCY WITH ELECTRICAL LOAD .....	133
FIGURE 5.15: ENERGY FLOW DIAGRAM (SANKEY CHART) OF THE COCOA POD HUSK GASIFIER ENGINE-GEN SET .....	136
FIGURE 5.16: COMPARISON OF THE DEVELOPED MODEL WITH EXPERIMENTAL RESULTS .....	137
FIGURE 5.17: COMPARISON OF MODIFIED MODEL WITH EXPERIMENTAL RESULTS. .....	140

## List of Tables

TABLE 2.1: COMPARATIVE OF THERMOCHEMICAL PROCESSES .....	13
TABLE 2.2: ENERGY POTENTIAL FROM CROP RESIDUES GENERATED IN 2020.....	38
TABLE 2.3: TOTAL MANURE OUTPUT AND ENERGY POTENTIAL OF AVAILABLE LIVESTOCK MANURE .....	42
TABLE 3.1: PROXIMATE ANALYSIS (WT %) AND HHV (MJ/KG) OF CPH SAMPLES FROM GHANA .....	55
TABLE 3.2: ULTIMATE ANALYSIS, WT % (DRY BASIS) AND HHV (MJ/KG) OF CPH SAMPLES FROM GHANA.....	69
TABLE 4.1: COEFFICIENTS OF SPECIFIC HEAT FOR THE EMPIRICAL EQUATION. ...	88
TABLE 4.2: ULTIMATE ANALYSIS OF CPH SAMPLES .....	92
TABLE 4.3: SIMULATED GAS COMPOSITION OF CPH FUEL .....	94
TABLE 5.1. PROPERTIES OF SAMPLE MATERIALS .....	114
TABLE 5.2. PERFORMANCE OF CPH GASIFIER SYSTEM .....	134

## List of Acronyms and Nomenclature

MW	Megawatt
PJ	Petajoule
GDP	Gross Domestic Product
UN SDG	United Nations Sustainable Development Goal
CPH	Cocoa pod husk
EFB	Empty fruit bunch
RPR	Residue-to-Product Ratio
MJ/kg	megajoules per kilogram
mm	millimetre
rpm	revolutions per minute
min	minute
ASTM	American Society for Testing and Materials
TGA	Thermogravimetric analysis
mg	milligram
N <sub>2</sub>	Nitrogen gas
°C	Degree Celsius
°C/min	Degree Celsius per minute
mL/min	millilitre per minute
CO <sub>2</sub>	Carbon dioxide
H <sub>2</sub> O	Water
wt%	Weighted percentage
HHV	Higher heating value
PA	Proximate Analysis
UA	Ultimate Analysis

FC	Fixed Carbon
VM	Volatile Matter
C	Carbon
H	Hydrogen
S	Sulphur
O	Oxygen
N	Nitrogen
H/C	Hydrogen–Carbon ratio
O/C	Oxygen–Carbon ratio
CH <sub>4</sub>	Methane
H <sub>2</sub>	Hydrogen gas
CO	Carbon Monoxide
CO <sub>2</sub>	Carbon Dioxide
m <sup>3</sup>	Cubic Metres
PAHs	Polycyclic Aromatic Hydrocarbons
NO <sub>x</sub>	Nitrogen Oxides

# CHAPTER ONE

## 1.0 INTRODUCTION

### 1.1 Research background

Ghana's energy sector faces two main challenges; the inability to provide a decent power supply and the upsurge in the use of wood fuel as the principal cooking fuel for families with no access to modern cooking fuels [1]. Currently, approximately 84% of urban households are grid-connected [2], whereas less than 30% of the rural population is connected to electricity [3]. Most rural communities are very deprived, with limited access to potable water, basic sanitation, and healthcare facilities due to inadequate energy services. The total population below the poverty line is about 24.2%, with rural poverty almost 4 times as high as urban poverty [4], [5]. Determinants such as cultural inclination, economic considerations, and resource accessibility necessitate the use of more biomass resources compared to other conventional energy reserves in rural communities [6]. Biomass provides a large proportion of energy services but in overly unproductive forms, notably firewood and charcoal for domestic purposes [7]. The current inefficient application of biomass in conventional form raises serious environmental and health concerns, including indoor air pollution. The sourcing strategy for firewood or wood for charcoal production, apart from being unsustainable, also puts Ghana's dwindling forest under extreme stress and could subsequently lead to far-reaching deforestation, with severe ramifications for climate change, crop production, and water resources [8]. Modern applications of biomass such as biofuel development are gradually gaining ground and efforts are being made to control wood fuel consumption and indoor

air pollution with the introduction of improved cook stoves in the country [9]. Notwithstanding, Ghana is far from harnessing half of its energy potential from biomass. The electricity generation mix is predominated by hydro and thermal sources, with the former contributing about 43% and the latter 57% [10]. Renewable energy sources only contribute about 0.2% of the total generation mix [11]. The power plants in current use are unable to reach full power capacity due to fuel supply limitations. The insufficient and unreliable rainfall patterns due to climate variability have also resulted in low water influx into the hydroelectric power dams, consequently leading to the dominance of thermal power usage in Ghana. Other challenges, such as high levels of transmission losses and the remoteness of some rural communities, have necessitated the need to decentralize the power supply in Ghana [11]. Currently, more than 50% of rural communities without access to electricity live in communities with a population of less than 500. Since there are no indications of these rural communities' increasing population any time soon, chances are that these rural communities would never be connected to the grid by Ghana's current electrification criteria [2]. Rural communities located far from the national grid are therefore prime candidates for stand-alone and mini-grid systems, which have been shown to be a more cost-effective way of connecting rural populations than main grid extension [12]. As most of these rural communities in Ghana are involved in agriculture and produce huge amounts of biomass resources, bioenergy development could be promoted as an energy security and rural development strategy [13]. Biomass resources used in the production of bioenergy typically enhance regional energy access and reduce dependence on fossil fuels.

Bioenergy can also strengthen the forestry and agriculture sectors of an economy while increasing the use of renewable resources as feedstocks for a wide range of industrial processes. Biomass utilisation could help to mitigate climate change, reduce risks to life and property, and help provide a secure, competitive energy source that is sustainable.

One promising biomass resource that is available in large quantities but not yet being utilised to its full potential is cocoa pod husks (CPH). Due to the economic importance of cocoa, it is one of the most predominantly grown and accessible crops in Ghana [14]. Ghana produces about 858,720 tonnes of CPH annually, which is equivalent to 19% of the total global production [15]. This abundant potential biomass energy resource is wasted every year as it has not been adequately exploited. The cocoa industry provides livelihood for about 800,000 families, which represents approximately 13% of the country's total population [16]. However, cocoa farmers continue to live despicable lives without access to basic energy services. Given the high abundance of CPH, it could be exploited for power generation for rural communities.

Whiles CPH conversion to useful energy vectors can promote economic development among farmers, it can also boost cocoa production. Recent studies conducted by Syamsiro et al [17], Tsai et al [18] and Adjin-Tetteh et al [19] revealed that CPH has a relatively high energy density of 17-18 MJ/Kg which is competitive with firewood. The energy density of CPH can however be affected by factors such as cultivation methods, environmental influences and differences in soil contaminations [19]. CPH, like other biomass materials, has inherent diversity that may be attributed to factors such as geographic location, variety, climatic conditions, harvesting methods, and the kind of soil in which it was

grown. Soil properties such as structure, texture, porosity, moisture, nutrient content, pH, salinity, and microbial activities affect plant development and therefore influence the quality of biomass fuel [20]. Nutrient deficiency and toxicity can have a negative impact on total biomass; hence, an optimum nutrient level in soil is crucial for biomass production [21]. The ash content of biomass, for instance, can be highly influenced by the soil type in which it was grown. Crops grown in clay soils are known to produce higher ash levels than crops grown in sandy soils [22]. Since ash content plays a significant role in the determination of energy density of biomass feedstock, it may be imperative to investigate how soil conditions and types affect the energy content of CPH.

In as much as a number of research have investigated the thermochemical properties of CPH and their potential conversion processes, no single research has been conducted on the different types of CPH and the variation in their thermochemical properties. It is against this background that this extensive research is being conducted across the cocoa growing regions.

## **1.2 Aim and Objectives**

The main aim of this thesis was to develop an integrated bio-rural energy scheme for Ghana by utilizing cocoa pod husks as the raw material. This would enable sustainable power generation and consequently improve living conditions thereby reducing poverty in rural communities in Ghana. The specific objectives were therefore to:

1. Review various types of biomass materials and their energy conversion technologies in order to select potential materials and technology for the proposed bio-rural energy scheme.

2. Characterize various types of selected CPH materials for their thermochemical properties using proximate and ultimate analysis.
3. Develop a mathematical model for predicting the thermal performance of selected CPH energy conversion system.
4. Evaluate the performance of the CPH-fed energy generation system with a dedicated rig.

### **1.3 Significance of the research**

The ability of a nation to obtain a sufficient, inexpensive, and reliable energy supply for its domestic and industrial needs is crucial for the economic advancement of that country. Most developing countries, including Ghana, rely on wood fuel to meet their growing domestic energy demands. The enormous national dependence on wood fuel for cooking in Ghana has resulted in a soaring rate of deforestation in the country. In addition, electricity access especially in rural households is very low. It has therefore become extremely important to search for sustainable alternatives. This thesis identifies CPH as a potential biomass resource that can contribute to the energy mix policy in Ghana. Governments, energy planners, policymakers, utilities, and international organisations involved in appraising renewable energy technology development in Ghana would benefit from the findings of this thesis. The study specifically has the following significance:

- The study should help to advance the field of bioenergy and allow for the selection of acceptable systems for bio-rural energy projects. The

research elucidates various biomass conversion technologies and how they can be useful in diversifying the energy mix in Ghana.

- The study determined the thermochemical properties of cocoa pod husks and therefore, should help policy makers and energy regulators in their choice of biomass resources for energy generation purposes.
- The findings of this study should be useful for investors, corporate bodies, NGO's and other stakeholders who may be interested in bioenergy development and production.

#### **1.4 Novelty**

This research breaks new ground in the bio-rural energy development sector, particularly in Ghana. While there is a great deal of study on bioenergy production, the majority of it is generic and places little attention on individual biomass resources. In the present research, the notion of using cocoa pod husks to generate electricity for remote rural populations in Ghana was studied for the first time. This thesis is the first of its kind to examine the thermochemical properties of all four varieties of cocoa pod husks in Ghana.

A thermodynamic equilibrium model simulating and predicting the performance of a cocoa pod husk-fed downdraft gasifier was effectively created. The equilibrium model was validated against experimental data from a 5 kW cocoa pod husk-fed gasifier system.

#### **1.5 Thesis structure**

The thesis is outlined as follows:

**Chapter 1** covers the research background, aims and objectives of study, significance of the research, structure of thesis and the limitations of the study.

**Chapter 2** covers a review of biomass resources in general as well as biomass materials available in Ghana. The various categories of biomass such as energy crops, agricultural crop residues, forest resources and animal waste are covered. Bioenergy conversion technologies are also be covered in this chapter.

**Chapter 3** presents the material characterization of different varieties of cocoa pod husks from the cocoa growing regions of Ghana. The elemental composition of the different types of cocoa pod husks together with their thermal properties are reviewed.

**Chapter 4** covers the development of a mathematical model for predicting the performance of cocoa pod husk gasification.

**Chapter 5** covers the experimental performance of a 5kW downdraft gasifier fed by cocoa pod husks. The result of the experimental study is used to validate the mathematical model.

**Chapter 6** summarises the outcomes of the study by providing the general conclusions and recommendations for further research.

## **1.6 Limitations of Study**

Although downdraft gasifiers create less tar than updraft gasifiers, producer gas containing tar cannot be utilised directly in internal combustion engines and gas turbines without further purification. In gasifier modelling, the prediction of tar generation with the purpose of limiting its quantity is essential. However, the present study does not include tar formation in the model.

# CHAPTER TWO

## 2.0 LITERATURE REVIEW

### 2.1 Introduction

This chapter begins with a general literature review of biomass resources covering energy crops, agricultural crop wastes, forest resources, animal waste and their conversion technologies. The chapter also reviews the biomass resources in Ghana in order to establish the most sustainable materials for rural power generation.

### 2.2 General biomass resources

Biomass is a broad term used to describe materials of contemporary biological origin that can be used as a source of energy or for its chemical components. Biomass is described in the EU Renewable Energy Directive as: ‘the biodegradable fraction of products, waste and residues from biological origin from agriculture (including vegetal and animal substances), forestry and related industries including fisheries and aquaculture, as well as the biodegradable fraction of industrial and municipal waste [23]. It is derived from organic material such as trees, plants, and agricultural and urban waste. Biomass contains stored energy from the sun and can therefore be considered as a form of stored solar energy. In other words, the primary step in the build-up of biomass is photosynthesis. In this process, sunlight is absorbed by chlorophyll in the chloroplasts of green plant cells and is used by the plant to produce carbohydrates from water and carbon dioxide (CO<sub>2</sub>) [24]. Biomass can be burnt directly or converted to liquid biofuels or biogas that can be burnt as fuels [25].

Biomass is a key renewable energy resource that generally comes from a variety of sources. There is currently a wide range of biomass sources available worldwide. The most easily accessible biomass resources are derived from agriculture, forestry and industry. Biomass resources include: wood from natural forests and woodlands, forestry plantations, forestry residues, agricultural residues such as straw, stover, cane trash and green agricultural waste, agro-industrial waste such as sugarcane bagasse and rice husk, animal waste (cow manure, poultry litter etc.), industrial waste such as black liquor from paper manufacturing, sewage, municipal solid waste (MSW), and food processing waste [26]. Biomass that are specifically grown for their energy content are called 'energy crops'. Dedicated energy crops are non-food crops that can be grown on marginal land (land not suitable for traditional crops like corn and soybeans) specifically to provide biomass [27]. Energy crops can take various forms and can be converted to several different products. Many crop species have multi-purpose uses, thus they can be used to produce more than one type of energy product, for example, hemp (both oil and solid biomass) and cereals (ethanol and solid biomass from straw) [28]. Energy crops are broken down into two general categories: herbaceous and woody. Herbaceous energy crops are perennial (plants that live for more than 2 years) grasses that are harvested annually after taking 2 to 3 years to reach full productivity. They include switchgrass, miscanthus, bamboo, sweet sorghum, tall fescue, kochia, wheatgrass, and others. Short-rotation woody crops are fast-growing hardwood trees that are harvested within 5 to 8 years of planting. They include hybrid poplar, hybrid willow, silver maple, eastern cottonwood, green ash, black walnut, sweetgum, and sycamore. Most of these species can help improve water

and soil quality, as well as wildlife habitat and overall farm productivity compared to annual crops [27].

Biomass can also be derived from waste and residues. Biomass wastes and residues encompass materials of biological origin that emerge as by-products and wastes from agriculture, forestry, forest or agricultural industries, and households. Unlike dedicated energy crops that are produced specifically for use as an energy resource, biomass waste and residues are produced as a result of economic activity and production of goods. Crop residues comprise all agricultural waste such as bagasse, straw, stem, stalk, leaves, husk, shell, peel, pulp, stubble, etc. Enormous quantities of agricultural residues are produced globally every year and are hugely under-exploited. Rice for example produces both straw and rice husks at the processing plant which can be easily converted into energy. Maize and sugar cane harvesting produce significant quantities of biomass in the form of cob and bagasse which can both be converted into energy. Harvesting and processing of coconuts also produce quantities of shell and fibre which can serve as a good source of energy [26].

### **2.3 Classification of biomass materials**

Biomass can be categorized broadly as woody, non-woody, and animal wastes. Woody biomass comprises forests, agro-industrial plantations, bush trees, urban trees and farm trees. Wood, bark, branches and leaves are also classed as woody biomass. This category of biomass in general is a high-valued commodity and has various uses such as timber, raw material for pulp and paper, pencil and matchstick industries and cooking fuel [29].

Non-woody biomass comprises crop residues like straw, leaves and plant stems (agro-wastes), processing residues like sawdust, bagasse, nutshells and husks, and domestic wastes (food, rubbish and sewage). They are essentially harvested in villages and used either as fodder or cooking fuel [24].

Animal waste comprises the waste from animal husbandry [29]. Animal dung is a potentially large biomass resource and dried dung has the same energy content as wood. The efficiency of animal dung is only about 10% when burnt for heat. However, by using anaerobic digestion (to generate biogas), the efficiency of converting animal waste might be increased to 60%. Dung is only easily recovered from confined cattle or in environments where the labour expenses involved with collecting dung are low. Each year, around 150 Mt (dry) of cow dung is used as fuel on a global scale [24].

## **2.4 Biomass Conversion Technologies**

Biomass can be converted into several useful forms of energy using different conversion technologies. Generally, the choice of biomass conversion technology depends on the type, quantity and characteristics of biomass feedstock available, infrastructural requirements, environmental standards, economic conditions, project specific factors and end-use applications [6], [30]. However, in most cases it is the end-use application (form in which the energy is required) and the biomass feedstock available (type, quantity and characteristics) that determines the biomass conversion technology and process pathway. Several processing stages are required to convert raw biomass into useful energy using the two main conversion methods available: thermo-chemical, and biochemical conversion [31]. The biomass feedstock usually

undergoes stages such as harvesting/collection, transportation, storage, and drying where necessary before being processed into a suitable form for the chosen energy conversion technology [30]. A review of the various biomass energy conversion technologies and processes are discussed in the following sections.

#### ***2.4.1 Thermochemical conversion***

Thermo-chemical conversion comprises of all conversion processes of biomass based on thermal energy. Thermo-chemical conversion is a high-temperature chemical reaction that disintegrate the bonds of organic matter and regenerate these intermediates into biochar (solid), highly oxygenated bio-oil (liquid) and synthesis gas [32]. There are four main process options within thermo-chemical conversion; combustion, pyrolysis, gasification and liquefaction. The main difference between these process options is the amount of excess air and temperature within the process that leads to the conversion of final product CO<sub>2</sub> and water, or to intermediate useful products [33]. Table 2.1 shows a comparative of thermochemical processes for biomass conversion. The operating conditions (temperature and pressure) and the end-products are displayed.

Table 2.1: Comparative of thermochemical processes [32]

<b>Process</b>	<b>Temperature (°C)</b>	<b>Pressure (MPa)</b>	<b>Products</b>
Combustion	700-1400	0.1	Thermal energy  Biochar
Pyrolysis	500-800	0.1	Gas  Bio-oil
Gasification	500-1300	0.1	Syngas
Liquefaction	250-350	5-20	Liquid biofuel

#### **2.4.1.1 Direct Combustion**

Biomass combustion simply means burning organic material. Combustion can be defined as a complete oxidation of fuel [32]. Direct combustion is the best established and most commonly used technology for converting biomass to heat. Biomass fuel burns in excess air to produce heat during combustion [34]. Combustion is the oldest energy production process in the history of humanity, and is responsible for over 97% of the world's bio-energy production [35]. Combustion is a high temperature exothermic reaction between oxygen and the hydrocarbons in biomass. The process occurs in the presence of more oxygen than pyrolysis and gasification thereby resulting in higher air emissions [32]. Combustion of biomass results in the production of hot gases at temperatures around 800-1000 °C and these hot gases may be used for direct heating purposes

or for electricity generation. Although it is possible to burn any type of biomass, combustion is practically feasible for biomass with a moisture content less than 50% unless the biomass is pre-dried [30]. Figure 2.1 shows an image of the combustion process. Some biomass combustion systems can be used or adjusted to burn multiple types of biomass, however most combustion systems are designed to burn a single type of biomass [36]. Combustion of biomass in coal-fired power plants (co-firing) has become increasingly popular and is an effective way of lowering greenhouse gas emissions [37].

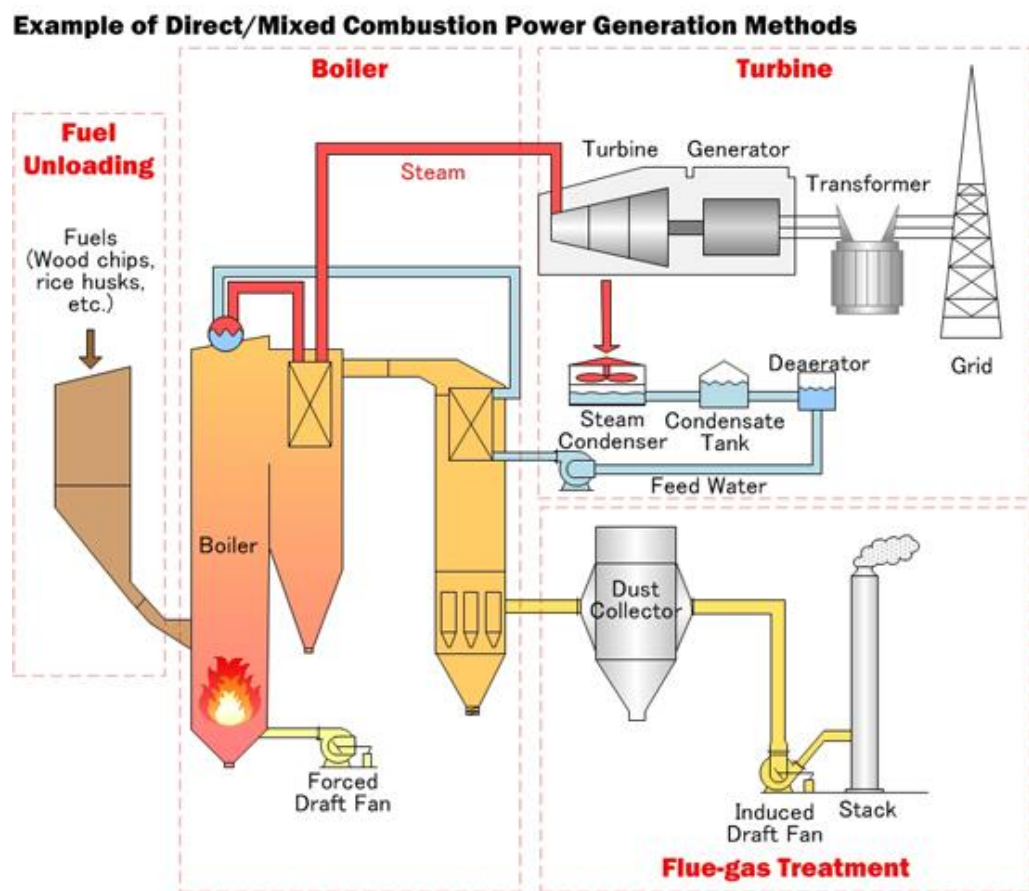


Figure 2.1: Schematic of combustion process [38].

Combustion is the most highly developed and marketable biomass technology worldwide. However, there are no available reports on biomass combustion in Ghana despite the availability of a diverse range of agricultural biomass

resources including crop residues, forest residues and dry animal dung which make combustion a potentially viable means of electricity generation in Ghana [6].

#### **2.4.1.2 Gasification**

Gasification is a thermochemical process that converts carbonaceous feedstock (biomass, coal, and plastics) into a fuel gas through partial oxidation [32]. Unlike combustion where oxidation is complete in one process, gasification converts the intrinsic chemical energy of carbon in biomass into a combustible gas in two stages [39]. Biomass gasification technology has historically been based on partial oxidation or partial combustion principles, resulting in the production of a hot, dirty, low calorific value gas that can be burnt directly or used as a fuel for gas engines and gas turbines [35]. Biomass-sourced gas for example, can be burnt directly for heating or cooking, converted to electricity or mechanical energy (through a secondary conversion device such as an internal combustion engine), or used as a synthetic gas for producing higher quality fuels or chemical products such as hydrogen and methanol [40]. Gasification takes place at high temperatures (800-1100°C) in the presence of a gasifying agent (air, steam or oxygen) [41], and the resulting fuel gas produced (synthetic gas or syngas) is a mixture of Carbon Monoxide (CO), Hydrogen (H<sub>2</sub>), Carbon Dioxide (CO<sub>2</sub>), Methane (CH<sub>4</sub>) and light hydrocarbons [32]. Gasification processes have several advantages over other conversion technologies. Gasification feedstock can be any type of biomass including agricultural residues, forestry residues, by-products from chemical processes, and even organic municipal wastes. Figure 2.2 depicts a biomass gasification process, illustrating both the feedstock

flexibility inherent to gasification and the vast array of products and applications of gasification technology.

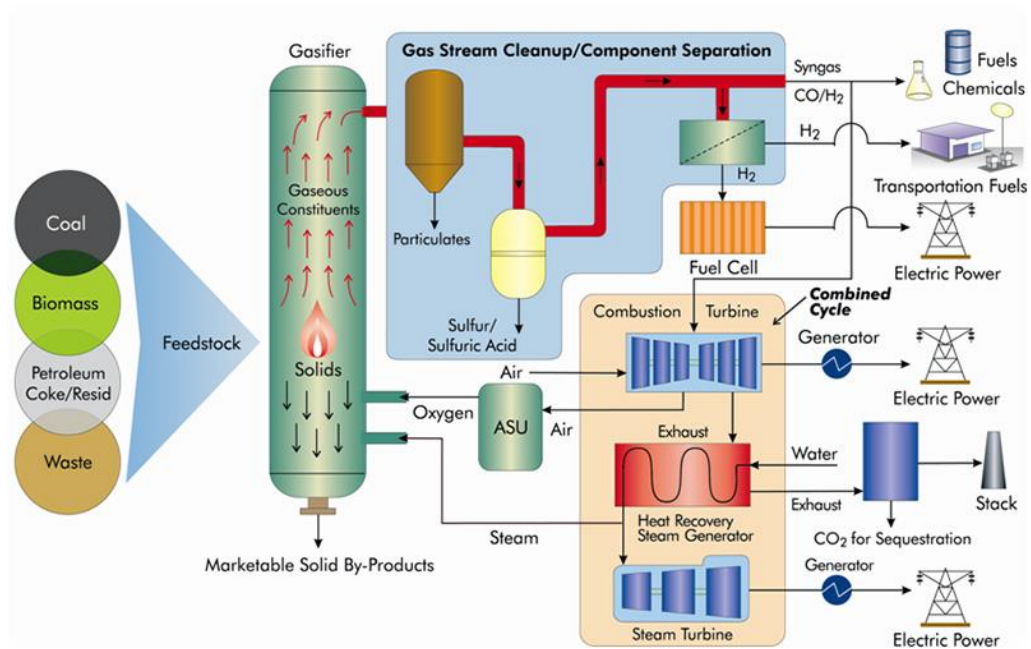


Figure 2.2: Schematic of gasification process [42].

Gasification traditionally converts the entire carbon content of the feedstock, making it more attractive than enzymatic ethanol production or anaerobic digestion where only portions of the biomass material are converted to fuel [37]. Syngas derived liquid fuels such as methanol, dimethyl ether, and synthetic diesels are also clean transportation fuels [43]. The main steps involved in gasification process can be classified as upstream processing, gasification, and downstream processing [44]. Figure 2.3 illustrates how each of the main steps are sub-divided and the various sub-processes that take place during gasification.

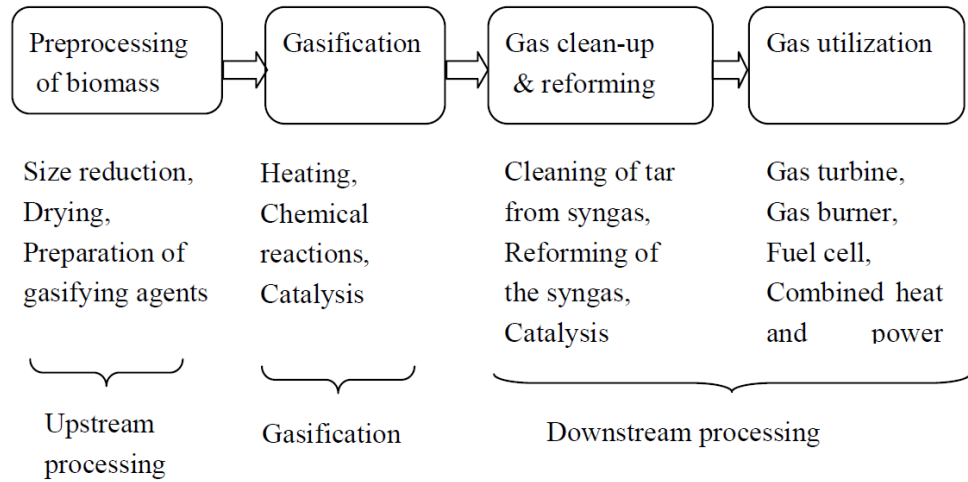


Figure 2.3: Processes involved in biomass gasification [44].

Upstream processing also known as pre-processing involves processing of biomass to make it suitable for gasification operations. This includes size reduction of biomass samples using hammer-mills, knife mills and tub grinders, and also drying to reduce moisture content of feedstock. Waste heat, perforated bin dryers, band conveyor dryers and rotary cascade dryers are all used in drying feedstock. Downstream processing on the other hand is the refining stage where the low calorific value product gas containing contaminants of varying degrees is processed further for effective use [44]. Cold cleaning (at temperatures  $<30^{\circ}\text{C}$ ), warm cleaning (at temperatures between 30 and  $300^{\circ}\text{C}$ ) and hot cleaning (at temperatures  $>300^{\circ}\text{C}$ ) may be administered depending on the final application of the syngas [45]. Recent studies by [44], [46], [47], [48], [49], [50], and [51] have all provided various alternatives for optimizing syngas yield, improving syngas quality and reducing tar yield in the application of gasification technologies. There are two categories of tar removal techniques namely primary (in-situ) and secondary removal techniques (post-gasification). While primary removal technique minimizes the tar yield in syngas internally through

optimization of the design and operating conditions of the gasifier without the need for an additional reactor, secondary removal technique requires additional reactor to destroy and reform the tar yield to acceptable levels in the syngas [44]. Although post-gasification or secondary treatment techniques have been tried and tested, in-situ tar removal techniques are becoming more popular as they may phase out the need for an additional clean up [52]. On the whole, a synthesis of both primary and secondary treatment methods is more productive since it may not always be possible to achieve a desired tar reduction and maintain the quality of the product gas using one gas cleaning technique.

Biomass Gasification in Ghana is still at the research and development and plant evaluation stage. A number of feasibility studies have been carried out to assess the potential for co-generation (combined heat and power) from wood residues. These include feasibility study on Letus Power Plant, and case study on the potential for co-generation from wood residues in three cities in Ghana [53]. A co-generation facility with a capacity of around 6 MW has been erected, with sawmill residues and oil palm waste serving as feedstock. This plant has powered some industries and surrounding communities without grid electricity [53], [6], [54]. A few industries such as SAMATEX Ltd. at Samreboi in the Western region, and STP in Kumasi currently use co-generation [53]. Gasification is one of the most promising bioenergy technologies for rural development and potential gasification feedstocks are in enormous abundance. Notable amongs them are agricultural residues such as coconut shells, coconut husks, maize cobs, cocoa pod husks, palm kernel shells, rice husks, rice straw, wheat straw, sawdust, and empty fruit bunch. Coconut husks and empty fruit bunch are fibrous in nature and hence require pre-treatment (densification, briquetting, and pelleting)

without which they may cause blockages in the gasifier [55]. Conversely, cereal crops like rice husks, rice straw and wheat straw generally have higher ash contents (>10%) and can cause slagging, fouling, and blockages in the gasifier [56]. Ash content can however be controlled by optimizing the operating conditions in order to achieve the desired results.

#### **2.4.1.3 Pyrolysis**

Pyrolysis is a thermal degradation process which occurs in the absence of oxygen and produces a variety of products such as fuel gas, bio-oil, char, and tar which can subsequently be used for power generation [57]. Biomass is heated in the absence of oxygen, or partially combusted in a limited amount of oxygen supply, to produce a hydrocarbon rich gas mixture, an oil-like liquid and a carbon rich solid residue [35]. The amount of useful products from pyrolysis process (CO, H<sub>2</sub>, CH<sub>4</sub> and other hydrocarbons) and their proportion depends entirely on the biomass type, rate of heating, operational temperature and residence time [58]. Pyrolysis is the first step in combustion and gasification processes, and the operating conditions of biomass pyrolysis are key factors in managing the quality and distribution of the output [59]. For example, a low-to-medium temperature pyrolysis process and a vapour residence time that is regularly prolonged up to 30 minutes tend to produce a higher quantity of solids whereas a high temperature biomass pyrolysis process and a long vapour residence time generally produces a higher quantity of gas. Alternatively, a moderate temperature pyrolysis process accompanied by a vapour residence period generally below 2 seconds, favours the formation of higher quantity of liquids rich in organic molecules and significant char yields [60]. Pyrolysis produces

much lower amounts of gaseous products compared to combustion and gasification, thereby enabling the elimination of a gas cleaning subsystem [41]. Biomass pyrolysis usually takes place in a temperature range of 300-600°C [61]. Based on reaction temperature, heating rate and residence time, pyrolysis may be broadly classified as slow pyrolysis and fast pyrolysis [62]. Slow pyrolysis is a batch process which is carried out at low temperatures and slow heating rates, for long residence times [63], [64]. Conventional slow pyrolysis is used primarily for the production of char and the process is more tolerant of feedstock with high moisture content [65]. Slow pyrolysis is categorized into two types; carbonization and torrefaction. Torrefaction occurs at a very low and narrow temperature range (200-300°C) whereas carbonization takes place at a much higher and broad temperature range. Carbonization is a slow pyrolysis process in which biochar is the desired product and it is the oldest technique of treating biomass for the production of charcoal [61]. An illustrative slow pyrolysis facility for the production of biochar is pictured in Figure 2.4.

Torrefaction, on the contrary is used as a pretreatment process to increase the energy density and biomass fuel properties such as grindability before it is sent for bio-oil production or for further use [66].

Fast pyrolysis unlike slow pyrolysis is a high temperature process in which biomass is rapidly heated in the absence of oxygen to form a dark brown mobile bio-liquid [67]. The primary objective of fast pyrolysis is to increase the production of bio-oil [61]. Although fast pyrolysis is relatively new, it has attracted lots of attention in recent times due to the benefits that bio-oils offer in terms of easy storage, transport and comparatively higher power generating efficiencies at small scales of operation [68]. Nonetheless, there are critical

issues with fast pyrolysis that need to be addressed, predominant among them is the quality of bio-oil yield. Bio-oils are known to be extremely corrosive and this nature poses serious handling and transportation problems.

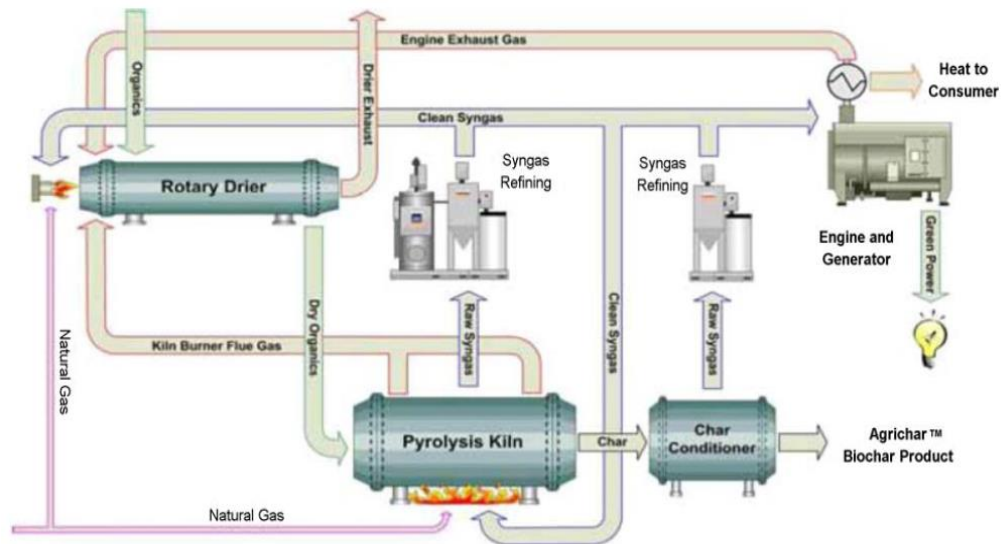


Figure 2.4: Schematic of slow pyrolysis process [69].

Pyrolysis can be exploited to Ghana's advantage since feedstock such as sawdust, waste from furniture factories and other wood processing industries, shells (almond, groundnut, palm kernel, coconut), husks (rice, coconut, cocoa), corn cobs, stalk (corn, cotton, cassava), straws (corn, cotton, wheat, rice), bagasse (sugarcane, sorghum, sunflower) banana leaves, jatropha residue, sunflower seeds, palm fronds, palm trunks, palm leaves, cassava rhizome, bamboo, elephant grass, cattle manure, household waste, municipal solid waste, poultry litter, sewage sludge and used oils [63], [64], [70], [71], [72], [73] have not been fully exploited.

There has only been a single pyrolysis project in Ghana. A 6-tonnes pyrolysis plant using sawdust as feedstock was installed in Kumasi in 1980 as an alternative power supply for a brick kiln. This project was a feasibility study

carried out jointly by the Building and Road Research Institute, the Technology Consultancy Centre of the Kwame Nkrumah University of Science and Technology (KNUST), and Georgia University of Technology, USA. Char and oil yields were envisaged at 25% and 18% respectively, however low yields between 6% and 13%, together with poor supply and drying of feedstock, and utilisation of manual process controls resulted in the closure of the pyrolysis plant [74], [53]. A pilot-scale pyrolysis plant for the production of bio-oil in Ghana using agricultural crop residues and wood processing wastes was started by the Institute of Industrial Research of the Council for Scientific and Industrial Research (CSIR-IIR) in collaboration with the University of Southampton in the UK [53], [75]. Unfortunately, that project was never completed.

#### **2.4.1.4 Liquefaction**

Liquefaction is a low temperature and high-pressure thermochemical process during which biomass is broken down into fragments of small molecules in water or another suitable solvent [32]. Liquefaction is sometimes confused with fast pyrolysis as both thermochemical processes convert feedstock organic compounds into liquid products. In the case of liquefaction, feedstock macromolecule compounds are decomposed into fragments of light molecules in the presence of a suitable catalyst whereas in pyrolysis, a catalyst is usually unnecessary [76]. Another point is that liquefaction reactions take place in a liquid medium and hence can handle biomass feedstock with high moisture content whereas pyrolysis generally requires feedstock with moisture content less than 10% in order to reduce the amount of water in the bio-oil yield [46]. The products of biomass liquefaction are determined by various factors,

including substrate type, heating conditions, solvent type, reactor configuration and catalyst [77]. There are three categories of biomass liquefaction namely; (1) Hydrothermal liquefaction; (2) Liquefaction with solvents, and (3) Liquefaction with solvent and catalysts [46]. Hydrothermal liquefaction (HTL) typically works at temperature range of 200-450°C and pressure of 5-25MPa [78], [79]. Hydrothermal liquefaction (also known as direct liquefaction) is basically pyrolysis in hot liquid water [80]. Water is mostly used as a working medium for hydrothermal processes as it enhances heat transfer and biomass decomposition. Liquefaction has been demonstrated for a range of biomass feedstocks with and without the presence of catalysts using different solvents. Figure 2.5 is an illustration of biomass liquefaction for the conversion of bio-crude to renewable diesel, gasoline, and jet fuel.

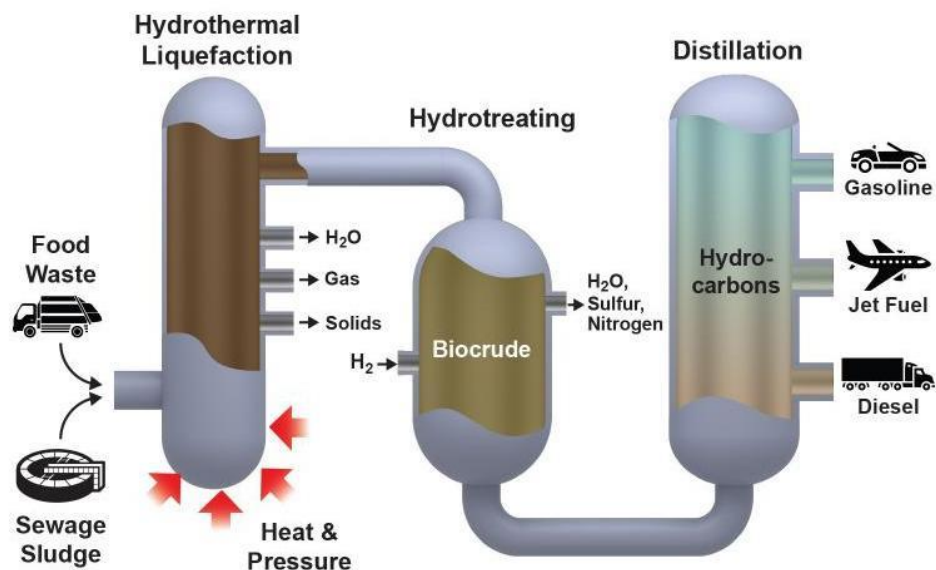


Figure 2.5: Schematic of biomass liquefaction [81].

Other studies have also investigated the effects of operating conditions such as temperature, pressure, and reaction time on product yield and composition [82]. Recent studies on biomass liquefaction indicate that bio-crude yield increases

with temperature increase, nonetheless there is an optimum temperature beyond which any further temperature increase reduces the bio-crude yield [83], [84]. A possible reason for the increase and decrease in product yield after the optimum temperature is the competition of the two reactions involving hydrolysis and repolymerization during liquefaction [85], [86]. Behrendt et al [87] stated in their review of biomass liquefaction that an increase in system pressure potentially increases the bio-oil yield in conformity to Le Chatelier's principle. Although pressure maintains liquefaction medium in the liquid phase, the effect of pressure on bio-oil yield and composition is less significant after a certain threshold. This is because in the supercritical region, influence of pressure on the properties of water or solvent medium is very minimal [88]. Reaction/residence time is another important parameter in biomass liquefaction as it affects the product composition and conversion efficiency of HTL [89]. An increase in residence time increases the product yield, however after a certain threshold, product yield decreases with increasing reaction time [90]. Apart from water which is environmentally friendly and comparatively cheaper, organic solvents such as ethanol, methanol, acetone, etc., have been used as the reaction medium for biomass liquefaction. Water plays a triple role during HTL, as it serves as a solvent, a reactant and a catalyst [86]. The thermochemical liquefaction of sewage sludge in methanol, ethanol, and acetone was studied by Huang et al [77]. Conclusions from the study by Huang and colleagues stated that, while using an ester-forming solvent like ethanol, which is more efficient than using an N-containing solvent like acetone, resulted in higher levels of N-containing compounds being formed, ethanol was the best solvent for thermochemical liquefaction of waste because of its efficiency and renewable nature. Yuan et al

[91] also studied the liquefaction characteristics of microalgae under different organic solvents and their findings were not different from Huang et al's [77]. They also concluded that ethanol is the most promising solvent in terms of efficiency and reproducibility.

Biomass resources such as palm, corn stalk, rice straw, sawdust, swine manure, wood stalk, empty fruit bunch, sugarcane bagasse, palm kernel shell, bamboo, cassava rhizome, rice husk, coffee husk, peanut shell and sludge can be used for energy production through liquefaction [82], [89].

#### ***2.4.2 Biochemical conversion***

Microbial processes are used in biological conversion technologies to convert biomass into valuable products. Biochemical conversion entails producing fermentable carbohydrates and converting them into liquid fuels (e.g., ethanol, butanol) or gaseous molecules (methane) using a particular microbial community. Because sugars are important intermediates in this process, this is referred to as the sugar platform. [92]. In the process of biochemical conversion, enzymes are used to convert structural carbohydrates (such as the cellulose and hemicellulose found in plant cell walls) into sugars. These sugars are then fermented by microorganisms to produce alcohol, organic acids, or hydrocarbons. Biochemical conversion can be thought of as the reverse of chemical conversion. Conversions are typically carried out at atmospheric pressure and temperatures ranging from room temperature to 70 degrees Celsius. [93]. The two main biochemical conversion processes used are fermentation and anaerobic digestion.

### **2.4.2.1 Fermentation**

Fermentation is a biological process that converts sugar and starchy foods into ethanol. Sugar cane, sugar beet, and sweet sorghum are sugar crops, while maize, cassava, yam, potatoes, and wheat are starchy crops [6]. Enzymes and yeasts are commonly used in the production of bio-ethanol. Continuous and batch yeast fermentations are both possible, although batch fermentations are favoured since the danger of contamination is smaller [33]. Microorganisms are introduced into predetermined volumes of medium during batch fermentation, and the fermentation continues until all sugars have been destroyed. This method works well with sugars because it is easy, cheap, and has a low chance of getting contaminated [92]. In order to achieve good quality ethanol, purification of the raw ethanol produce is essential. Purification of ethanol by distillation is an energy-intensive step, with about 450 litres of ethanol being produced per ton of dry corn. One of the advantages of fermentation is that the solid residue produced can be used for other purposes such as animal feeding, and the bagasse from sugar cane as fuel for electricity generation in a boiler or gasifier [30]. The ethanol-making power plant can use the residues for self-generation. Bio-ethanol fermentation plants are practically large, and an optimal sized plant produces about 200,000-300,000 tonnes of ethanol per year [33]. The diverse range of biomass feedstock used in the production of ethanol through fermentation can be classified into three main types: sugars, starches, and cellulose materials. Although sugars (from sugarcane, sugar beets, molasses, and fruits) can be directly converted into ethanol, starches (from corn, cassava, potatoes, and root crops) must first be hydrolyzed to fermentable sugars by the action of enzymes whereas cellulose (from wood, agricultural residues, waste sulfite liquor from

pulp, and paper mills) must also be converted into sugars, by the action of mineral acids before enzymes from microorganisms can readily ferment them to ethanol [94]. Ligno-cellulosic materials including forestry, agricultural and agro-industrial wastes are rich in sugars and easily assimilated by microorganisms, making them good feedstocks in the production of biofuels by fermentation [95]. Pretreatment is an essential step in biochemical conversion of ligno-cellulose materials into biofuels and generally an acid catalyzed thermo-chemical treatment is mostly used for this purpose [96]. Effective pretreatment of biomass feedstock is necessary to increase the enzyme-available surface area, improve the substrate solubility, and promote substrate utilization to ensure high biofuel yield [97]. Fermentation of starch is more complex than fermentation of sugars because starch must first be converted into sugar by hydrolysis and then into ethanol. This requires high-temperature cooking (140–180°C) to raise starch saccharification efficiency and increase ethanol yield under complete sterilization of harmful microorganisms [94]. Fermentation is used commercially to produce ethanol in a number of jurisdictions, including Brazil from sugar cane at over 300 distilleries, the USA, Spain and France from maize and other cereal crops, and currently in Canada and Sweden from ligno-cellulosic sources [33]. El-Dalatony et al [98] have recently introduced a novel integrated approach to improve energy conversion efficiency of microalgal biomass (*Chlamydomonas mexicana*). In their proof-of-concept, successive throughput fermentations attained 46% energy recovery from microalgae and 89% of biomass was converted into biofuels with minimal waste production. The leftover biomass was then converted to biodiesel by transesterification, thereby making the process a cost-effective one. Figure 2.6 depicts the sequential

fermentation process used to completely decompose microalgal biomass, beginning with carbohydrates and progressing to protein to produce ethanol (C2) and higher alcohols (C3-C5), respectively. Lipid being the primary component of the preceding fermentation, was transformed to biodiesel by transesterification.

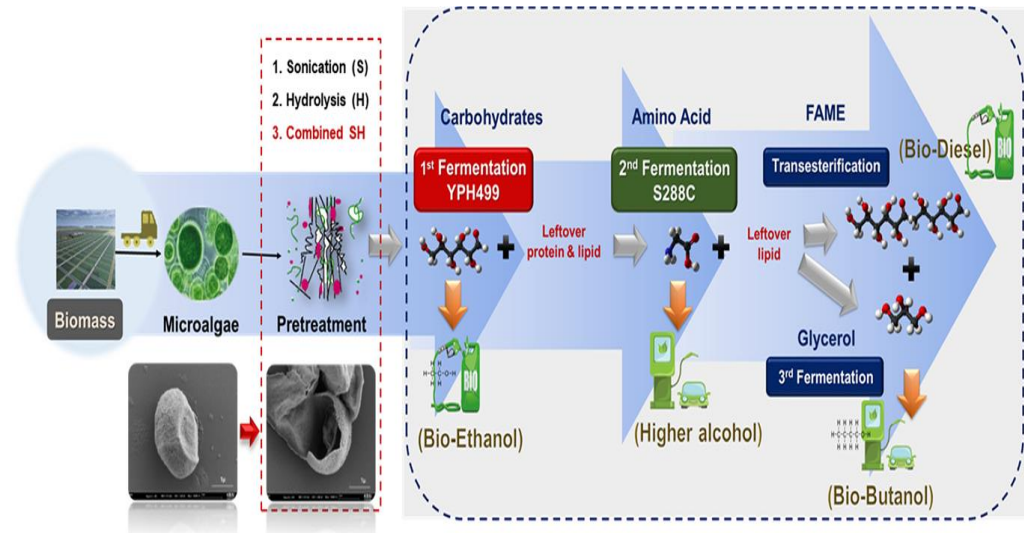


Figure 2.6: Schematic of serial fermentation using microalgae [98].

There is a great potential for ethanol production in Ghana and any attempt to synthesize the use of petrol with ethanol would result in a massive reduction in greenhouse gas emission. The addition of bio-ethanol to gasoline increases the oxygen content of the fuel, facilitate gasoline combustion and minimise the exhaust emissions such as carbon monoxide and unburned hydrocarbons that are normally associated with incomplete combustion in motor vehicles [99], [100], [101], [102]. Available feedstock for the production of ethanol through fermentation includes sugarcane bagasse, municipal solid waste (MSW), corn stover, corn stalk, rice straw, rice husk, sawdust, cassava, cocoa pod husk, coconut husk fibre, oil palm empty fruit bunch, among others [94], [103], [104], [105].

#### **2.4.2.2 Anaerobic digestion**

Anaerobic digestion is a biological process by which organic material is broken down by micro-organisms in the absence of oxygen, to produce biogas, a methane-rich gas used as a fuel, and digestate, a source of nutrients used as fertiliser [33]. The biogas produced from this process can be used in alternate gas-engine, CHP systems or micro-turbines as the prime mover. This is common in the water-treatment industry and where ‘wet’ biomass such as animal slurries are produced [57]. Anaerobic digestion is a commercially established process that is commonly used for recycling and treating organic waste and waste fluids with a high moisture content, i.e., 80–90% moisture. Gas generated by anaerobic digestion, like gas produced by gasification, may be used directly for cooking or heating following adequate treatment. It may also be used to generate power or shaft work in secondary conversion devices such as internal combustion engines. An Anaerobic digestion plant usually takes 15 to 30 days to process an organic waste. Essentially, any biomass except lignin (a major component of wood) can be converted to biogas - including animal and human wastes, sewage sludge, crop residues, industrial processing by-products, and landfill material. The conversion of animal wastes and manure to methane/biogas has significant health and environmental benefits. Aside avoiding greenhouse gas impacts by trapping and utilizing methane, the pathogens existing in manure are eradicated by the heat generated in the bio-digestion process and the resulting material provides a valuable, nutrient-rich fertilizer [40].

Despite its many benefits, the production of bioenergy from waste using anaerobic digestion presents several limitations. Environmental and health concerns could have an impact on social acceptability. H<sub>2</sub>S, Si, VOCs, CO, and

$\text{NH}_3$  are among the undesirable and harmful compounds found in biogas.  $\text{H}_2\text{S}$  and  $\text{NH}_3$  are toxic and very corrosive, causing damage to combined heat and power units and metal components.  $\text{H}_2\text{S}$  impacts the amount and quality of biogas produced, in addition to emitting toxic pollutants and corroding the biogas filtration system. Since anaerobic digestion-produced biogas includes contaminants, it often requires preventive treatment to increase methanol yield and post-treatment to remove  $\text{H}_2\text{S}$ . These methods are both energy-intensive and costly [106]. The complex nature of anaerobic digestion therefore requires accurate prediction, process monitoring, real-time control, and modelling of the performance of microbial communities in the anaerobic digestion system to optimize anaerobic digestion operation [107]. The Anaerobic digestion process begins with sludge hydrolysis and continues with fermentation, hydrogen-producing acetogenesis, and homoacetogenesis until the ultimate product, biogas, is generated. The hydrolysis of particulate organic matter into soluble molecules is often regarded as the most rate-limiting of these activities [108]. Li et al [109] used ultrasound at 20 kHz and an energy density of 0.5 W/mL as pre-treatments for mesophilic anaerobic digestion of waste activated sludge in their quest to discover a remedy for sluggish hydrolysis rate during anaerobic digestion. After sonication for 0-100 minutes, the sludge was digested at a hydraulic retention time (HRT) of 20 days. The results demonstrated that ultrasonic pre-treatment aided in the dissolving of soluble chemical oxygen demand (SCOD) from waste activated sludge, as well as the quick deterioration of the sludge's dewatering ability. The reactor that was fed with sonicated sludge produced the most gas and methane at 80 minutes. Darwin et al [110] evaluated anaerobic co-digestion of cocoa husk with digested swine manure in a batch

system under mesophilic conditions and a hydraulic retention period of 25 days as part of an investigation to assess biodegradation efficiency in methane generation. The findings indicated that anaerobic co-digestion of cocoa husk with digested swine manure produced less methane (60.31.6 ml CH<sub>4</sub>/g) than anaerobic digestion of swine manure alone (104.14.4 ml CH<sub>4</sub>/g). Due to the high cell wall composition of cocoa husk, anaerobic bacteria may have been inhibited from converting cocoa husk to methane, resulting in a reduced biodegradation efficiency and methane output of the former. Figure 2.7 gives a general overview of biogas plant.

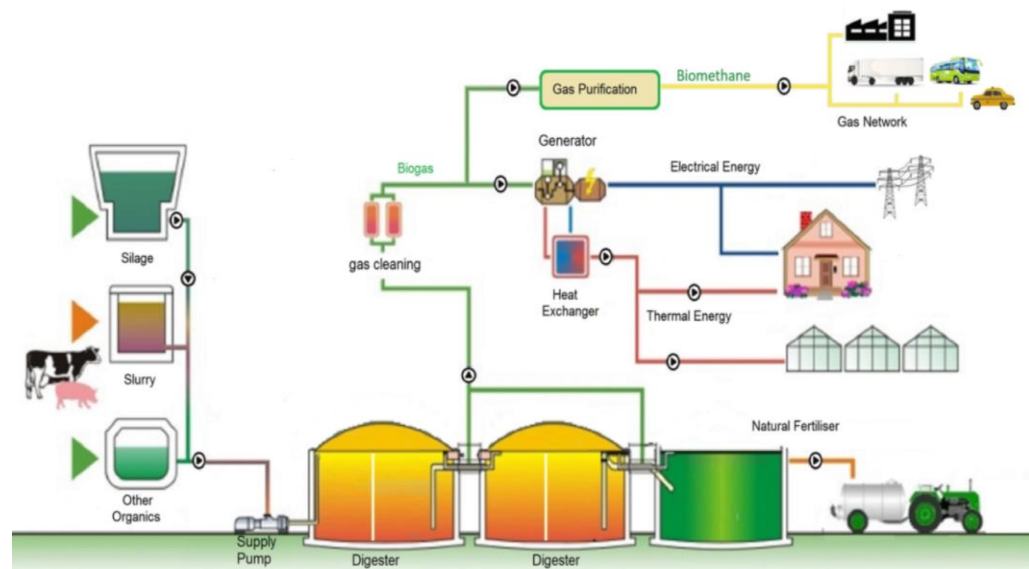


Figure 2.7: Illustration of biogas plant operation [111].

In Ghana, the only grid-connected biogas plant, a 100 kWe plant (Safisana), treating human faecal matter and organic waste from the market, began feeding electricity into the national grid in September 2016 [112], [113]. Several biogas systems have been installed in public places such as schools, prisons, healthcare centres and district assemblies, by the Institute of Industrial Research of the Council for Scientific and Industrial Research (CSIR-IIR), as part of Ghana's

bio-sanitation scheme [53], [6]. A feasibility study by Mohammed et al [114] suggest that the use of biogas for cooking is a viable option with a payback period of 5 years. However, biogas service companies face a number of challenges, notably, high costs of biogas digesters, poor image of biogas as a modern energy source, and socio-cultural stigmatization on the use of ‘faecal gas’ for cooking and ‘faecal fertilizer’ in agriculture. Other major challenges include low government commitment, low follow-up services on the part of biogas companies, lack of concrete policy on biogas, lack of well-tested standardized designs, and lack of microfinance schemes for cattle farmers interested in biogas digesters [115]. Having said that, biogas for electricity generation is competitive with diesel plants if the feedstock is obtained at little or no cost to the site [116].

## **2.5 Biomass Resources in Ghana**

Biomass as previously described in section 2.2, are materials of contemporary biological origin that can be used as a source of energy or for their chemical components. Ghana’s economy is traditionally oriented towards agriculture and hence produces a significant amount of biomass materials. In Ghana, biomass already supplies the bulk of energy services but in very inefficient forms, particularly as firewood and charcoal for cooking and heating [7]. Firewood is the main source of cooking fuel for about 80% of the rural inhabitants in Ghana [117].

A 2018 report by the Energy Commission of Ghana reveals that woodfuel consumption in Ghana has increased approximately 6% from 2517.8 kilo tonnes in 2008 to 2829.4 kilo tonnes in 2017 [118]. Biomass is Ghana’s dominant

energy resource in terms of endowment and consumption. Biomass resources cover about 20.8 million hectares of the land mass of Ghana (23.8 million hectares) and is the source of supply of about 60% of the total energy used in the country [119]. Biomass resources in Ghana include wood and wood wastes, agricultural crops and their waste by-products, municipal solid waste, animal wastes, wastes from food processing, aquatic plants and algae. However, there are competing uses for these biomass resources due to their economic and environmental value [53]. The Ghana Energy Commission acknowledges that woodfuel consumption in Ghana is second to petroleum at 40.5%, making woodfuel one of the most dominant primary energy sources in Ghana today [118].

Ghana's agricultural sector is characterised by many dispersed small-scale producers that employ manual cultivation techniques and depend mainly on rainfall. Nonetheless, it provides over 90% of the food needs of the country. Although crop production in Ghana is impeded by land degradation, improper field development, use of low-yield varieties, lack of organised seed production and distribution systems, and inadequate storage structures, Ghana still produces major crops such as maize, rice, sorghum, cassava, yams, plantain, groundnut, cowpeas, cocoa, oil palm, rubber, coconut, pineapple and coffee [53]. The availability of agricultural resources in Ghana vary from one agro-ecological farming zone to the other due to different mean annual rainfall and land area allocation for each zone [6]. Crop production dominates the agricultural sector with about 75 percent of total output whereas livestock, fishing, and forestry comprise the remaining 25 percent. Cocoa alone makes up about 10% of total crop production in Ghana [120] and hence a huge bioenergy generation potential.

### ***2.5.1 Energy crops***

Energy crops like sugarcane, sweet sorghum, maize, and cassava could well be used to produce ethanol. Palm oil, coconut, sunflower, soy, and jatropha may all be used to produce biodiesel [54]. Brazil and the United States generate ethanol from sugarcane and maize, respectively, for the transportation industry. They are both cultivated in most parts of Ghana, making them popular food crops. Approximately 1.96 million -tonnes of maize were harvested from an area of 1,000,000 ha in 2017. Sugarcane production in the country increased slightly from 145,000 tonnes in 2008 to 151,762 tonnes in 2017. Cassava production on the hand has increased massively from 11.35 million tonnes harvested in 2008 to 18.47 million tonnes in 2017 [14]. The increase in cassava production can partly be attributed to the introduction of high-yielding new varieties, and the Special Initiative on cassava production in the country. Sweet sorghum is cultivated mainly in the savannah zones. In 2008, approximately 350,000 tonnes of sorghum were produced from an area of 340,000 ha [53]. There is a huge potential for biodiesel production from jatropha and oil palm fruit, both of which have received significant investment from private and government bodies. A National Jatropha Plantation Initiative (NJPI) was introduced in 2006 with the main aim of developing up to one million hectares of jatropha plantations on available idle and degraded lands in phases for the next five to six years. In recent times, private institutions have emerged and over 20 companies (mostly foreign owned) are cultivating large tracts of jatropha plantations all over [121]. Jatropha plantation occupies over 1500 ha of land under the control of prominent institutions such as the UNDP, New Energy, Jatropha Africa Ltd., AngloGold

Ashanti Ltd and Valley View University, which places Ghana at an advantage as a potential leader in biodiesel production from jatropha in Africa [6].

Oil palm plantations cover approximately 320,000 ha and are located mostly in the rainforest and deciduous zones of the Ashanti, Western, and Eastern regions. Production of oil palm fruits increased from 1.1 million tonnes in 2001 to 1.9 million tonnes in 2008 [53]. Oil palm cultivation is carried out in varying scales such as smallholder farms, and medium to large-scale plantations. Ghana has the potential to produce biodiesel from almost all the oil-bearing energy crops apart castor beans. In 2017, approximately 383,960 tonnes of coconut were harvested across an area of 71,288 ha [14]. About 4,000 ha of these plantations mainly in the coastal belt have been affected by the Cape Saint Paul Wilt Disease, a lethal yellowing disease. The government however implemented a Coconut Sector Development Project between 1990 and 2005, which yielded results and resulted in the rehabilitation of about 800 ha of coconut farms. The Council for Scientific and Industrial Research (CSIR) has also developed a coconut hybrid to replace the affected trees [53]. Other oil-bearing energy crops such as sunflower and soybeans are cultivated mainly on small scale farms for local use. Maize, cassava, oil palm, coconut, sunflower, sugarcane, and sorghum could all play important roles in biofuel generation.

### ***2.5.2 Agricultural crop residues***

Agricultural crop residues are classified into two main categories: crop residues and agro-industrial by-products. Crop residues are the waste materials left or burnt on the farms after harvesting the target crops whiles Agro-industrial by-products are produced mainly after crop processing [53]. Major crop residues

produced in Ghana include straw or stalk of cereals such as rice, maize/corn, sorghum and millet, and cocoa pod husk, while agro-industrial by-products include corn/maize cob, cocoa husk, coconut shell and husk, rice husk, oil seed cake, oil palm empty fruit bunch (EFB), and sugarcane bagasse [69]. The harvesting and processing of maize produces major residues such as stalk, cob and husk which are potential biofuel feedstock. The stalk of sweet sorghum which is rich in sugar is also a potential feedstock for ethanol production. Coconut residues, mainly the husk and shells, oil palm empty fruit bunch (EFB) and sugarcane bagasse can serve as potential feedstock for biochar production. Oil palm produces three main residues; empty fruit bunches (EFB), shells and fronds. These residues have competing uses. The EFBs, which are rich in potassium, can be used as fertiliser, and the shells for production of activated carbon and heating, while the fronds are usually used for mulching. Coffee husk which is a residue from coffee processing, can be used as an organic fertiliser or for power generation. It can also be a potential feedstock for biochar production. Rice husk and straw are also potential feedstock for biofuel generation that are virtually unutilised in Ghana. Traditionally, most of the agricultural crop residues are burnt on the farms to facilitate the harvesting process or as a pest control mechanism while some of the residues are also used as substitutes for firewood [53]. Cocoa is the single most important export product of Ghana. Cocoa production occurs in the forested areas and covers approximately 1.75 million ha [69]. The main residue generated from cocoa production is the cocoa pod husks (CPH) which at present are left on the farms to decompose. Table 2.2 presents the theoretical energy potential of various crop residues generated in Ghana. Approximately 45 million tonnes of agricultural crop

residues were generated in Ghana in 2020, which is equivalent to a theoretical potential of 728.43 PJ of energy. Theoretical potential of residue assumes 100% availability of all residues considered during the calculation. Practically, not all generated residues are technically available for energy production due to a number of reasons. Firstly, some of the residues may be left on the farmland intentionally to mulch and also for re-fertilisation. Secondly, there may be practical challenges when collecting field residues, due to poor road conditions especially when it comes to small-holder farms in rocky and mountainous agricultural fields. In other words, not all the existing agricultural residues can be collected and used for bioenergy generation due to technical constraints, ecosystem functions, and other uses (e.g. animal fodder, fertiliser, domestic heating and cooking). Utilisation of all these residues in bioenergy production can potentially have adverse impacts on soil fertility [84]. Hence, it is expedient to assume recoverable percentage in order to get the technical potential of generated residues. Assuming that 60% of generated residues were available for energy production in 2020, the technical energy potential of Ghana was 437 PJ. There is a huge difference in estimated energy potentials of crop residues between this study and that of Duku et al [53] and Mohammed et al [6] who estimated 75.20 PJ and 91.60 PJ respectively. The differences in estimated potential may be attributed to the number of cash crops considered in this study. While this study considered 14 crops, the other two studies above only considered 8-9 crops and left out staple Ghanaian food crops like cassava and yam which have enormous energy potentials as per Table 2.2

Table 2.2: Energy potential from crop residues generated in 2020

<b>Crop</b>	<b>Annual production (10<sup>3</sup> t)<sup>a</sup></b>	<b>Residue type</b>	<b>Residue to product ratio (RPR)<sup>b</sup></b>	<b>Total residue produced (10<sup>3</sup> t)</b>	<b>Lower heating value (MJ/kg)<sup>c</sup></b>	<b>Residues Energy Potential (PJ)</b>
Cassava	21812	Stem/ Stalk	1.24	27046.88	17.5	473.32
Cocoa beans	800	Husk	1	800	15.48	12.38
Coconut	412	Husk/ Shell	0.54	222.48	14.71	3.27
Coffee, green	0.74	Husk	2.1	1.554	12.56	0.02
Groundnut	450	Husk/Shell/ Straw	2.08	936	17.5	16.38
Maize	3071	Stalk/ Husk/Cob	0.63	1934.73	18.08	34.98
Millet	170	Stalk	5.53	940.1	15.51	14.58
Oil palm fruit	2472	EFB/ Kernel Shell/ Fibre	0.44	1087.68	15.23	16.57
Plantain	4668	Trunk/ Leaves	0.5	2334	15.48	36.13
Rice	973	Straw/ Husk	3.28	3191.44	14.3	45.64
Sorghum	356	Stalk	4.75	1691	17	28.75
Sugarcane	154	Bagasse	0.2	30.8	13.38	0.41
Sweet potato	139	Straw	0.5	69.5	10.61	0.74
Yams	8533	Straw	0.5	4266.5	10.61	45.27

<b>Total</b>						<b>728.43</b>
--------------	--	--	--	--	--	---------------

<sup>a</sup> Annual crop production in 2020 [14]

<sup>b</sup> Residue to product ratio (RPR) based on [122]

<sup>c</sup> Lower heating value based on [122], [53], [6]

### ***2.5.3 Residues from forestry***

Ghana's forests portray a high diversity with the southern wet evergreen closed forests and the northern open semi-deciduous forests. The country's forest resources have gradually been reduced by factors such as excessive logging, unsustainable agricultural practices, bush burning, mining, quarrying, settlement, population growth and migration to forest areas [123],[124]. It is therefore critical to investigate how bioenergy may be produced from forest residues in order to lessen the amount of stress on forestry. Forest biomass is mostly in the form of wood fuel, with various forest wood-based resources serving as a significant source of domestic bioenergy [6]. Approximately 90% of the wood fuel consumed in Ghana are obtained directly from the natural forest and the savannah woodlands. The other 10% comes from wood waste, like logging and sawmilling waste [125], [126]. Wood residues are generated as co-products of logging and timber processing [7]. Hence, there are two categories of forest residues, namely: logging residues and wood processing residues. Logging residues include off-cuts, stumps, sawdust etc. and the average logging recovery is approximately 75% [53]. Wood processing residues on the other hand include discarded logs, bark, sawdust, off-cuts, sander dust, chips, trim ends and shavings. Wood processing residues are generated through sawmill and plywood mill processing operations. Figure 2.9 shows different residue types

that are generated in the production of plywood. Wood residues are mostly available at centralized locations and hence fairly easier to recover significant amounts for use as feedstock. Estimate by Kemausuor et al [122] place bioenergy potential from wood residues at 4.8 PJ which can replace portions of local cooking fuel (firewood and charcoal) in Ghana.

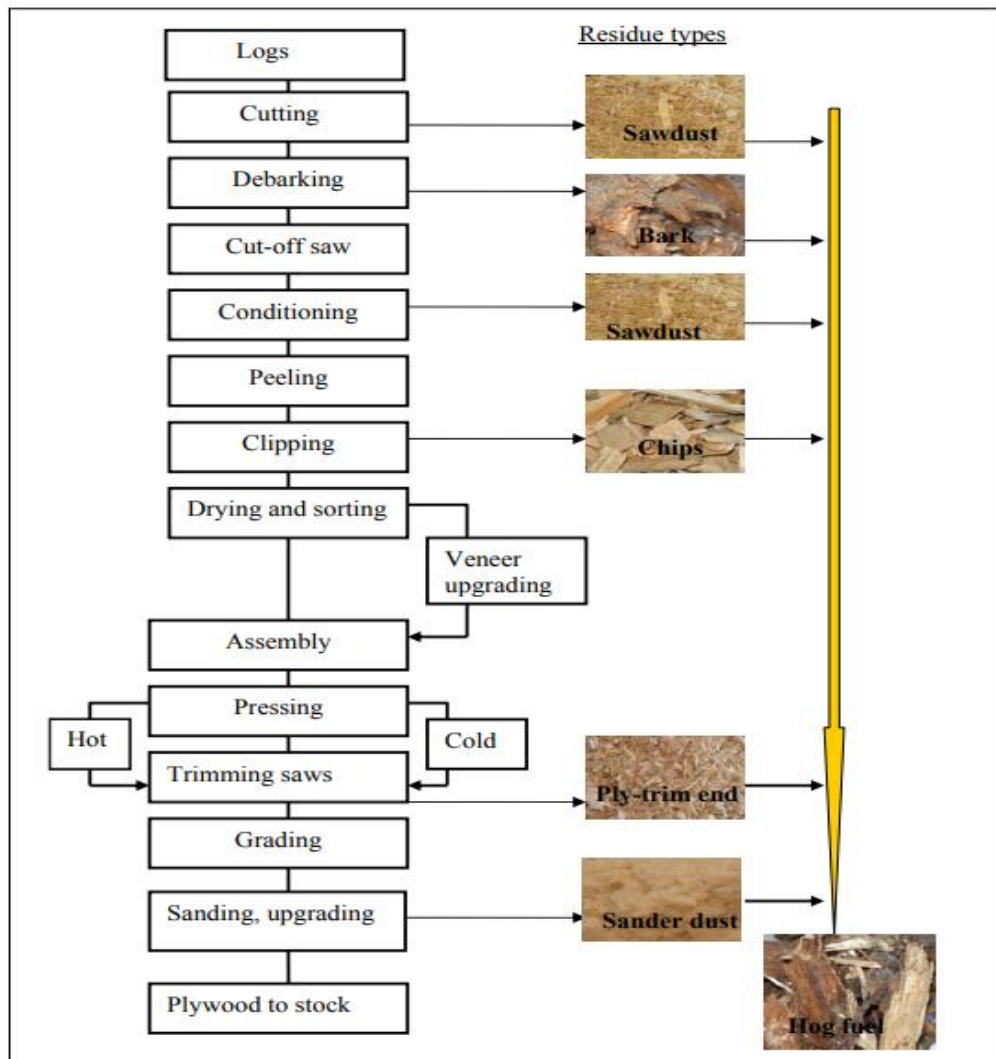


Figure 2.8: Forest residues from the production of plywood [127].

#### 2.5.4 Animal waste

Animals produce a lot of waste, which is generally referred to as "livestock manure." Animal waste such as dung and slaughter waste can be used as a source

of energy and as feedstock for biogas generation. Anaerobic digestion of livestock manure improves sanitation by reducing the pathogenic content of substrate materials [122]. The process also benefits farmers as it provides an opportunity for secondary income generation through the production and sale of biogas for cooking and electricity [6]. Livestock production generates a considerable amount of animal manure, however the quantity of manure produced depends on the type of animal, the amount of fodder eaten, the quality of the fodder, the physiological state (lactating, growing, etc.) and the body weight of the animal [53]. Estimates of the potential quantities of livestock manure resources are calculated using number of livestock, average annual manure production per livestock, and dry manure fraction [122][128]. Data on livestock production was obtained from the Food and Agriculture Organization of the United Nations [129]. The most popular livestock types in Ghana, in terms of numbers are cattle, sheep, goats, pigs and chicken [122]. Table 2.3 shows that chickens produce the smallest quantity of waste per animal, however large quantities of manure can be expected from large production quantities. Cattle by virtue of their big body sizes, produce the highest quantity of waste per animal as well as the highest total energy potential. Livestock production alone could generate a total energy potential of 76.72 PJ per year based on 2020 production data. While the calculated energy potential in this research is greater than the estimated theoretical potential of 47.59 PJ revealed by Mohammed et al. [6], the discrepancy is attributable to a time lag in the analysis. Similar to crop residues, not all produced manure can be practically available for collection and use. Cattle are mostly allowed to graze in open fields thereby making the manure produced during grazing periods uncollectible. Cattle are also used as draught

animals for agricultural operations and their manure cannot be collected [122]. Hence, on the basis of assumption that half of the manure generated by livestock is not recoverable, there is still a technical energy potential of about 38.36 PJ. For the purposes of modern energy generation, this is a huge potential that can be exploited in biogas generation through anaerobic digestion. It is promulgated that in India, four to five cattle is enough to feed a 2 m<sup>3</sup> household biogas plant [122], hence a small to medium family sized livestock farm would be enough to produce biogas for a household in Ghana.

Table 2.3: Total manure output and energy potential of available livestock manure

Livestock type	Production stocks (1000 head) <sup>a</sup>	Dry dung output (Kg h <sup>-1</sup> d <sup>-1</sup> ) <sup>b</sup>	Total dung output (tonnes)	Energy value (GJ t <sup>-1</sup> ) <sup>c</sup>	Total energy potential (PJ)
Cattle	1922	1.80	1262754	18.5	23.36
Chickens	95455	0.06	2090464.5	11.0	23.00
Goats	8203	0.40	1197638	14.0	16.77
Pigs	759	0.80	221628	11.0	2.44
Sheep	5458	0.40	796868	14.0	11.16
Total					76.72

<sup>a</sup> Production stocks [129]    <sup>b</sup> Dry dung output [6]    <sup>c</sup> Energy value [6]

## **2.6 Concluding Remarks**

This chapter reviewed types of biomass materials and their conversion technologies. Due to the paucity of data on Ghana's biomass resource base and feedstock distribution, it was necessary to estimate the quantity of biomass resources available for energy generation in the country. The estimation was limited to crop residues and livestock manure and based on annual production data, residue to product ratios, and a lower heating value. The crop residues considered in this study have an estimated energy potential of 728.43 PJ while the livestock manure have an estimated energy potential of 76.72 PJ. When conversion efficiency and other practical challenges and technological limits are taken into account, not all of this potential will be accessible as usable energy. On assumption that a 50% recoverable percentage is achievable, there is a technical energy potential of 364 PJ and 38.36 PJ from crop residues and livestock manure respectively. Bioenergy generation from this potential source of energy, particularly in rural areas, is crucial due to the socioeconomic benefits such as energy service provision, job creation, and poverty eradication that comes with it.

There are several biomass conversion methods that may be used to harness the country's vast bioenergy potential. However, it is the type and characteristics of the biomass feedstock together with the end-use application that determines the choice of the conversion technology. In addition to their primary end products, some conversion methods like fermentation and pyrolysis provide solid residues that may be used to generate power. Generally, an integration of biomass conversion technologies is more beneficial as it enables simultaneous production of power and other energy carriers. Nevertheless, evidence from literature shows

that gasification has the best potential to expand electricity access rate for the rural populace. Unlike other conversion processes, gasification has different feedstock requirements and transforms the full carbon content of feedstock, resulting in a higher calorific value output with improved energy capture.

Cocoa is a strategic economic crop in Ghana, and hence cocoa pod husk was identified as a potential biomass resource that could be exploited for power generation in off-grid, remote, and isolated rural communities through gasification. Research on CPH as an energy resource for power generation in Ghana is limited. The very few studies that consider CPH for its power generation potential do not give any attention to how different types of CPH vary in thermochemical properties and energy potential. The effect of feedstock location, climate, and soil conditions on thermochemical properties as well as the energy potential of CPH have also not been critically examined. Additionally, there is hardly any research in Ghana that evaluates the performance of CPH gasification systems. Hence, in order to provide further justification in support of CPH being used in energy production, the next chapter evaluates the power production potential through material characterization processes of different varieties of CPH available in Ghana.

## CHAPTER THREE

### 3.0 CHARACTERIZATION OF COCOA POD HUSKS

#### 3.1 Introduction

Biomass materials have significant differences in physical and chemical properties such as moisture content, fixed carbon, ash content, volatiles, energy density and chemical composition. Biomass feedstocks may have high moisture content like animal waste, or low moisture content like wheat straw [130]. It is the differences in biomass composition and the form in which the energy is required that determines the type of conversion technology to be used [131]. Characterization of biomass could help establish the thermo-physical properties, which are useful in the prediction of energy density and environmental impacts associated with energy conversion processes [132].

#### 3.2 Materials and Methods

##### *3.2.1 Material Selection and Classification*

As of 2018, the majority of Ghana's cocoa production was concentrated in six administrative regions: Volta, Eastern, Ashanti, Brong-Ahafo, Western, and Central. Ghana grows four (4) distinct cocoa types, namely Amelonado, Amazonia, Trinitario, and Hybrid.

All four CPH varieties were taken from Ghana's six cocoa growing regions. A total of twenty-four (24) CPH samples were obtained and coded with letters and numbers for easy analysis as presented in Figure 3.1. The regions were designated with letters A to F whiles CPH types were designated with numbers

1 to 4. For example, Amelonado from Volta region was designated as A1 while Amelonado from Ashanti region was designated as E1.

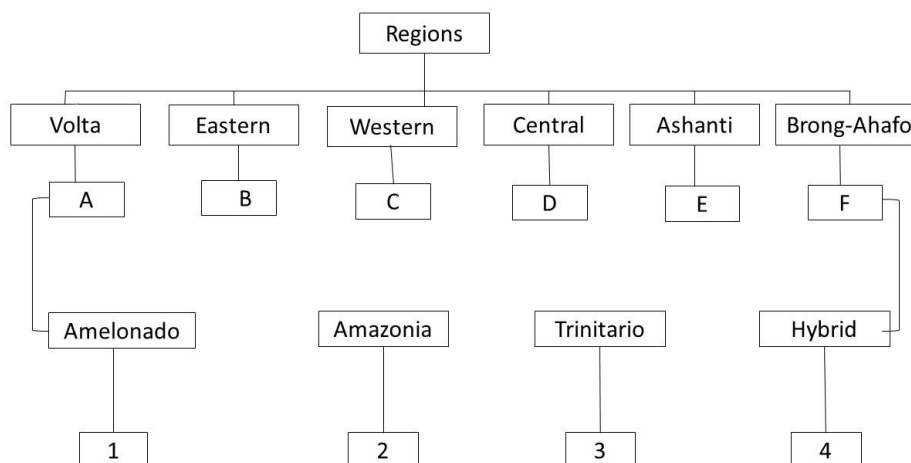


Figure 3.1: Regional designation of CPH samples

### 3.2.2 Material Preparation

#### 3.2.2.1 Drying

Drying is a critical step in the production of a wide variety of final goods, including chemicals and energy carriers. It reduces the moisture content of biomass, thereby resulting in a net lower energy density by mass. This reduces processing costs as well as storage and transportation expenses. There is a clear and significant link between the degree of dryness of biomass fuel and its calorific value. High amount of water in biomass fuel can reduce combustion temperature below optimum and reduce overall system efficiency. Most biomass gasifiers are designed to run on feedstock with a low moisture content of 10 to 20% [133]. Hence, the CPH samples were sun-dried for approximately 1-2 weeks to reduce the moisture level to below 20%. During the drying process, the CPH were constantly mixed and turned to ensure uniform drying. The moisture

content of the drying CPH were measured intermittently with a hand-held moisture meter. Drying was stopped as soon as moisture content was measured to be less than 20%.

### **3.2.2.2 Crushing and Grinding**

Biomass crushing is a necessary first step in both the consumption and conversion of biomass energy [134]. CPH samples were broken down into smaller chips with a hammer. This was done to reduce the size of the CPH material before the grinding stage.

The Retsch Planetary Ball Mill PM 100 (Figure 3.2) was used to mill the crushed CPH samples at 350 rpm for 3 min and sieved with a Retsch Electromagnetic Shaker AS 200 (Figure 3.3) for 5 minutes to obtain a homogeneous particle size distribution of 212  $\mu\text{m}$ . The aforementioned procedure was repeated until the whole sample was reduced to a particle size less than 212  $\mu\text{m}$ . During thermal conversion, particle size distribution plays a significant role in the thermal degradation behaviour of biomass. Heterogeneous sample sizes can cause variations and errors in the fuel characterization results [135], [136], [137]. Hence, to ensure effective combustion behaviour and enhance energy efficiency, a homogeneous particle size distribution with grain size controlled below 212  $\mu\text{m}$  was considered desirable.

The AS 200 uses vibratory sieving, in which the sample material is propelled upward by the vibrating sieve bottom and then falls back down onto the sieve mesh fabric owing to gravitational forces. As a result, the sample material undergoes a three-dimensional movement in which a horizontal circular motion superimposes atop a vertical tossing action. As a result, the sample material is

distributed equally throughout the whole surface of the sieve bottom, while the particles are accelerated upward. During this procedure, they execute free rotations and are properly oriented while falling back down. An electromagnetic motor moves a spring-mass system and sends vibrations to the sieve stack in the Retsch Electromagnetic Shaker.



Figure 3.2: Retsch Planetary Ball Mill PM 100



Figure 3.3: Retsch Electromagnetic Shaker AS 200 with sieve mesh on the side

The processed samples were stored in airtight plastic sample bottles and labelled (Figure 3.4) to perform corresponding fuel characterisation experiments.



Figure 3.4: Milled CPH packaged in sample bottles and labelled.

### ***3.2.3 Characterisation Methods***

#### **3.2.3.1 Proximate analysis**

Proximate analysis is a method for determining product distribution when samples are heated under prescribed circumstances. Proximate analysis is critical for biomass energy usage as it helps to determine the percentage of material that burns in a gaseous form (volatile matter), in a solid state (fixed carbon), and the percentage of inorganic waste material (ash) [138]. It is used to show the ratio of combustible to incombustible constituents in a biomass sample and also covers the determination of moisture. Standards for proximate analysis have traditionally been developed by a number of organisations, including the International Organization for Standardization (ISO), the American Society for Testing and Materials (ASTM), the German Institute for Standardization (DIN),

and the British Standards Institution (BSI). Even though there are a variety of standards for proximate analysis, the measuring concept and process seem to be very comparable [139].

Generally, the several proximate analytical determinations entail heating the sample to a constant weight under circumstances prescribed by ASTM. However, these assessments are time-consuming and require a substantial quantity of laboratory equipment. Thermogravimetric analysis (TGA) is an alternative technique for proximate analysis. Although this thermal analysis approach similarly involves heating the sample to a consistent weight under specific circumstances, the smaller sample sizes and controlled temperature and atmosphere significantly minimise the analysis time and equipment required for proximate analysis [140].

In this research, the thermal degradation behaviour of CPH was studied under inert and oxidative atmospheres using thermogravimetric analyzer, TGA Q500 with circular platinum crucibles measuring 2 mm in height and 5 mm in diameter. Figure 3.5 is a set-up of the thermogravimetric analyzer.

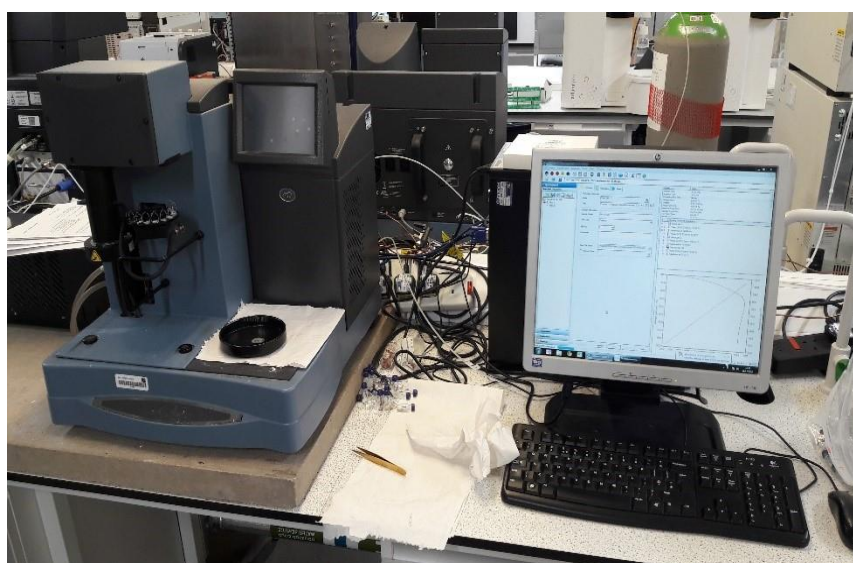


Figure 3.5: Thermogravimetric analyser – TGA Q500 set-up

The TG approach has been described by Saldarriaga et al [141] and El may et al [142]. The proximate TG method used in this thesis involved heating the sample ( $10 \pm 0.5$  mg) in a nitrogen atmosphere at a constant flow rate of 50 ml/min from room temperature to 110 °C at a heating rate of 10 °C/min and a hold-up time of 10 minutes to obtain the weight loss associated with moisture. The sample was heated further to 900 °C at a rate of 20 °C/min and a hold-up time of 20 minutes to obtain the weight loss associated with volatiles release. The nitrogen gas was then substituted with air, with the temperature and flow rate being the same for 20 minutes to ensure the oxidation of the char formed and a complete stabilisation of the sample. The weight loss associated with this step is the fixed carbon. The remaining material after oxidation is the ash. At the start of each experiment, 20 minutes of N<sub>2</sub> purging was conducted. To ensure repeatability, the proximate analysis experiments were conducted at least twice. A third sample was used if results differed by more than 5%. Experiments were performed based on ASTM standards (ASTM E871-82 for moisture, ASTM E1755-01 for ash, and ASTM E872-82 for volatile matter). Figure 3.6 shows a typical weight loss and heating rate profile with corresponding fractions considered in the proximate analysis of the samples.

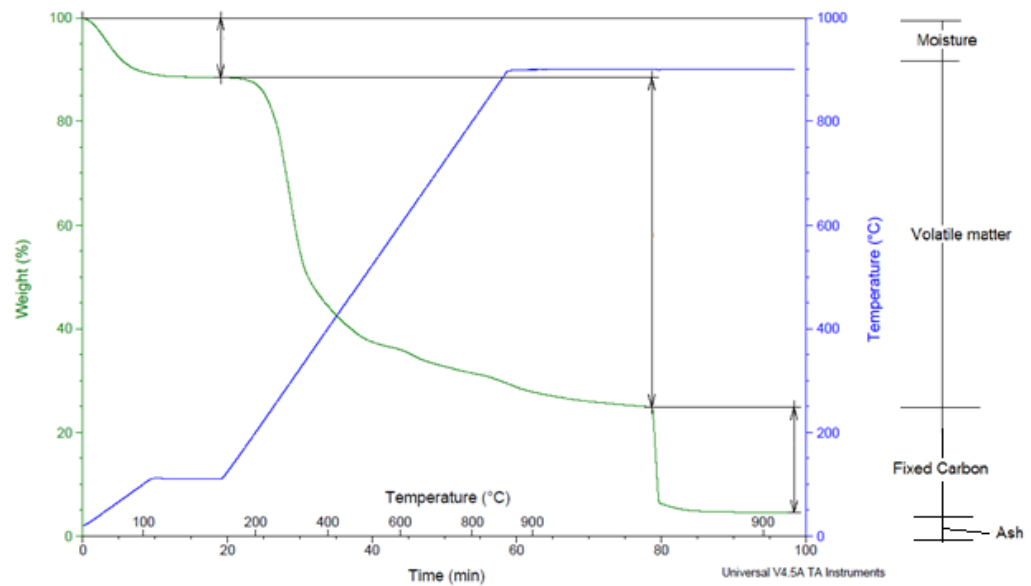


Figure 3.6: Typical weight loss and heating profile of a TG proximate analysis technique.

### 3.2.3.2 Ultimate analysis

Ultimate analysis is conducted to determine the composition of biomass in terms of percentages of carbon, hydrogen, nitrogen, oxygen, and sulphur in elemental form. It is useful during mass balance calculations for chemical and thermal processes. Additionally, the information obtained from the ultimate analysis may be used to assess the efficiencies and emission potentials of solid fuel materials. The information provided by ultimate analysis can also help to calculate efficiencies and emission potential for solid fuel materials [143].

Based on the Standard UNE EN 5104, the ultimate analysis of the CPH samples was carried out using Thermo flash equipment (Leco, CHN-628) and the sulphur add-on module (CHN-628S). Figure 3.7 shows the analytical tools used for the ultimate analysis.

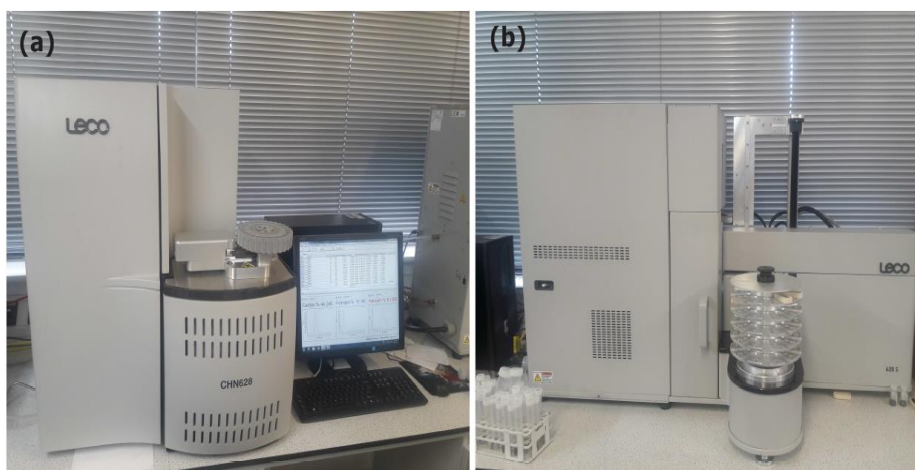


Figure 3.7: (a) Leco, CHN-628 analyser and (b) Leco sulphur add-on module CHN-628S

The Leco CHN-628 is a combustion elemental carbon, hydrogen, and nitrogen instrument that use only pure oxygen in the furnace to ensure full combustion and better elemental recovery. A system for the collection and management of combustion gases reduces the total cost per analysis and increases the lifespan of reagents. A carrier gas sweeps the combustion gas to separate infrared cells intended for the detection of H<sub>2</sub>O and CO<sub>2</sub>, and a thermal conductivity cell is used for the detection of nitrogen. Oxygen content is determined by difference. The sulphur add-on module 628S is intended particularly for determining the sulphur content of a broad range of organic materials.

An analysis starts when a sample is loaded into a combustion boat and put in a furnace containing generally 1350 °C-regulated pure oxygen. Sulphur in the sample evolves into SO<sub>2</sub> and escapes the sample. First, the sample gases from the furnace are swept through the boat stop to the rear of the inner combustion tube, then forward between the inner and outer combustion tubes. This permits the sample gases to stay in the high-temperature zone for a longer period of time, allowing for effective oxidation. From the combustion system, gases go via an

anhydrous tube to eliminate moisture, followed by a flow controller that regulates the flow of sample gases through the sulphur infrared detection cell inside the 628 Series instrument. While the 628 Series instrument and sulphur add-on module are capable of loading, analyzing, and operating independently of one another, the module needs the 628 Series instrument system's detecting capabilities and PC in order to conduct the analysis.

### **3.2.3.3 Heating values**

The higher heating values (HHV) of the CPH samples were determined using available formulae from literature. A correlation developed by Parikh, Channiwala, and Ghosal [144] in equation 3.1 with an average absolute error of 3.74% after considering the entire spectrum of solid carbonaceous materials such as coals, lignite, all types of biomass material, and char to residue-derived fuels was used to calculate higher heating values based on the proximate analysis (PA). The accuracy of the proposed correlation has been previously analysed by researchers such as Saldarriaga et al. [141] and Jarunghammachote and Dutta [145].

$$\text{HHV (MJ/kg)} = 0.3536 \text{ FC} + 0.1559 \text{ VM} - 0.0078 \text{ Ash} \quad 3.1$$

Where FC, VM and Ash are fixed carbon, volatile matter and ash content obtained from the proximate analysis on dry basis respectively (ASH + VM + FC = 100%).

Many authors have proposed a correlation for calculating higher heating values based on elemental analysis. However, the correlation by Channiwala and Parikh [146] in equation 3.2 is more pronounced because the weighing coefficients have

been analysed for fuels with a wide range of elemental composition and offer an average absolute error of 1.45%, thereby establishing their versatility and validity [19], [147].

$$\text{HHV (MJ/kg)} = 0.3491\text{C} + 1.1783\text{H} + 0.105\text{S} - 0.1034\text{O} - 0.0151\text{N} - 0.0211\text{Ash} \quad 3.2$$

Where C, H, S, O, N, and Ash are percentages of carbon, hydrogen, sulphur, oxygen, nitrogen, and ash as determined by ultimate analysis on a dry basis.

### 3.3 Results and Analysis

#### 3.3.1 Proximate Analysis

Table 3.1 shows the moisture, volatile matter, fixed carbon, and ash contents of the CPH samples as determined by the proximate analysis. Each of the properties of CPH plays a crucial role in determining its energy potential. They also help to predict potential technical challenges that may be encountered during biomass energy conversion.

Table 3.1: Proximate analysis (wt %) and HHV (MJ/kg) of CPH samples from Ghana

Sample	Type	Moisture (%)	Ash (%)	VM (%)	FC (%)	HHV <sup>a</sup> (MJ/kg)
A1	Amelonado	10.35	14	65.24	20.76	17.40
A2	Amazonia	7.64	11.98	60.45	19.93	16.38

---

A3	Trinitario	10.12	9.17	60.57	20.14	16.49
A4	Hybrid	9.75	13.94	69.05	17.01	16.67
B1	Amelonado	9.43	9.45	68.96	21.59	18.31
B2	Amazonia	5.57	11.41	62.04	20.98	17.00
B3	Trinitario	13.21	13.57	53.75	19.48	15.16
B4	Hybrid	10.06	12.43	64.48	23.09	18.12
C1	Amelonado	7.81	11.84	70.56	17.60	17.13
C2	Amazonia	6.56	9.80	60.78	22.86	17.48
C3	Trinitario	5.90	9.81	62.51	21.80	17.38
C4	Hybrid	8.81	11.24	69.23	19.53	17.61
D1	Amelonado	8.65	10.09	66.39	23.52	18.59
D2	Amazonia	6.14	10.34	61.92	21.61	17.21
D3	Trinitario	9.64	9.92	59.44	21.02	16.62
D4	Hybrid	9.2	14	66.18	19.82	17.22
E1	Amelonado	7.62	7.87	67.3	24.83	19.21
E2	Amazonia	5.82	9.54	62.34	22.30	17.53
E3	Trinitario	4.98	11.35	63.37	20.30	16.97
E4	Hybrid	8.51	9.98	68.65	21.37	18.18
F1	Amelonado	7.76	12.1	69.96	17.94	17.16

---

F2	Amazonia	4.63	10.80	63.48	21.08	17.27
F3	Trinitario	8.59	8.28	62.81	20.32	16.91
F4	Hybrid	6.67	11.29	72.44	16.27	16.96

<sup>a</sup> By calculation based on equation 3.1

### 3.3.1.1 Moisture Content

Moisture content is critical in choosing a biomass conversion technology as it can affect the amount of energy that can be generated from a feedstock. Feedstock with lower moisture contents are preferred for thermochemical conversion whereas higher moisture feedstock are great for biochemical conversion. Water serves as a binder and a lubricant thereby facilitating pre-treatment processes such as densification [136]. However, during thermochemical conversion, heat is required to reduce the moisture content of high moisture feedstock which inversely affects the overall energy output and solid fuel performance [131]. Moisture content affects biomass handling costs and conversion efficiency. Biomass is usually transported from one location (the production site) to another, where it is processed into energy, and the higher the weight of the biomass, the higher the cost of its transport [148]. The moisture content is relevant not only for the calorific value but also for the storage conditions, the combustion temperature and the amount of exhaust gas emission [93]. Moisture content of biomass can vary widely depending on the time of harvesting, the geographic location, type and duration of the storage and the potential contamination of the harvested biomass by soil and other debris [149]. Biomass harvested in autumn for instance, may contain significant amounts of

moisture compared to biomass harvested in winter, which decreases to about 20% mass [148]. The moisture content of a feedstock has implications for how much of the energy embodied in biomass can be converted to useful work. Feedstock with higher moisture content are very difficult to ignite and they also produce gas of poor quality and yield [150]. The moisture contents of the CPH samples were between 4.63 wt% and 13.21 wt%, thereby making them suitable for thermochemical conversion processes such as gasification.

Apart from Amelonado and Trinitario from the Volta region and Hybrid and Trinitario from the Eastern region that recorded high moisture contents of more than 10%, the moisture content of all other CPH samples was less than 10% (see Figure 3.8).

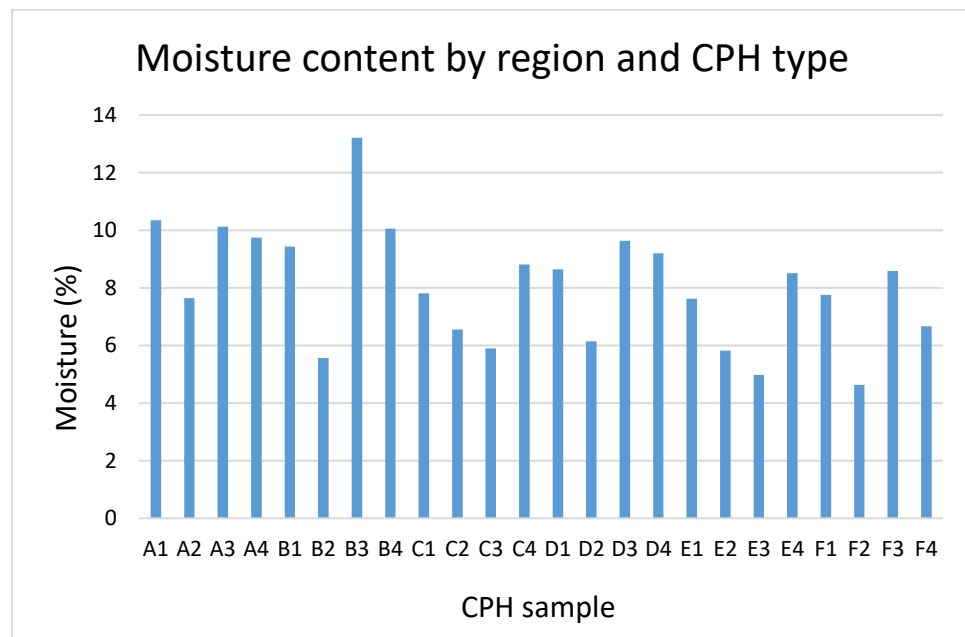


Figure 3.8: Variation in moisture content of CPH samples

The moisture contents of the CPH samples measured were generally within a range that was comparable to previously reported moisture values for

CPH. Although studies such as [136] and [147] put the moisture content of CPH over 10 wt.%, 83% of the samples tested in the current study recorded moisture contents of less than 10 wt.%. This means that the moisture content of the CPH samples tested were comparatively lower than reported values. There were also differences in moisture contents of the CPH samples across the different regions which can be attributed to the variations in soil composition, cultivation methods, and climatic and storage conditions.

The Hybrid and Trinitario varieties of the CPH samples had higher moisture content than Amelonado and Amazonia. However, the total moisture content of Amazonia was significantly low in comparison with the other three varieties.

Figure 3.9 shows the differences in moisture content based on CPH type.

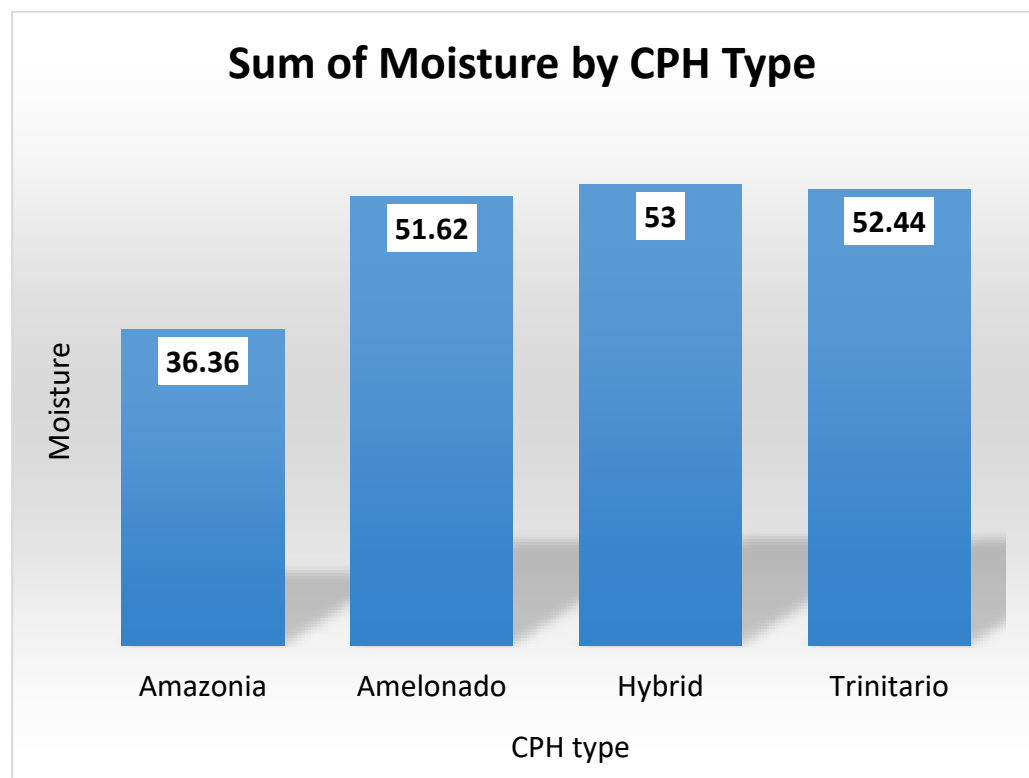


Figure 3.9: Differences in moisture content by CPH type

Although the moisture content of all four varieties were reasonably low and hence suitable for thermochemical conversion, Amazonia would be much preferred because it may reduce the process energy demand and cost while facilitating conversion efficiency.

Out of the six cocoa growing regions in Ghana, the CPH samples from Eastern and Volta regions had the highest moisture content while CPH from Ashanti region had the lowest moisture content. Figure 3.10 displays regional variation of total moisture content among the CPH samples.

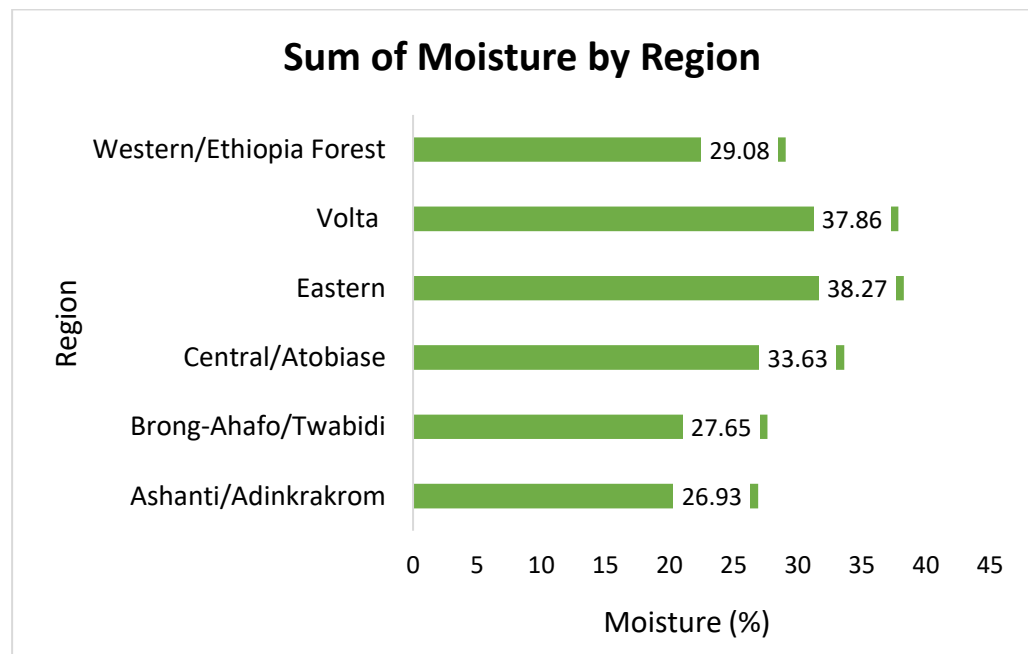


Figure 3.10: Moisture content of CPH based on regions

CPH from Ashanti region is therefore preferable for thermochemical conversion as low moisture content increases energy efficiency during combustion. High moisture impacts negatively on calorific value, hence it can be expected that the calorific values of CPH from Eastern and Volta may be relatively low.

### **3.3.1.2 Ash Contents**

Ash is the mineral and inorganic matter in biomass that is obtained after complete combustion [93]. The percentage composition of ash in biomass can vary depending on the type of biomass. Wood for example has 0.5% ash, agricultural crop residues have 5-10% ash and rice husk has 30-40% ash [151]. Higher ash content in biomass is usually the result of higher levels of inorganic compounds, which can inherently act as catalytic effect on the thermal conversion technique. On the contrary, high-ash content affects combustion characteristics and reactor design by causing slagging, fouling and blocking problems in the reactor. Ash content also affects both the handling and processing costs of the biomass as well as reduces the higher heating value [19].

The ash contents of CPH samples measured from 7.87% to 14% which is in line with other studies such as [17], [19], [136], [147]. The Amelonado species from the Ashanti region had the lowest ash content, while hybrids from the Central region and amelonado from the Volta region had the highest. Figure 3.11 depicts a comparison of CPH types across several geographies.

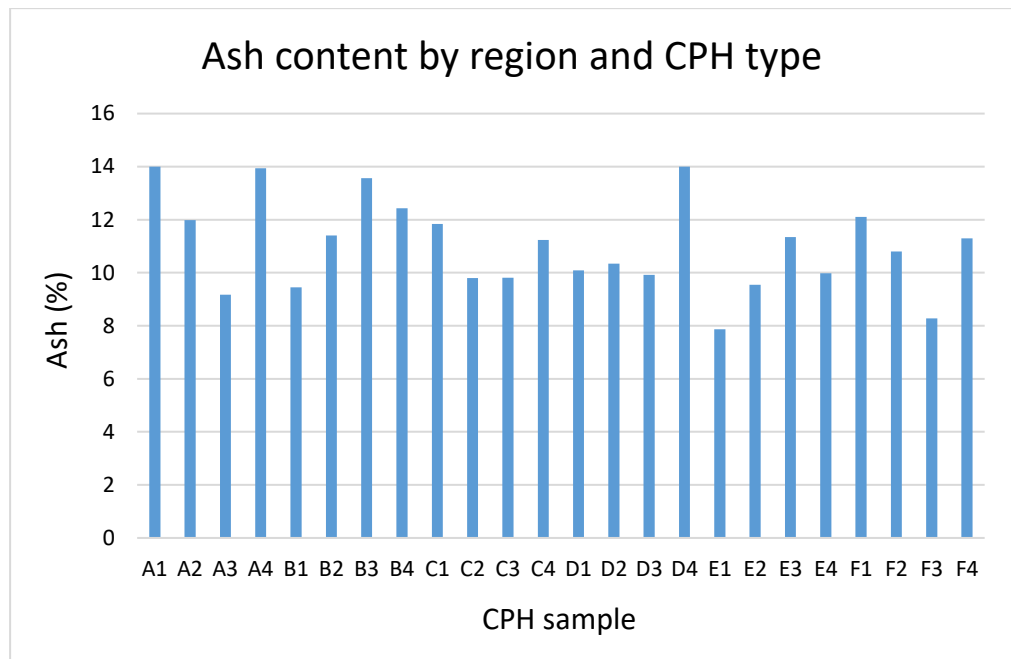


Figure 3.11: Ash content of CPH types in the various regions

Ash contents less than 10% can be classified as low whereas those less than 25% can be classified as medium. Hence, the CPH samples under investigation can generally be classed as medium ash-content feedstock.

Comparatively, the hybrid species had higher ash content than the other three varieties and could be due to the type of soil in which the hybrid species were grown. Trinitario, on the other hand, had the lowest ash content of them all. Figure 3.12 shows the variation in ash content between the four types of CPH analysed.

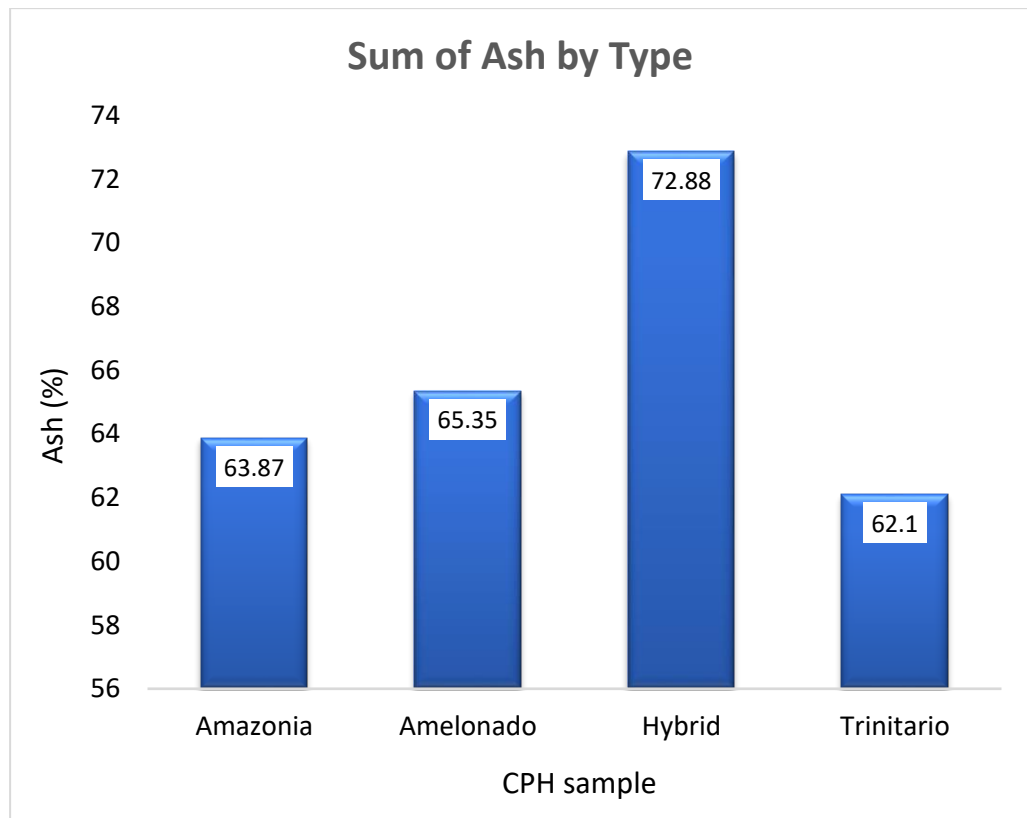


Figure 3.12: Ash content of CPH sample types

High ash content reduces calorific value of a biomass feedstock and causes complications during combustion. The hybrid varieties may therefore benefit from pre-treatment to minimise the ash content before energy conversion.

While CPH from the Volta and Eastern region had the greatest ash concentration, CPH from the Ashanti region had the lowest. Figure 3.13 depicts region-specific ash content of CPH. CPH samples from Ashanti region would therefore be preferred for energy conversion.

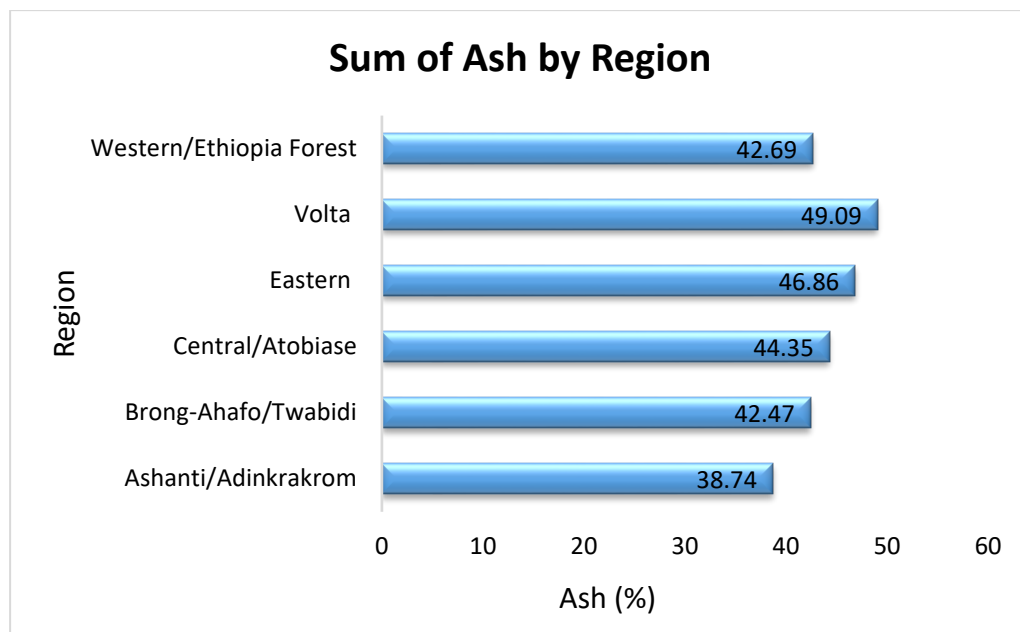


Figure 3.13: Ash concentration of CPH based on region

### 3.3.1.3 Volatile Matter

Many biomass materials generally have high content of volatile matter. It is this biomass property that enhances ignition, flame stability, reactivity and improves carbon burnout [152]. During thermochemical conversion processes such as gasification, feedstock with high volatile matter tend to increase tar formation which can cause clinkering and feed blockages in the reactor. Hence, volatile matter is a determining factor in the design of a gasifier to ensure effective tar removal [153].

The volatile matter concentration of the CPH samples measured between 53.75% and 72.44%, which is consistent with what has been written in sources such as [19], [147], [154]. Figure 3.14 compares the volatile matter content of various sample types from different geographic locations. The highest volatile matter was recorded by Hybrid from Brong-Ahafo region while the lowest was recorded by Trinitario from Eastern region.

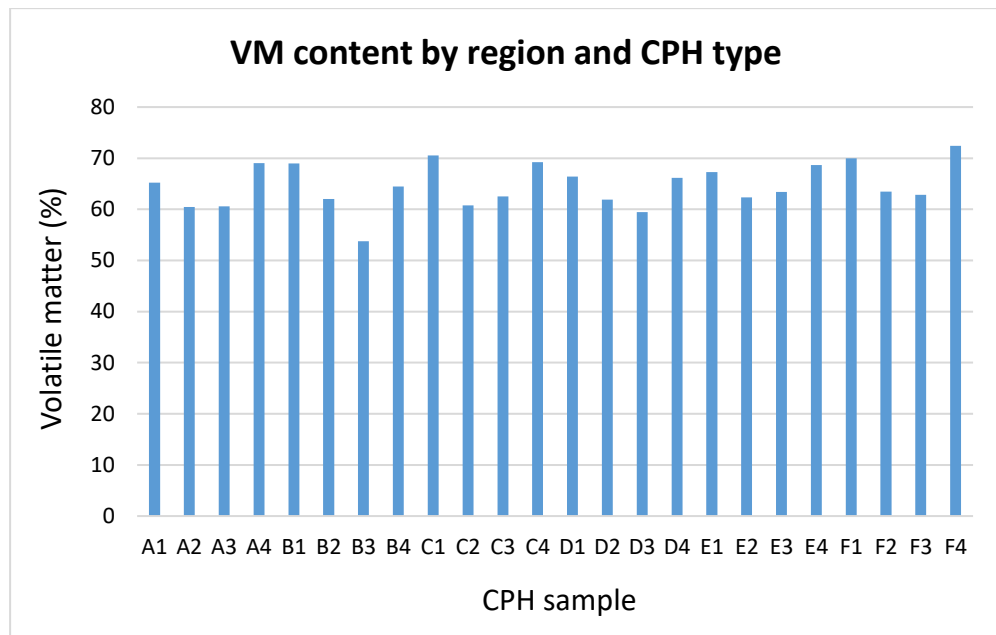


Figure 3.14: Volatile matter content of CPH types in various regions

The higher the volatile matter in biomass feedstock, the faster the ignition potential [136]. The Hybrid species had the highest volatile matter, followed by Amelonado, Amazonia, and Trinitario in descending order.

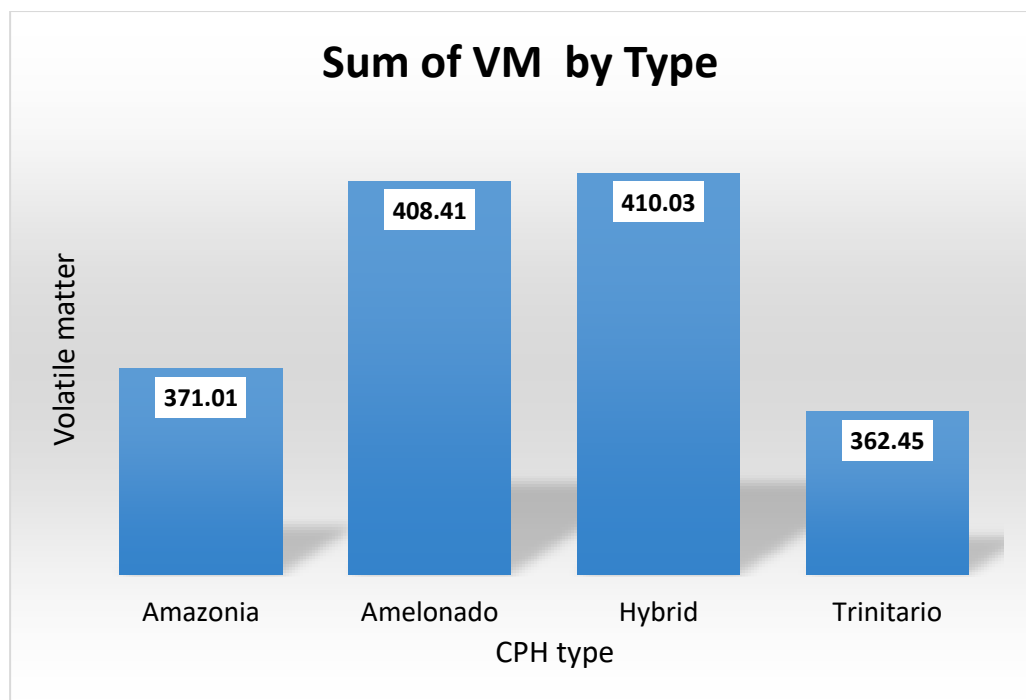


Figure 3.15: Variation in volatile matter of CPH types

The Hybrid CPH is more likely to have the fastest ignition potential due to its high volatile matter.

Figure 3.16 shows the volatile matter content of CPH from the six regions. CPH samples from Brong-Ahafo region had the highest volatile matter whereas CPH from Eastern region had the lowest volatile matter. This implies that CPH from Brong-Ahafo region will be easier to ignite, sustain flame better and maintain a low carbon loss due to better combustion efficiency.

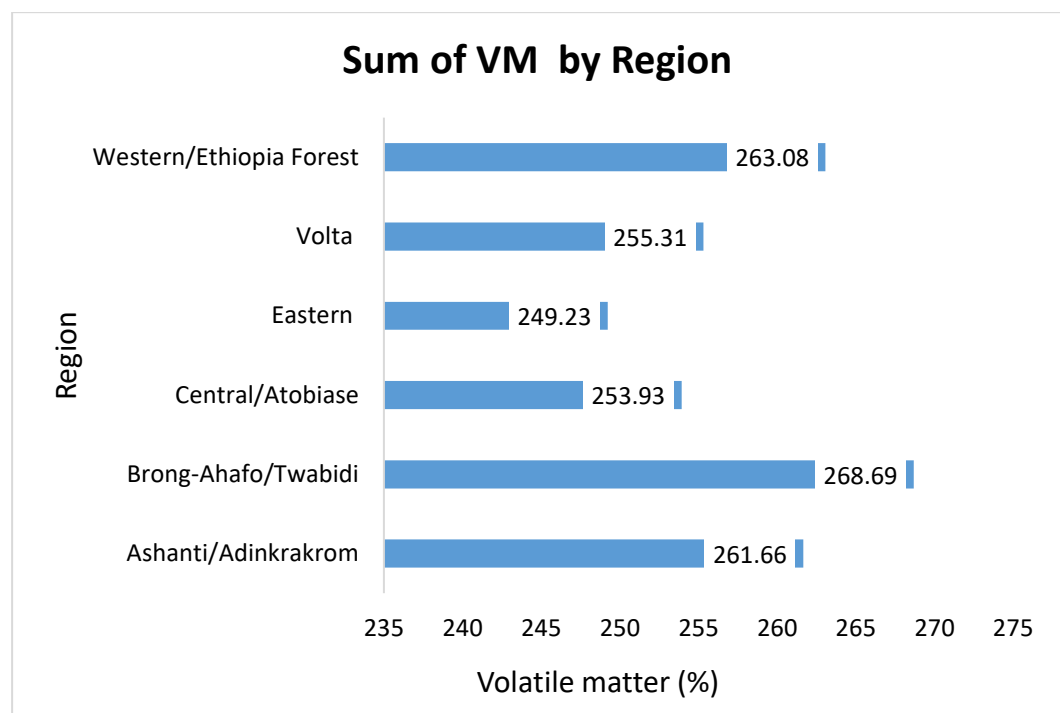


Figure 3.16: Region-specific volatile matter content of CPH

### 3.3.1.4 Fixed Carbon

Fixed carbon content is without doubt the most essential parameter that directly reflects the energy potential of any biomass feedstock; thus feedstocks with higher fixed carbon content possess inherent higher heating values [19]. The fixed carbon content of the CPH samples was between 16.27% and 24.83%.

Figure 3.17 shows the individual CPH types and their fixed carbon content across the various regions.

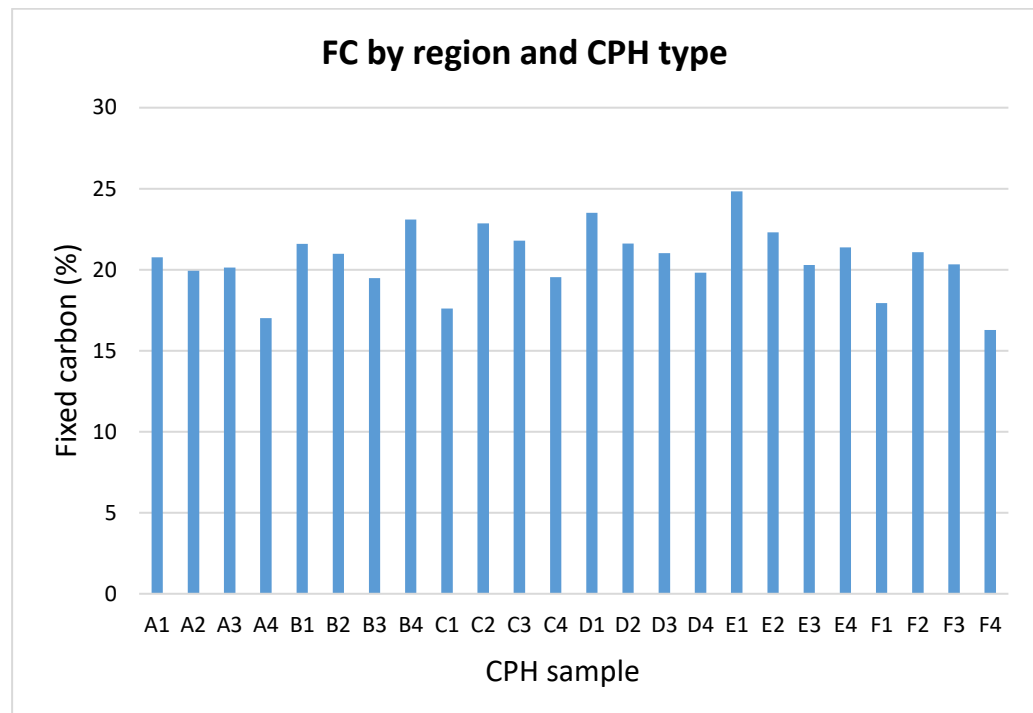


Figure 3.17: Fixed carbon content of CPH types in the various regions

The highest fixed carbon content was recorded by Amelonado species from Ashanti region (24.83%) and the lowest was recorded by Hybrid from Brong-Ahafo region (16.27%). The higher the fixed carbon content of a biomass feedstock, the higher the calorific value. This is consistent with Table 3.1 as the sample that recorded the highest fixed carbon content (Amelonado from Ashanti region) also recorded the highest heating value (19.21 MJ/Kg).

When it came to CPH varieties, Amazonia had the greatest fixed carbon concentration, whereas Hybrid had the lowest. Figure 3.18 compares the fixed carbon content of the four varieties of CPH.

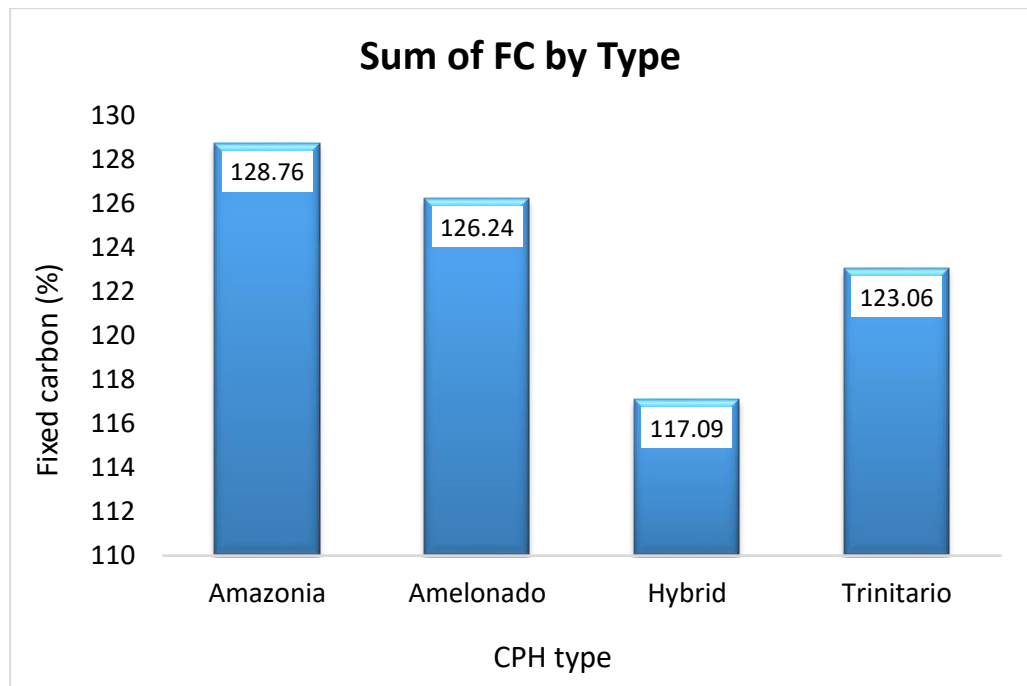


Figure 3.18: Fixed carbon content of CPH types

Ashanti region appeared to be the region with the highest fixed carbon whereas Brong-Ahafo region had the lowest. Figure 3.19 compares the fixed carbon content of CPH among the six regions.

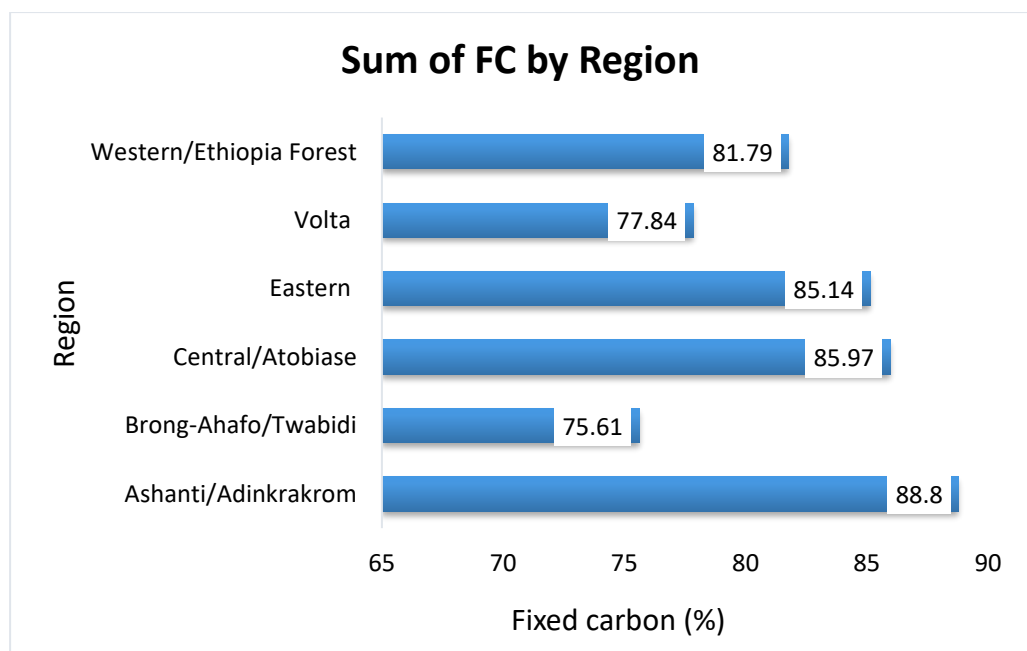


Figure 3.19: Region-specific fixed carbon content of CPH

An increase in fixed carbon causes an increase in higher heating value, hence it is expected that samples from Ashanti region may have the highest heating value.

### 3.3.2 Ultimate Analysis

In Table 3.2, the basic elemental composition of the CPH samples and their respective heating values together with the molar H/C and O/C ratios are given. The higher heating values of CPH based on the wt% of the main elements ranges from 14.44 MJ/Kg to 16.82 MJ/Kg. Although the heating values calculated by the ultimate equation were lower than their corresponding values calculated by the proximate equation, they were also similar to reported values in literature such as [19], [147]. The increased oxygen content of the CPH might have contributed to the downward trend in computed heating values.

Table 3.2: Ultimate analysis, wt % (dry basis) and HHV (MJ/kg) of CPH samples from Ghana

Sample	Type	C (%)	H (%)	N (%)	S (%)	O <sup>c</sup> (%)	HHV <sup>b</sup> (MJ/kg)	H/C <sup>a</sup>	O/C <sup>a</sup>
A1	Amelonado	41.53	5.81	0.92	0.13	51.61	15.71	0.14	1.24
A2	Amazonia	42.32	5.37	1.28	0.16	51.03	15.57	0.13	1.21
A3	Trinitario	42.87	5.55	1.31	0.16	50.27	16.11	0.13	1.17
A4	Hybrid	40.38	5.89	1.02	0.24	52.47	15.32	0.15	1.30
B1	Amelonado	39.82	6.11	1.27	0.16	52.63	15.46	0.15	1.32
B2	Amazonia	42.43	5.06	1.74	0.16	50.77	15.27	0.12	1.20

---

B3	Trinitario	39.9	5.28	2.63	0.16	52.19	14.44	0.13	1.31
B4	Hybrid	41.5	5.86	0.84	0.29	51.81	15.78	0.14	1.25
C1	Amelonado	40.47	5.87	1.63	0.31	51.72	15.46	0.15	1.28
C2	Amazonia	42.8	5.34	1.04	0.16	50.82	15.77	0.12	1.19
C3	Trinitario	41.66	5.87	2.41	0.16	50.06	16.06	0.14	1.20
C4	Hybrid	42.33	5.98	1.63	0.13	49.94	16.41	0.14	1.18
D1	Amelonado	42.78	5.83	1.31	0.14	49.94	16.42	0.14	1.17
D2	Amazonia	43.48	5.08	1.35	0.16	50.09	15.76	0.12	1.15
D3	Trinitario	43.06	5.47	2.14	0.16	49.33	16.15	0.13	1.15
D4	Hybrid	41.47	5.78	1.14	0.16	51.45	15.67	0.14	1.24
E1	Amelonado	43.81	5.79	0.77	0.12	49.52	16.82	0.13	1.13
E2	Amazonia	42.37	5.73	1.33	0.16	50.57	16.11	0.14	1.19
E3	Trinitario	41.18	5.35	1.68	0.16	51.79	15.08	0.13	1.26
E4	Hybrid	42.32	5.76	1.42	0.08	50.43	16.12	0.14	1.19
F1	Amelonado	41.22	5.73	1.13	0.08	51.85	15.51	0.14	1.26
F2	Amazonia	41.98	5.18	0.96	0.16	51.88	15.17	0.12	1.24
F3	Trinitario	42.42	5.27	1.63	0.16	50.68	15.6	0.12	1.19

---

F4	Hybrid	41.45	5.86	1.48	0.12	51.09	15.84	0.14	1.23
----	--------	-------	------	------	------	-------	-------	------	------

<sup>a</sup> H/C and O/C molar ratios

<sup>b</sup> By calculation based on equation 3.2

<sup>c</sup> By difference

All CPH samples studied have homogenous levels of Carbon, Hydrogen and Oxygen. The measure of Carbon in the samples was 37.36%-43.81% while Oxygen measured 49.33%-56.10%. Hydrogen content ranged from 4.72% to 6.11%, which is much lower in comparison to the carbon and oxygen contents. Hydrogen has the highest calorific value amidst other fuels, hence fuels with high hydrogen contents have high burning velocity. Higher proportions of oxygen in biomass feedstock reduce the energy density of the fuel as it increases the emission of carbon dioxide (CO<sub>2</sub>) and water (H<sub>2</sub>O) formation. Sulphur and Nitrogen contents of all CPH samples were similar and very low. The nitrogen content was found to be 0.72%-2.63% as compared to 0.5%-3% for coal whereas the sulphur content range was 0.08%-0.31 compared to 2%-4% for coal. The trace amounts of nitrogen and sulphur observed in the CPH samples allude to the eco-friendly nature of cocoa pod husks. When sulphur is oxidized, it produces sulphur dioxide which can potentially cause acid deposition. Sulphur dioxide is very corrosive in the presence of water and could cause chimney corrosion, hence the lower the sulphur content, the better. The low levels of sulphur in the CPH samples is therefore an added advantage in our pursuit of green energy.

The atomic ratios H/C ranges from 0.12 to 0.15 and O/C from 1.13 to 1.32. While H/C indicates the stability of the CPH material, O/C gives a general indication of its polarity. A high H/C ratio indicates that there is a higher concentration of hydrogen molecules in the fuel mix. The higher the H/C ratio, the higher the energy density of the feedstock, since hydrogen has the highest heating value among other fuels. The O/C ratios of the CPH samples are higher than the H/C ratios due to the higher concentration of oxygen molecules. There is therefore a higher possibility of producing more carbon monoxide (CO) than methane (CH<sub>4</sub>) and hydrogen gas (H<sub>2</sub>) in a thermochemical conversion to syngas.

### ***3.3.3 Higher Heating Value***

The heating value is defined as the energy contained in a sample of a given material [155]. It can be expressed as higher heating value and lower heating value. Heating value is one of the most essential parameters of biomass fuels for design calculations and numerical simulations of biomass thermal conversion systems. It is directly proportional to carbon content and inversely proportional to ash content [156]. Figure 3.20 compares the higher heating values of CPH samples determined by both ultimate and proximate analyses. The higher heating values calculated by the proximate analysis are all higher than the corresponding values calculated by the ultimate analysis. However, the results provided by the ultimate analysis is more accurate because the proximate analysis only provides an empirical composition of the biomass [157].

Based on both the ultimate and proximate analyses, Amelonado from the Ashanti region had the highest calorific value, while Trinitario from the Eastern region had the lowest.

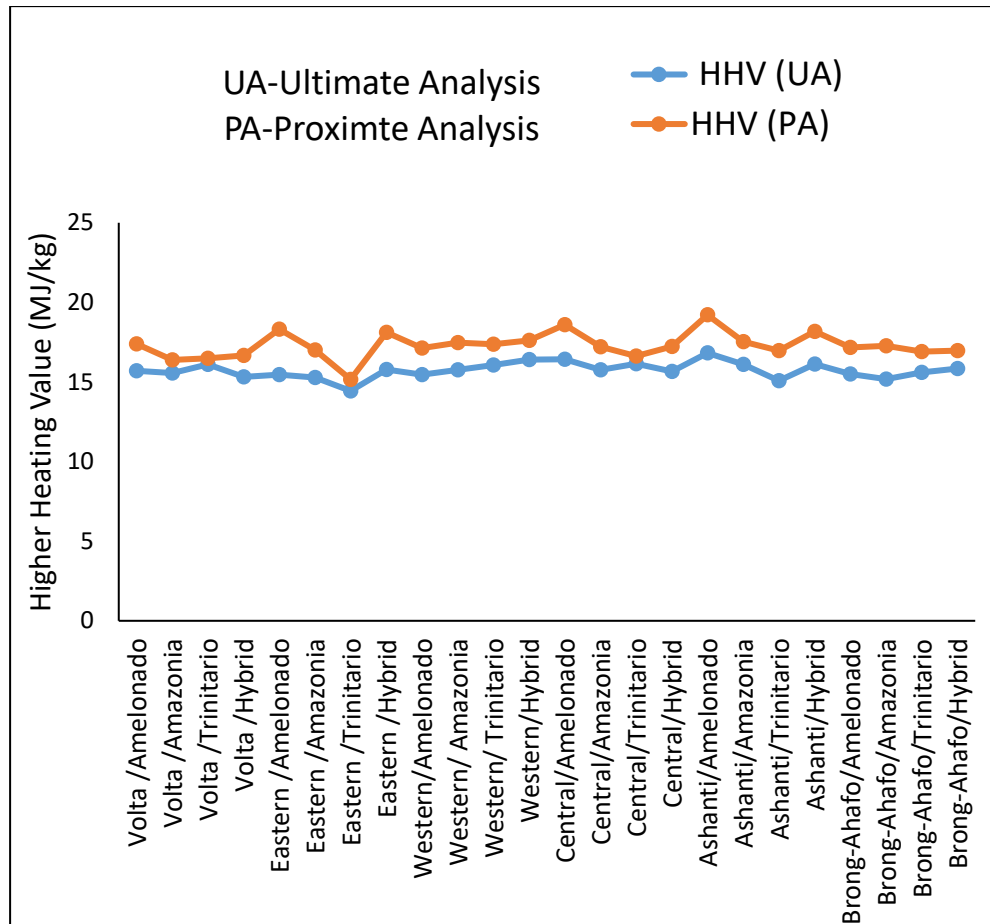


Figure 3.20: Comparison of Higher Heating Values of CPH samples by ultimate and proximate analysis.

According to the proximate analysis, Amelonado had the highest heating value of the CHP types, while Trinitario had the lowest. Figure 3.21 depicts the higher heating values of the four types of CPH as calculated by the proximate analysis.

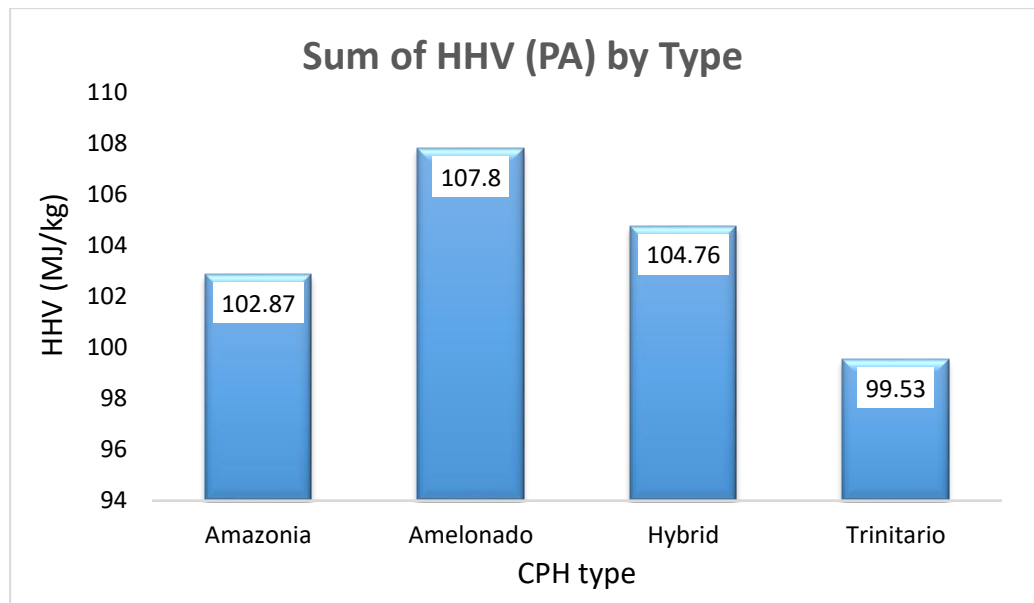


Figure 3.21: The higher heating value of the CPH types based on proximate analysis

Again, based on the ultimate analysis, Amelonado had the highest heating value, and Trinitario had the lowest, as depicted in Figure 3.22.

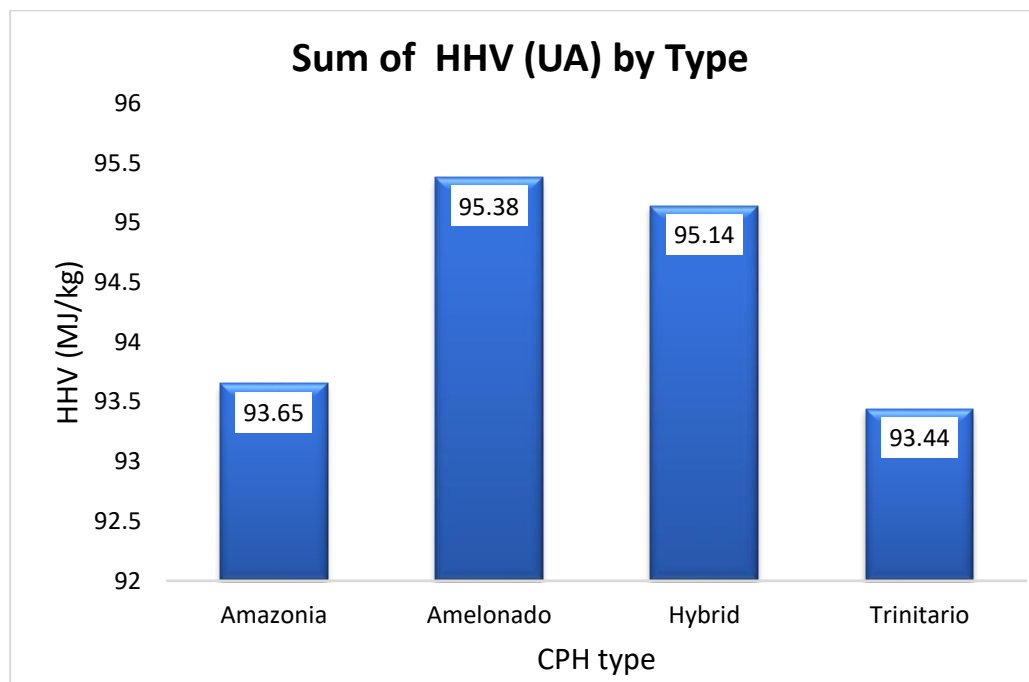


Figure 3.22: The higher heating value of the CPH types based on ultimate analysis

The high calorific value of Amelonado may be due to its high hydrogen-to-carbon ratio and fixed carbon content. On the other hand, the low calorific value of Trinitario could be a result of its low volatile matter and high moisture content.

In consonance with the ultimate analysis, Ashanti region had the highest heating value while Eastern region had the lowest. Figure 3.23 portrays the Ashanti region as the region with the greatest energy potential, as per the higher heating value calculated using the ultimate analysis.

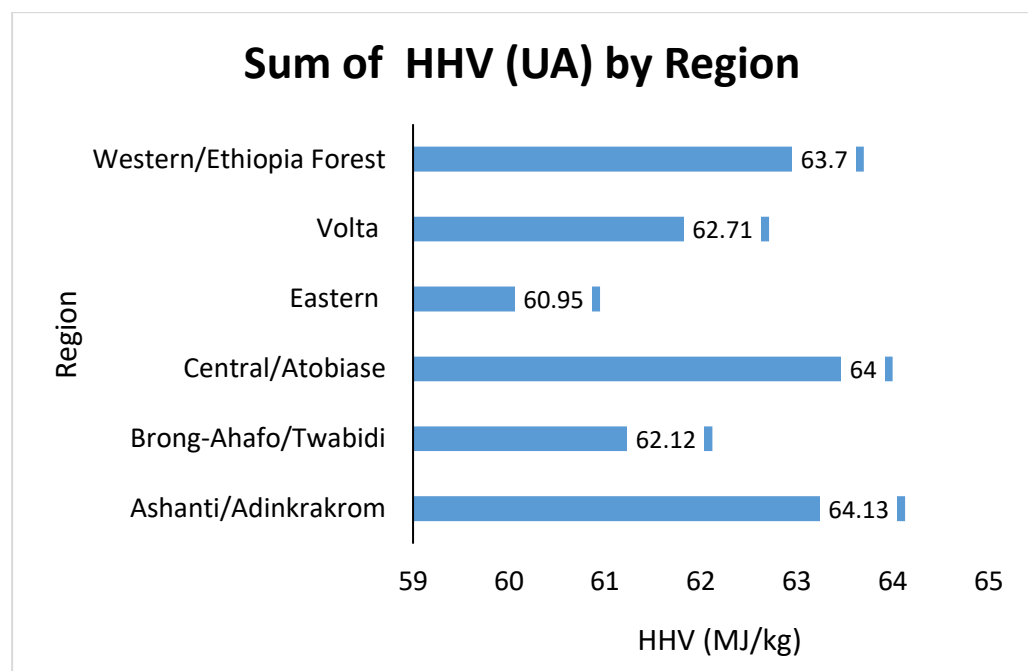


Figure 3.23: Region-specific higher heating value based on ultimate analysis

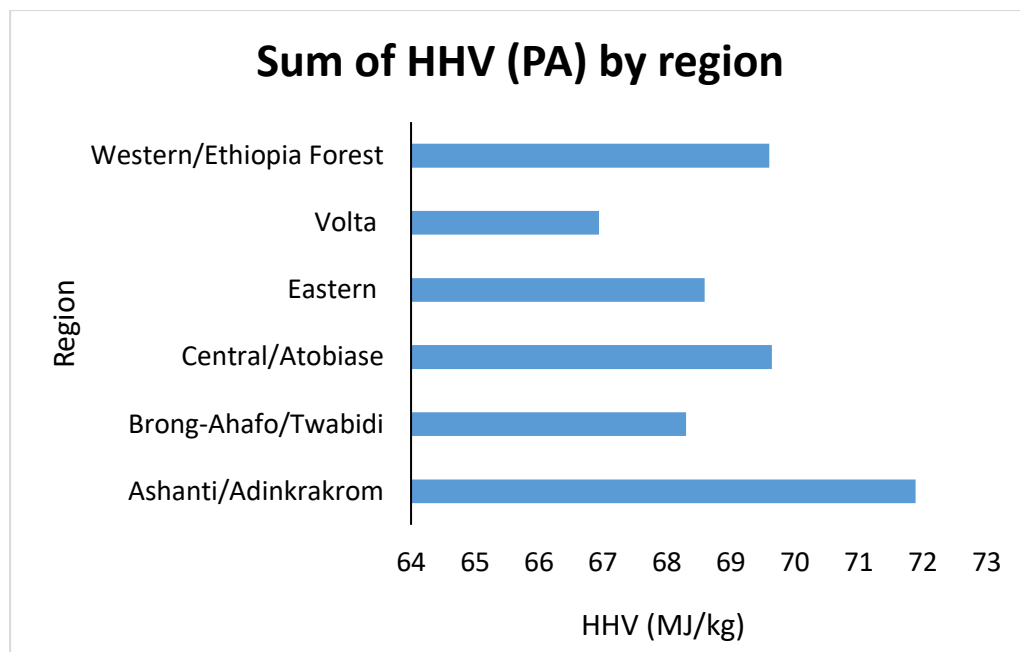


Figure 3.24: Region-specific higher heating value based on proximate analysis

Just as in the ultimate analysis, the proximate analysis also revealed that the Ashanti region had the highest heating value, although the lowest heating value was recorded by the Volta region instead of the Eastern region. The high calorific values of CPH samples from the Ashanti region can be attributed to the high fixed carbon and low ash content. Meanwhile, the low calorific value of CPH samples from Eastern and Volta regions may be due to the high moisture and ash content of samples from the two regions. Since soil type affects ash content and therefore indirectly influences calorific value, it is very likely that the CPH samples that exhibited superior heating values were cultivated in optimum soil conditions.

### 3.4 Concluding Remarks

Twenty-four (24) locally produced cocoa pod husks from the six cocoa growing regions of Ghana were characterised for their thermo-physical properties and

energy conversion potential. The results based on ultimate and proximate analyses show that cocoa pod husk has a high calorific value of 14.44-19.21 MJ/kg and hence, a tremendous source of energy for power generation.

The proximate analysis produced similar results to those reported in literature. The volatile matter contents of cocoa pod husk samples studied were reasonably high, which makes them good feedstock for combustion, gasification and pyrolysis. The high content of volatiles in CPH suggest that they would be easy to ignite, have better flame stability and would maintain a low carbon loss during combustion. The moisture content of the CPH samples were all less than 14% with over 83% of samples recording moisture contents less than 10%. Any biomass material with a moisture content below 15% is good enough for a hassle free operation of a gasification plant. Hence, cocoa pod husk as feedstock for electricity generation via gasification would be very effective and economical. In order to promote energy efficiency, the steam generated during gasification of CPH could also be recovered and reused as a gasifying agent. Although ash content of the CPH samples measured an average of 11.01% which is quite high and could increase power plant maintenance cost, operational conditions during thermochemical conversion could be optimised to get the best energy output.

The ultimate analysis demonstrated that carbon and oxygen contents of cocoa pod husks were high compared to hydrogen. Trace amounts of nitrogen and sulphur were observed in the CPH samples, hence cocoa pod husk is an eco-friendly feedstock for energy production. Ghana can therefore reduce cocoa waste by using it for the production of clean electricity. The slight differences in thermal properties observed between the cocoa pod husk samples could be

attributed to differences in location, soil contamination, cultivation methods, climatic, and storage conditions.

Whiles Amelonado was the CPH species with the highest calorific value, Trinitario had the lowest calorific value. Among the six cocoa growing regions in Ghana, Ashanti region recorded the highest calorific value, while Eastern and Volta had the lowest calorific values. Ashanti region recorded the lowest ash and moisture content as well as the highest fixed carbon content, which could be the influential factor for its high calorific value. On the whole, Amelonado from Ashanti region of Ghana exhibited the highest energy potential at 19.21 MJ/Kg. Ashanti region could therefore be prioritised for any future demonstration of a bio-energy plant.

Notwithstanding, the material characterization has provided a foreknowledge of the inherent properties of CPH, such as calorific value, which are imperative for numerical modeling and simulation of thermochemical conversion systems. For this reason, the next chapter would develop a mathematical model for simulating cocoa pod husk gasification processes.

# CHAPTER FOUR

## 4.0 MATHEMATICAL MODELING AND SIMULATION OF CPH GASIFICATION PROCESS

### 4.1 CPH Gasification System

The gasification system comprises of a hopper, a reactor vessel, as well as a cooling and cleaning sub-system. Figure 4.1 illustrates how the gasification system is set out.

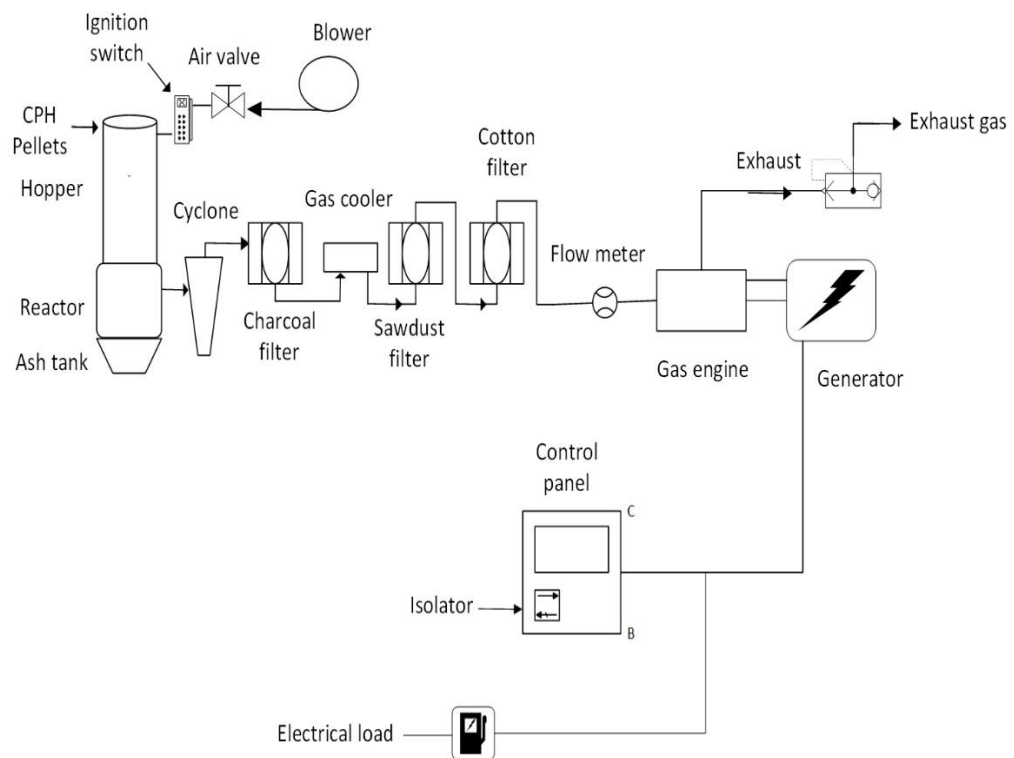


Figure 4.1: A schematic diagram of the gasification system

The reactor carries out four distinct operations, including feedstock drying, pyrolysis, combustion, and reduction. At the start of the operation, biomass feedstock is fed into the reactor via the hopper at predefined intervals. A regulated amount of air is then introduced into the reactor through an air valve

and a blower. As a result, the biomass undergoes partial oxidation and is converted into product gas. The product gas, which may contain tar, is then sent through a series of filters in order to remove the tar and any other impurities that may cause the gas engine to malfunction. The hot syngas is also routed via a gas cooler to reduce the temperature down to ambient. The syngas is finally introduced into the gas engine after going through a series of fine filters and textiles that have been specially designed for the purpose.

## **4.2 Mathematical Modelling and Simulation**

### ***4.2.1 Formulation of the model***

Gasification systems have been modelled in different ways, including with equilibrium and kinetic models. Equilibrium models predict the best possible yield of a desired product from a reacting system, whereas kinetic models predict the progression and product composition at various points in a reactor. Equilibrium models are less computationally intensive than kinetic models and can be used for preliminary comparisons. Despite their inability to provide very accurate results in all instances, they are considered a decent technique for modelling entrained-flow gasifiers and downdraft fixed-bed gasifiers as long as high temperatures and gas residence times are attained in the throat [158]. Some equilibrium models are based on the minimization of Gibbs free energy (non-stoichiometric approach), which has a constrained optimization problem that typically employs the Lagrange multiplier technique. The second type of equilibrium model relies on equilibrium constants (stoichiometric approach) [145]. The stoichiometric method is based on a set of selected independent

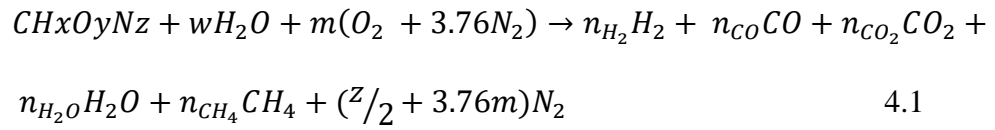
reactions and makes use of elemental balances and equilibrium relations. The non-stoichiometric method is based on the assumption that certain species are present in the syngas [159]. However, both the stoichiometric and non-stoichiometric methods follow the same concept.

For the purpose of modelling the biomass gasification process presented in this work, a thermodynamic equilibrium technique that is based on equilibrium constants was adopted. The following are the primary assumptions that were utilised in the development of the equilibrium model:

- CPH is generally thought to be composed of the elements carbon, hydrogen, oxygen, and nitrogen.
- It is anticipated that nitrogen will form an inert gas, and it is assumed that the gasification system is in a steady state and operating under isothermal circumstances.
- The behaviour of an ideal gas is assumed for each type of gas and its attributes.
- It is assumed that all of the carbon in the CPH has been gasified; as a result, the generation of char is not taken into consideration.
- The syngas is made up of carbon monoxide, carbon dioxide, nitrogen, methane, and hydrogen gas.
- Since it is presumed that tar goes through a full transformation into permanent gases, the model does not take this into account.

In order to properly use the thermodynamic equilibrium model that is based on the equilibrium constants method, the precise chemical processes that are employed in the computation need to be defined [160]. It is assumed that CPH is

dry and that it exclusively contains the elements carbon, hydrogen, oxygen, and nitrogen. Air is employed as the medium for the gasification process. Under conditions of equilibrium, the only components that are thought to be present are C(s), CO, H<sub>2</sub>, CO<sub>2</sub>, H<sub>2</sub>O, and CH<sub>4</sub>. Taking into account that the chemical formula for CPH is CH<sub>x</sub>O<sub>y</sub>N<sub>z</sub>, CPH gasification reaction based on the above assumptions can be written as;



Where  $n_{H_2}$ ,  $n_{CO}$ ,  $n_{CO_2}$ ,  $n_{H_2O}$ ,  $n_{CH_4}$ , and  $n_{N_2}$  are the number of moles of H<sub>2</sub>, CO, CO<sub>2</sub>, H<sub>2</sub>O, CH<sub>4</sub>, and N<sub>2</sub> respectively,  $m$  is the amount of air per kmol of CPH and  $w$  is the amount of water per kmol of CPH. All inputs on the left side of Eq. (1) are defined at 298 K (25 °C). On the right side, the number of moles of the individual product species ( $n_i$ ) are unknowns. The amount of water per kmol of CPH can be calculated using the equation as follows [161].

$$w = \frac{M_{CPH} \times MC}{M_{H_2O} \times (1 - MC)} \quad 4.2$$

where  $M_{CPH}$  and  $M_{H_2O}$  are the masses of the CPH and water respectively, and  $MC$  is the moisture content.

Equivalence ratio (ER) is one of the most important parameters for enhancing the quality of gas yield in gasification. It is the actual air–fuel ratio (used in the gasification) to the stoichiometric air–fuel ratio for combustion [162]. For a biomass with composition  $CH_xO_y$ , ER can be expressed using the following equation [163].

$$ER = \frac{m}{1 + \frac{x}{4} - \frac{y}{2}} \quad 4.3$$

Since gasification takes place in a reduced oxygen environment, ER is assumed to be 30% - 60% fraction of the calculated stoichiometric air [161].

Subscripts  $x$ ,  $y$  and  $z$  are numbers of atoms of hydrogen, oxygen, and nitrogen per one atom of carbon in the feedstock, respectively and are determined by the ultimate analysis of the CPH as follows [164].

$$x = \frac{HM_C}{CM_H} \quad 4.4$$

$$y = \frac{OM_C}{CM_O} \quad 4.5$$

$$z = \frac{NM_C}{CM_N} \quad 4.6$$

$M_C$ ,  $M_H$ ,  $M_O$  and  $M_N$  are the molecular weight of carbon, hydrogen, oxygen and nitrogen respectively and C, H, O and N are the mass fractions of those elements.

#### **4.2.2 Mass balance**

Taking into consideration the gasification reaction in Equation 4.1, there are five unknown product species which can be calculated using the relationships between mass balance and equilibrium constants. The mass balance equations for carbon, hydrogen and oxygen are given below:

Carbon balance,

$$n_{CO} + n_{CO_2} + n_{CH_4} - 1 = 0 \quad 4.7$$

Hydrogen balance,

$$2n_{H_2} + 2n_{H_2O} + 4n_{CH_4} - x - 2w = 0 \quad 4.8$$

Oxygen balance,

$$n_{CO} + 2n_{CO_2} + n_{H_2O} - w - 2m - y = 0 \quad 4.9$$

### 4.2.3 Thermodynamic equilibrium

The following chemical reactions describe the processes that take place in the gasification unit;

Boudouard reaction



Water gas reaction



Water gas shift reaction



Considering equilibrium constant  $K_1$  for the water gas shift reaction above,

$$K_1 = \frac{n_{CO_2} \times n_{H_2}}{n_{CO} \times n_{H_2O}} \quad 4.13$$

Methane reaction,



Using equilibrium constant  $K_2$  for methane reaction,

$$K_2 = \frac{n_{CH_4} \times n_{total}}{(n_{H_2})^2} \quad 4.15$$

Where  $n_{total}$  is total number of moles of producer gas.

The equilibrium constants  $K_1$  and  $K_2$  for ideal gases are dependent on temperature [165]. The equilibrium constant  $K_1$  can be determined using the relation with temperature (T) in K [164].

$$K_1 = \exp\left\{\left(\frac{4276}{T}\right) - 3.961\right\} \quad 4.16$$

The equilibrium constant  $K_2$  can be calculated from the relation used by Zainal et al [165].

$$K_2 = \exp\left(\frac{7082.848}{T} - 6.567 \ln T + \frac{7.466 \times 10^{-3}}{2} T - \frac{2.164 \times 10^{-6}}{6} T^2 + \frac{0.701 \times 10^{-5}}{2T^2} + 32.541\right) \quad 4.17$$

The composition of the product gas ( $n_{H_2}$ ,  $n_{CO}$ ,  $n_{CO_2}$ ,  $n_{H_2O}$ , and  $n_{CH_4}$ ) were obtained by simultaneously solving the three linear equations [Equations. 4.7-4.9] and two non-linear equations [Equations. 4.13 and 4.15] in MATLAB platform using Newton-Raphson method. To determine the temperature-dependent equilibrium constants  $K_1$  and  $K_2$ , the temperature in the gasification zone must be known. In this study, the temperature in the gasification zone was assumed.

#### **4.2.4 Energy balance**

There are endothermic as well as exothermic processes that take place in the gasifier during the gasification process. The gasifier's temperature increases as a result of the conversion of any excess heat that is produced by exothermic reactions into sensible heat by endothermic reactions [160]. Exothermic reactions are those that produce heat, while endothermic reactions are those that consume the heat produced by exothermic reactions. Because temperature is

such an important factor in thermodynamics, it was necessary to determine the temperature of the reaction that was taking place in the gasification zone before one could proceed with the calculation of the equilibrium constants. In order for the gasification process to be successful, it was necessary to adhere to the principle of energy conservation, which is sometimes referred to as the first law of thermodynamics [166]. It was presumed that the gasifier had a very modest footprint and that there was no significant heat loss throughout its entirety. The following is a description of how to write up the energy balance for the gasification process:

$$H_{Reatants} + Q_{in} = H_{Products} + Q_{out} \quad 4.18$$

Where  $H_{Products}$  and  $H_{Reatants}$  are the enthalpies of the products and reactants respectively while  $Q_{in}$  and  $Q_{out}$  are the heat exchanges between the gasifier and its surroundings. Because we assumed adiabatic conditions for this research, any heat exchanges that occurred between the gasifier and its environment were deemed to be inconsequential. Therefore, both  $Q_{in}$  and  $Q_{out}$  were equal to zero. So, the energy balance for the gasification process under adiabatic conditions can be shown by the following equation:

$$H_{Reatants} = H_{Products} \quad 4.19$$

Assuming an ideal gas behaviour, enthalpies are dependent on temperature and can be determined using the enthalpy of species at given temperature. When the temperature in the gasification zone was  $T_i$  and the temperature at the inlet of the gasifier was assumed to be 298 K (25 °C), the energy balance for the process was as follows.

$$H_{Reactants} = h_{f_{biomass}}^0 + w [h_{f_{H_2O}}^0 + \int_{298}^{T_i} C_{P_{H_2O}} \cdot dT_i] \quad 4.20$$

$$H_{Products} = \sum_{products} n_i [h_{f_i}^0 + \Delta h_{T,i}^0] \quad 4.21$$

$\Delta h_T^0$  is the enthalpy difference between any given state and at reference state.

It can be expressed as:

$$\Delta h_T^0 = \int_{298}^T C_p \cdot dT_i \quad 4.22$$

By substituting Equation 25 into equation 24:

$$H_{Products} = \sum_{products} n_i [h_{f_i}^0 + \int_{298}^{T_i} C_{P_i} \cdot dT_i] \quad 4.23$$

Where  $C_p$  is the specific heat at constant pressure in kJ/kmol K and  $h_f^0$  is the enthalpy of formation in kJ/kmol. All chemical elements at the inlet state (298 K, 1 atm) have zero enthalpies of formation.  $C_p$  is a function of temperature (T) in Kelvin (K) and can be defined by the empirical equation [145].

$$C_p = a + b \cdot T_i + c \cdot T_i^2 + d \cdot T_i^3 \quad 4.24$$

$$\int_{298}^{T_i} C_p \cdot dT_i = a \cdot T_i + b \cdot \frac{T_i^2}{2} + c \cdot \frac{T_i^3}{3} + d \cdot \frac{T_i^4}{4} \quad 4.25$$

Where  $a$ ,  $b$ ,  $c$ , and  $d$  are the coefficients of the specific heat in the empirical equation displayed in Table 4.1 [145].

Table 4.1: Coefficients of specific heat for the empirical equation.

Gas species	a	b	c	d	Temperature range (K)
H <sub>2</sub>	29.11	-0.1916 x 10 <sup>-2</sup>	0.4003 x 10 <sup>-5</sup>	-0.8704 x 10 <sup>-9</sup>	273 - 1800
CO	28.16	0.16750 x 10 <sup>-2</sup>	0.5372 x 10 <sup>-5</sup>	-2.222 x 10 <sup>-9</sup>	273 - 1800
CO <sub>2</sub>	22.26	5.981 x 10 <sup>-2</sup>	-3.501 x 10 <sup>-5</sup>	-7.469 x 10 <sup>-9</sup>	273 - 1800
H <sub>2</sub> O (vapour)	32.24	0.1923 x 10 <sup>-2</sup>	1.055 x 10 <sup>-5</sup>	-3.595 x 10 <sup>-9</sup>	273 - 1800
CH <sub>4</sub>	19.89	5.204 x 10 <sup>-2</sup>	1.269 x 10 <sup>-5</sup>	-11.01 x 10 <sup>-9</sup>	273 - 1800
N <sub>2</sub>	28.90	-0.1571 x 10 <sup>-2</sup>	0.8081 x 10 <sup>-5</sup>	-2.873 x 10 <sup>-9</sup>	273 - 1800

Since enthalpy of reactants equals enthalpy of products at adiabatic conditions,

Equation 4.22 can be rewritten as:

$$\begin{aligned}
 h_{f_{biomass}}^0 + w (h_{f_{H_2O(l)}}^0 + h_{(vap)}) + mh_{f_{O_2}}^0 + 3.76mh_{f_{N_2}}^0 = n_i h_{f_{H_2}}^0 + \\
 n_i h_{f_{CO}}^0 + n_i h_{f_{CO_2}}^0 + n_i h_{f_{H_2O(vap)}}^0 + n_i h_{f_{CH_4}}^0 + \Delta T (n_i C_{p_{H_2}} + n_i C_{p_{CO}} + \\
 n_i C_{p_{CO_2}} + n_i C_{p_{H_2O}} + n_i C_{p_{CH_4}} + (Z/2 + 3.76m) C_{p_{N_2}}) \quad 4.26
 \end{aligned}$$

At ambient temperature,  $h_{f_{H_2}}^0$ ,  $h_{f_{N_2}}^0$ , and  $h_{f_{O_2}}^0$  are zero. Hence Equation 4.29

reduces to:

$$\begin{aligned} h_{f_{biomass}}^0 + w (h_{f_{H_2O(l)}}^0 + h_{(vap)}) = n_i h_{f_{CO}}^0 + n_i h_{f_{CO_2}}^0 + n_i h_{f_{H_2O(vap)}}^0 + \\ n_i h_{f_{CH_4}}^0 + \Delta T (n_i C_{p_{H_2}} + n_i C_{p_{CO}} + n_i C_{p_{CO_2}} + n_i C_{p_{H_2O}} + n_i C_{p_{CH_4}} + (Z/2 + \\ 3.76m) C_{p_{N_2}}) \end{aligned} \quad 4.27$$

Where  $h_{f_{biomass}}^0$  is the enthalpy of formation of biomass,  $h_{f_{H_2O(l)}}^0$ , the enthalpy of formation of liquid water,  $h_{(vap)}$ , enthalpy of vaporization of water,  $h_{f_{H_2O(vap)}}^0$ , enthalpy of formation of water vapour,  $h_{f_{CO}}^0$ ,  $h_{f_{CO_2}}^0$ ,  $h_{f_{CH_4}}^0$ , are the enthalpies of formation of the gaseous products,  $C_{p_{H_2}}$ ,  $C_{p_{CO}}$ ,  $C_{p_{CO_2}}$ ,  $C_{p_{H_2O}}$ ,  $C_{p_{CH_4}}$ ,  $C_{p_{N_2}}$  are specific heats of the gaseous products,  $\Delta T = T_2 - T_1$ ,  $T_2$ , the gasification temperature at the reduction zone;  $T_1$  is the ambient temperature at the reduction zone.

From equation 4.30,

$$\begin{aligned} \Delta T (n_i C_{p_{H_2}} + n_i C_{p_{CO}} + n_i C_{p_{CO_2}} + n_i C_{p_{H_2O}} + n_i C_{p_{CH_4}} + (Z/2 + \\ 3.76m) C_{p_{N_2}}) = h_{f_{biomass}}^0 + w (h_{f_{H_2O(l)}}^0 + h_{(vap)}) - (n_i h_{f_{CO}}^0 + n_i h_{f_{CO_2}}^0 + \\ n_i h_{f_{H_2O(vap)}}^0 + n_i h_{f_{CH_4}}^0) \end{aligned} \quad 4.28$$

$\Delta T$

$$\begin{aligned} = \frac{h_{f_{biomass}}^0 + w (h_{f_{H_2O(l)}}^0 + h_{(vap)}) - (n_i h_{f_{CO}}^0 + n_i h_{f_{CO_2}}^0 + n_i h_{f_{H_2O(vap)}}^0 + n_i h_{f_{CH_4}}^0)}{(n_i C_{p_{H_2}} + n_i C_{p_{CO}} + n_i C_{p_{CO_2}} + n_i C_{p_{H_2O}} + n_i C_{p_{CH_4}} + (Z/2 + 3.76m) C_{p_{N_2}})} \end{aligned} \quad 4.29$$

$$\begin{aligned}
& T_2 - T_1 \\
&= \frac{h_{f_{biomass}}^0 + w \left( h_{f_{H_2O(l)}}^0 + h_{(vap)} \right) - \left( n_i h_{f_{CO}}^0 + n_i h_{f_{CO_2}}^0 + n_i h_{f_{H_2O(vap)}}^0 + n_i h_{f_{CH_4}}^0 \right)}{\left( n_i C_{p_{H_2}} + n_i C_{p_{CO}} + n_i C_{p_{CO_2}} + n_i C_{p_{H_2O}} + n_i C_{p_{CH_4}} + \left( \frac{Z}{2} + 3.76m \right) C_{p_{N_2}} \right)}
\end{aligned} \tag{4.30}$$

$$T_2 = \frac{h_{f_{biomass}}^0 + w \left( h_{f_{H_2O(l)}}^0 + h_{(vap)} \right) - \left( n_i h_{f_{CO}}^0 + n_i h_{f_{CO_2}}^0 + n_i h_{f_{H_2O(vap)}}^0 + n_i h_{f_{CH_4}}^0 \right)}{\left( n_i C_{p_{H_2}} + n_i C_{p_{CO}} + n_i C_{p_{CO_2}} + n_i C_{p_{H_2O}} + n_i C_{p_{CH_4}} + \left( \frac{Z}{2} + 3.76m \right) C_{p_{N_2}} \right)} + T_1 \tag{4.31}$$

Enthalpy of formation of biomass can be calculated based on its heating value [163].

$$h_{f_{biomass}}^0 = HHV_{biomass} + h_{f_{CO_2}}^0 + \frac{x}{2} h_{f_{H_2O(l)}}^0 \tag{4.32}$$

In order to work out the higher heating value (HHV) of the fuel, a correlation proposed by Channiwala and Parikh [146] was used.

$$\begin{aligned}
HHV &= 0.3491C + 1.1783H + 0.1005S - 0.1034O - 0.0151N - \\
&0.0211Ash
\end{aligned} \tag{4.33}$$

Where C, H, O, N, S and Ash are percentages of mass of carbon, hydrogen, oxygen, nitrogen, sulfur and ash in the dry solid fuel. The lower heating value (LHV) of the solid fuel was calculated using the following correlation [160], [167].

$$LHV_{fuel} = HHV - \frac{9m_H}{100} (h_{(vap)}) \tag{4.34}$$

Where  $m_H$  is the mass fraction of hydrogen in the solid fuel,  $h_{(vap)}$  is the enthalpy of vaporization of water, and  $LHV_{fuel}$  is the calorific value of the fuel.

The calorific value of the syngas ( $LHV_{syngas}$ ) was calculated using the following expression [159].

$$LHV_{syngas} = \frac{n_{CO} H_{CO,298}^o + n_{H_2} H_{H_2,298}^o + n_{CH_4} H_{CH_4,298}^o}{M_{syngas}} \quad 4.35$$

$H_{CO,298}^o$  is the heat of combustion of CO,  $H_{H_2,298}^o$  is the heat of combustion of H<sub>2</sub> and  $H_{CH_4,298}^o$  is the heat of combustion of CH<sub>4</sub>.  $M_{syngas}$  is the mass flow rate of the syngas,  $M_{fuel}$  is the mass flow rate of the fuel.

Cold gas efficiency (CGE) is the ratio of the energy content of produced gas in standard state to the energy content of the biomass fuel [168]. It is used as a measure of the efficiency of the CPH gasification system in this study and was calculated using the following expression [161].

$$CGE = \frac{\text{Heating value in produced syngas}}{\text{Heating value in fuel}} \times 100 \quad 4.36$$

#### **4.2.5. Calculation of the gas composition**

The data used to test the thermodynamic equilibrium model was obtained from the ultimate and proximate analyses. The iterative Newton-Raphson method built into Matlab was chosen as the best way to solve the system of equations. An initial temperature was assumed for the first calculation of equilibrium constants  $K_1$  and  $K_2$  in order to determine the  $n_{H_2}$ ,  $n_{CO}$ ,  $n_{CO_2}$ ,  $n_{H_2O}$ , and  $n_{CH_4}$ . This was done in order to ensure that the correct values were obtained. Both equilibrium constants were then substituted into equations 4.13 and 4.15 respectively.

Subsequently, the five simultaneous equations 4.7, 4.8, 4.9, 4.13 and 4.15 were solved using Newton-Raphson method in Matlab. The values of  $n_{H_2}$ ,  $n_{CO}$ ,  $n_{CO_2}$ ,  $n_{H_2O}$ , and  $n_{CH_4}$  once obtained, were entered into an excel spreadsheet and their individual percentage compositions calculated. Excel was then used to analyse the results and draw conclusions.

## 4.3 Results and Discussion

### 4.3.1 Model analysis

Table 4.2 shows the data used for testing the thermodynamic equilibrium model. Detailed composition of various cocoa pod husk samples obtained from the ultimate and proximate analyses were used for test simulation. A fixed temperature setting of 1100K and an ER of 0.3 were used in line with what was reported by both Jarungthammachote and Dutta [145] and Jayah et al [169].

Table 4.2: Ultimate analysis of CPH samples

Feedstock	C	H	N	S	O	Moisture	Ash	HHV
CPH A1	41.53	5.81	0.92	0.13	51.61	10.35	14	15.71
CPH A2	42.32	5.37	1.28	0.16	51.03	7.64	11.98	15.57
CPH A3	42.87	5.55	1.31	0.16	50.27	10.12	9.17	16.11
CPH A4	40.38	5.89	1.02	0.24	52.47	9.75	13.94	15.32
CPH B1	39.82	6.11	1.27	0.16	52.63	9.43	9.45	15.46
CPH B2	42.43	5.06	1.74	0.16	50.77	5.57	11.41	15.27

---

CPH B3	39.9	5.28	2.63	0.16	52.19	13.21	13.57	14.44
CPH B4	41.5	5.86	0.84	0.29	51.81	10.06	12.43	15.78
CPH C1	40.47	5.87	1.63	0.31	51.72	7.81	11.84	15.46
CPH C2	42.8	5.34	1.04	0.16	50.82	6.56	9.80	15.77
CPH C3	41.66	5.87	2.41	0.16	50.06	5.90	9.81	16.06
CPH C4	42.33	5.98	1.63	0.13	49.94	8.81	11.24	16.41
CPH D1	42.78	5.83	1.31	0.14	49.94	8.65	10.09	16.42
CPH D2	43.48	5.08	1.35	0.16	50.09	6.14	10.34	15.76
CPH D3	43.06	5.47	2.14	0.16	49.33	9.64	9.92	16.15
CPH D4	41.47	5.78	1.14	0.16	51.45	9.2	14	15.67
CPH E1	43.81	5.79	0.77	0.12	49.52	7.62	7.87	16.82
CPH E2	42.37	5.73	1.33	0.16	50.57	5.82	9.54	16.11
CPH E3	41.18	5.35	1.68	0.16	51.79	4.98	11.35	15.08
CPH E4	42.32	5.76	1.42	0.08	50.43	8.51	9.98	16.12
CPH F1	41.22	5.73	1.13	0.08	51.85	7.76	12.1	15.51
CPH F2	41.98	5.18	0.96	0.16	51.88	4.63	10.80	15.17
CPH F3	42.42	5.27	1.63	0.16	50.68	8.59	8.28	15.6
CPH F4	41.45	5.86	1.48	0.12	51.09	6.67	11.29	15.84

---

Table 4.3 displays the gas composition of the various CPH samples tested. The gas composition of carbon monoxide (CO) was between 22.80% and 27.17%, whereas the gas composition of carbon dioxide (CO<sub>2</sub>) was between 10.79% and 14.33%. In comparison to the other gases, the percentage composition of methane (CH<sub>4</sub>) was quite low, ranging from 0.39% to 0.55%. The composition of hydrogen gas (H<sub>2</sub>) was between 20.79% and 23.83%, while nitrogen gas (N<sub>2</sub>) had a compositional range that went from 39.47% to 40.85%.

Table 4.3: Simulated gas composition of CPH fuel

CPH Feedstock type	Gas composition (mole % dry basis)				
	CO	CO <sub>2</sub>	CH <sub>4</sub>	H <sub>2</sub>	N <sub>2</sub>
A1	23.75	12.61	0.52	23.24	39.88
A2	25.62	11.94	0.44	21.84	40.16
A3	24.79	11.96	0.48	22.56	40.20
A4	23.29	13.02	0.53	23.42	39.74
B1	22.80	12.96	0.55	23.83	39.86
B2	26.89	11.55	0.39	20.79	40.37
B3	22.87	14.33	0.49	22.84	39.47
B4	23.73	12.59	0.52	23.28	39.88

C1	23.92	12.37	0.51	23.06	40.14
C2	26.24	11.51	0.43	21.53	40.28
C3	24.99	11.06	0.50	22.60	40.85
C4	24.29	11.41	0.53	23.21	40.56
D1	24.78	11.37	0.51	22.86	40.49
D2	27.17	11.12	0.40	20.84	40.47
D3	25.14	11.54	0.47	22.30	40.54
D4	24.10	12.35	0.51	23.00	40.03
E1	25.61	10.79	0.49	22.50	40.61
E2	25.60	11.13	0.47	22.24	40.56
E3	25.95	11.95	0.43	21.44	40.23
E4	24.71	11.66	0.50	22.75	40.38
F1	24.49	12.28	0.49	22.70	40.04
F2	26.77	11.79	0.40	20.93	40.10
F3	25.52	12.08	0.44	21.79	40.17
F4	24.71	11.64	0.50	22.74	40.41

---

### ***4.3.2 Parametric study and performance analysis***

#### **4.3.2.1 Effects of equivalent ratio**

Equivalence ratio as previously defined is the ratio of the actual air amount in gasification process to the stoichiometric amount. The effect of equivalence ratio on the composition of syngas is depicted in Figures 4.1, 4.2 and 4.3. In Figure 4.1 for CPH sample A1, the CO content of syngas can be seen to decrease from 23.75% to 10.71% with an increase in equivalence ratio from 0.3 to 0.6. With the same range of equivalence ratio values, the H<sub>2</sub> percentage also decreased from 23.24% to 10.37% as equivalence ratio increased. This could be attributed to the presence of more oxygen in the reaction that caused further hydrogen oxidation [168]. While the CH<sub>4</sub> content of syngas remained low, it decreased further when equivalence ratio was increased. On the contrary, it was observed that the mole percentages of N<sub>2</sub> and CO<sub>2</sub> increased with increase in equivalence ratio. The same behaviour was observed for the other CPH samples A2 and A3 as can be seen in Figures 4.2 and 4.3 respectively. Modellers such as Barman et al [164], Ghassemi and Shahsavan-Markadeh [168], and Puig-Arnavat et al [158] have all reported similar findings. In Figure 4.4, the effects of equivalence ratio on syngas heating value and cold gas efficiency are displayed. As the equivalence ratio increases, both the heating value of syngas and cold gas efficiency decrease. This could be as a result of the decrement of the main fuel components (CO, H<sub>2</sub> and CH<sub>4</sub>) when equivalence ratio is increased.

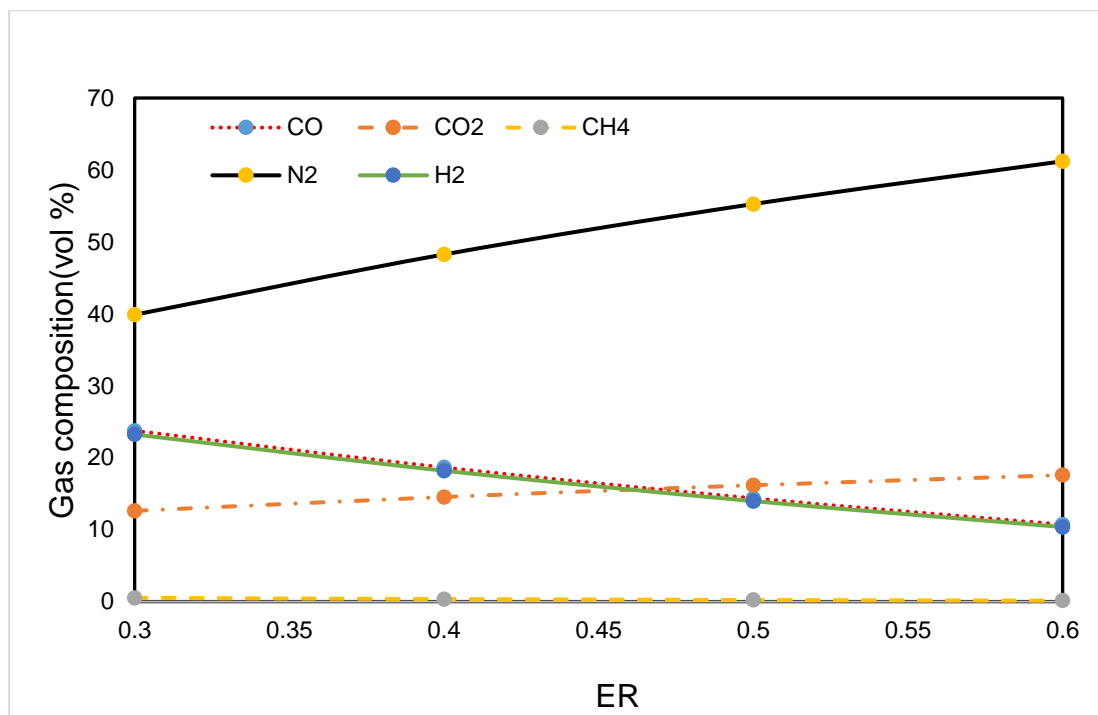


Figure 4.2: Syngas composition variation with equivalence ratio (A1)

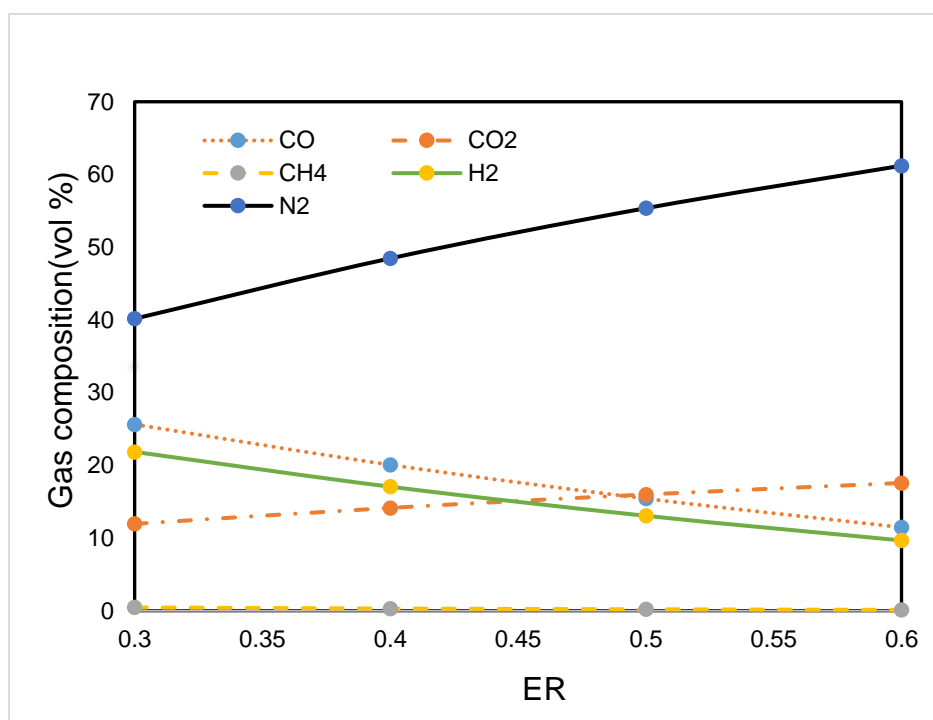


Figure 4.3: Syngas composition variation with equivalence ratio (A2)

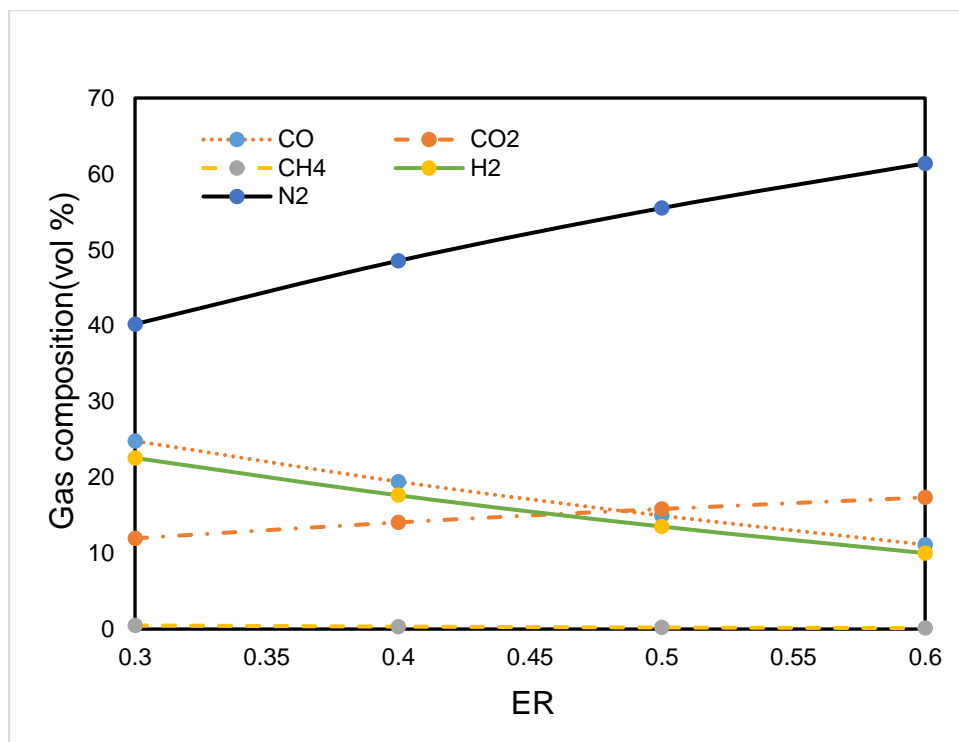


Figure 4.4: Syngas composition variation with equivalence ratio (A3)

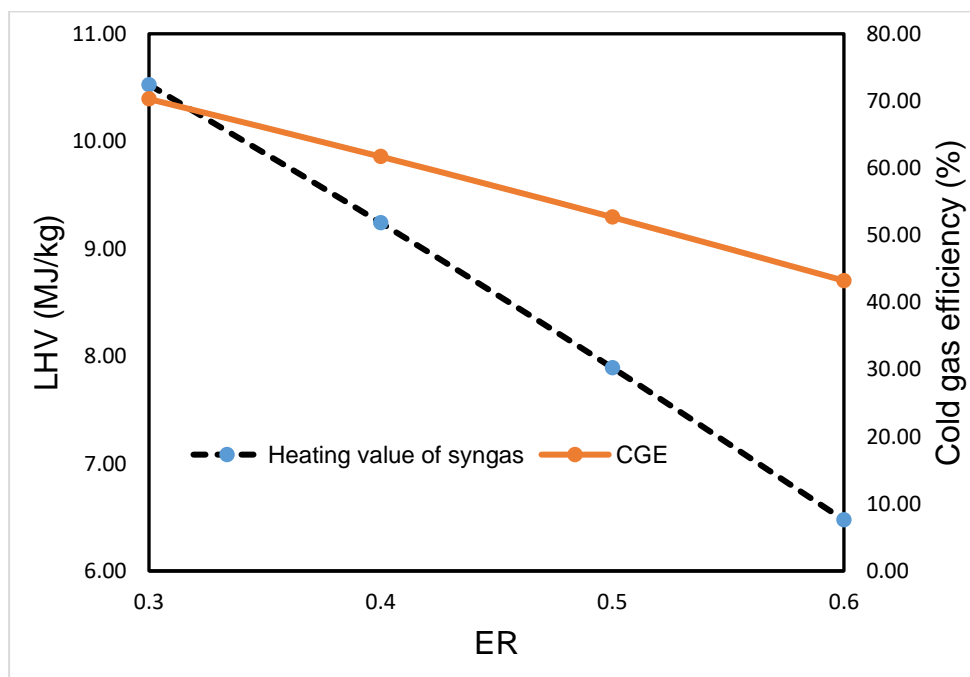


Figure 4.5: Effects of equivalence ratio on syngas heating value and cold gas efficiency

#### 4.3.2.2 Effects of moisture

The moisture content of biomass differs between different biomass materials and plays an important role in gasification efficiency and performance. The effect of moisture content on the gasifier performance was evaluated. To study the effect of moisture content on syngas composition, heating value and cold gas efficiency, temperature and equivalence ratio were kept fixed at 1100K and 0.3 respectively. The CPH sample with the highest moisture content (B3, 13.21%) and the CPH sample with the lowest moisture content (F2, 4.63%) were selected for the moisture test in addition to two other random samples (C1, 7.81% and B4, 10.06%). It can be seen from Figure 4.5 that the percentage composition of methane was very low (0.40-0.51%) and almost constant with variation in moisture content. The percentage composition of inert Nitrogen as expected was also relatively constant with changes in moisture content. The composition of hydrogen in the syngas increased with increase in moisture content. The only exception was CPH sample C1 which showed a higher hydrogen composition than CPH B4 and CPH B3 although both had higher moisture contents. Carbon dioxide exhibited akin trend to what was observed for hydrogen. While the CPH sample with the highest moisture content (B3) exhibited the highest carbon dioxide composition, the lowest carbon dioxide composition was not exhibited by the sample with lowest moisture content (F2). On the contrary, with the exception of CPH B4 which showed higher carbon monoxide composition than CPH C1, the carbon monoxide distribution in the syngas generally decreased as moisture content increased. This may be due to the increase in the proportion of carbon dioxide with upward variation in moisture content. A similar trend in behaviour for various other biomass has been reported by Zainal et al [165].

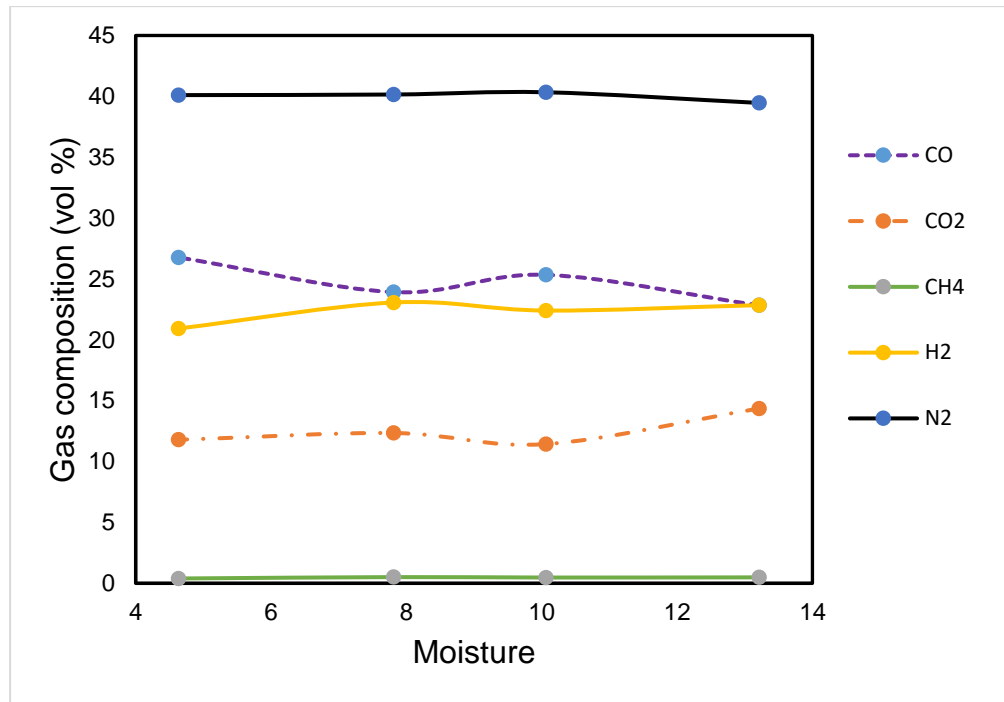


Figure 4.6: Effects of moisture on gas composition

#### 4.3.2.3 Effects of gasification temperature

Gasification temperature plays a crucial role in the performance of a gasifier. Temperature influences various aspects of the gasification process including evaporation of moisture from feedstock and eventually impacts on syngas quality. Looking at CPH samples C1 and A1 in Figures 4.6 and 4.7 respectively, it was observed that an increase in temperature from 900K to 1100K caused an increase in the carbon monoxide and hydrogen gas composition of the syngas while methane, carbon dioxide, and nitrogen compositions of the syngas decreased continuously.

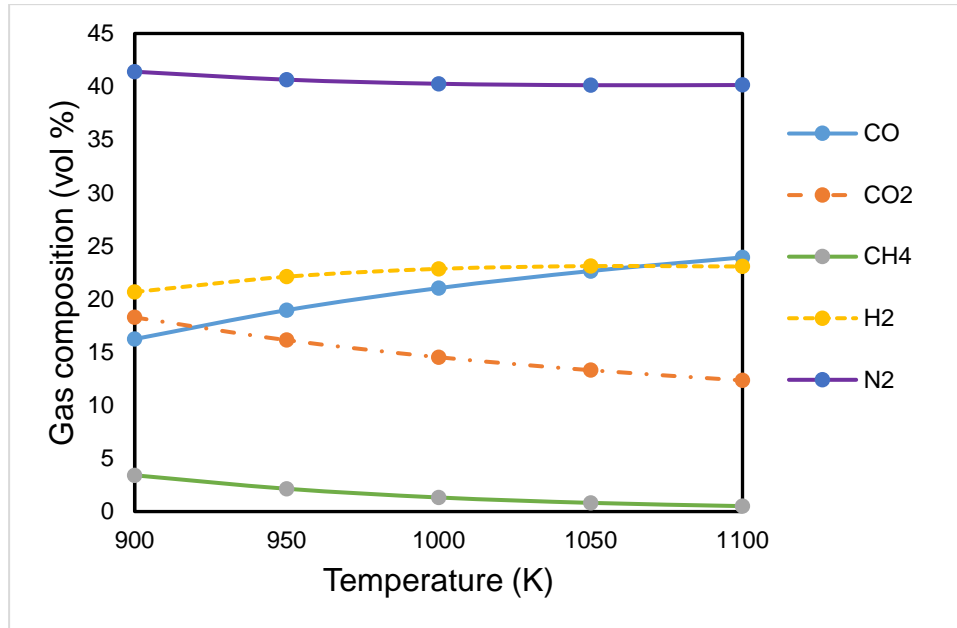


Figure 4.7: Effect of temperature on gas composition (CPH C1)

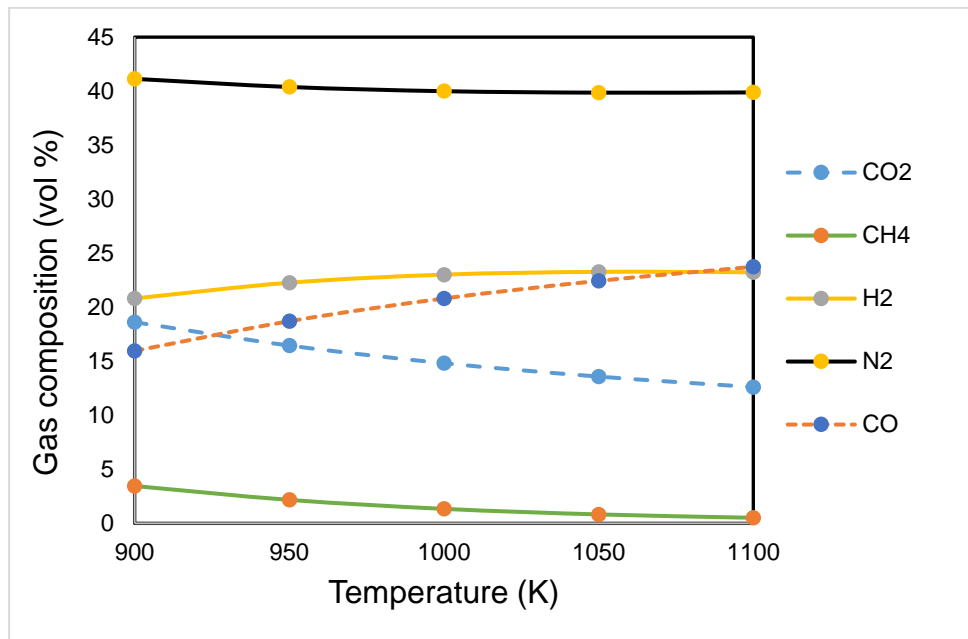


Figure 4.8: Effect of temperature on gas composition (CPH A1)

In Figures 4.8 and 4.9, the effect of temperature on heating value and cold gas efficiency are analysed. It was observed that an increase in temperature increased

both the heating value and cold gas efficiency. The increase in cold gas efficiency was due to the increase in heating value as temperature was increased. However, there was an optimum temperature beyond which any further increase in temperature caused a decrease in heating value and cold gas efficiency. Thus, the maximum point of efficiency for an effective gasification process was achieved at 1050K. For temperatures higher than 1050K, there was a dip in cold gas efficiency and heating value, although the variation in results were very small and negligible.

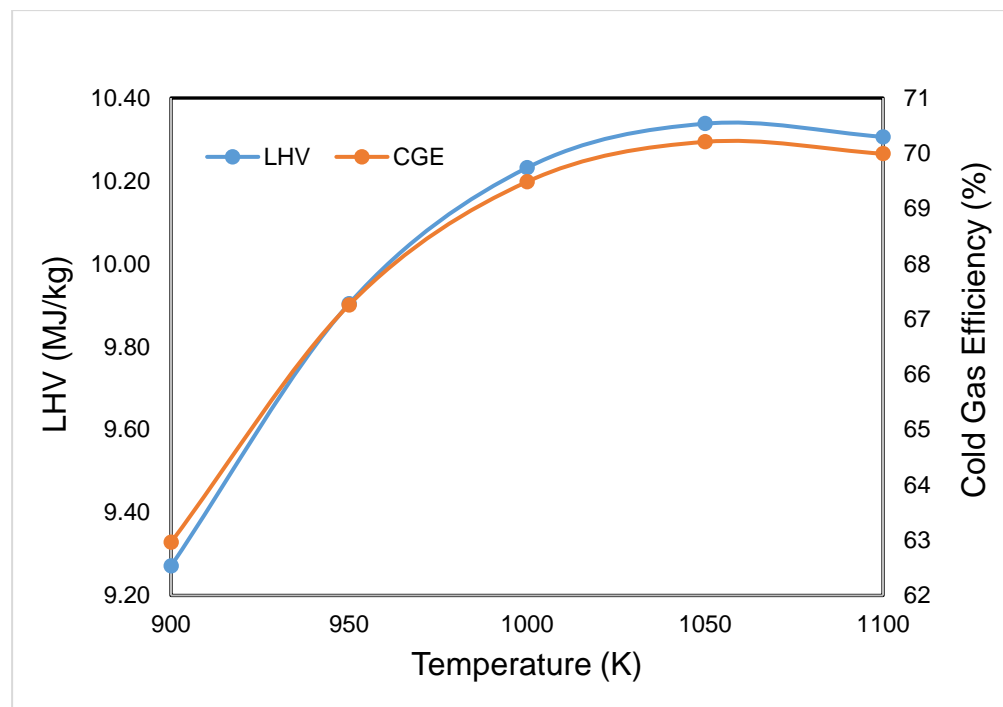


Figure 4.9: Effect of temperature on heating value and cold gas efficiency (CPH C1)

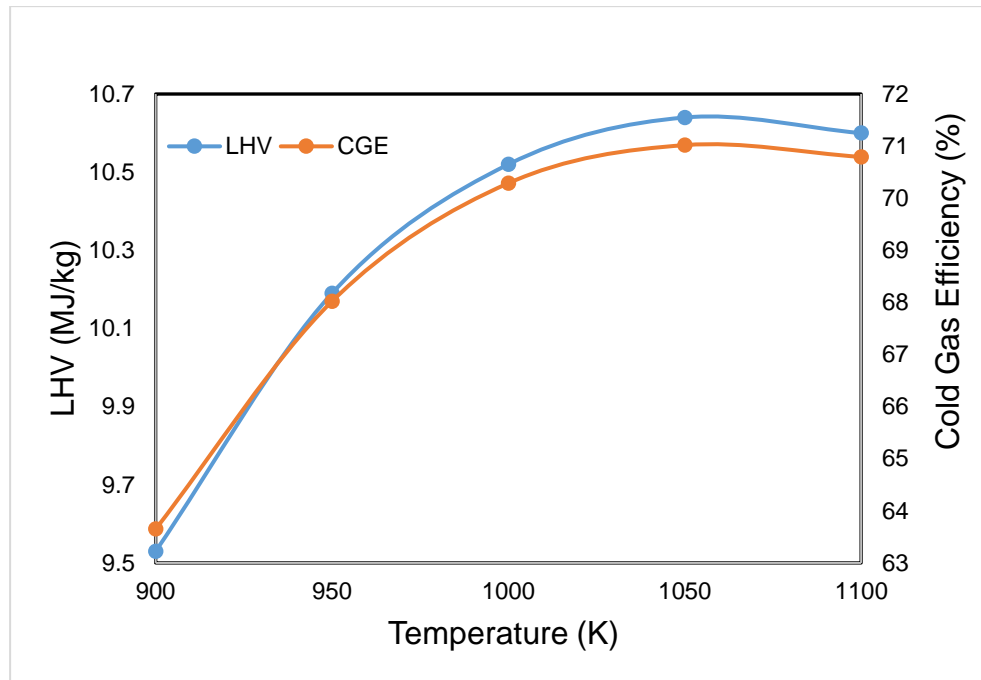


Figure 4.10: Effect of temperature on heating value and cold gas efficiency (CPH A1)

#### 4.4 Concluding Remarks

A thermodynamic equilibrium model for downdraft biomass gasifiers was created so that the composition of producer gas produced by CPH gasification could be calculated. The developed model was then utilised to perform a simulation of the gasification of Ghana's CPH. The outcomes predicted by the present model were found to be consistent with those predicted by other researchers who had built models that were conceptually comparable to the current one. Additionally, the impacts of equivalence ratio, moisture content, and gasification temperature, on the output of producer gas were examined. When the equivalence ratio was increased, the CO, H<sub>2</sub>, and CH<sub>4</sub> contents of the producer gas, which together comprise the primary component of the gas, all dropped. As was predicted, both the heating value of syngas and the efficiency

of cold gas decreased with an increase in the equivalence ratio. On the other hand, an increase in the equivalence ratio led to an increase in the mass fraction of nitrogen gas and carbon dioxide.

The percentage composition of methane and nitrogen gas were relatively constant, with only marginal variations as moisture content increased. As the amount of moisture grew, the mass fractions of hydrogen and carbon dioxide in the producer gas also rose. In most cases, a decrease in carbon monoxide percentage was seen in the producer gas as a result of an increase in moisture content. When the temperature of the gasification process was increased, the mass percentage of carbon monoxide and hydrogen gas in the producer gas likewise grew. On the other hand, the proportions of methane, carbon dioxide, and nitrogen gas in the producer gas decreased. As the temperature of gasification rose, both the heating value and the efficiency of the cold gas rose as well. At 1050 degrees Celsius, the gasification process finally reached its full efficiency.

The mathematical model has predicted the composition of the producer gas during the gasification of CPH. However, there is a need to validate the mathematical model using experimental data. Some studies use experimental data from literature to verify their models, but this thesis would generate its own experimental data from a 5kWe pilot-scale downdraft gasifier that runs on CPH. As a result, Chapter five would evaluate the performance of the pilot-scale downdraft gasifier system and use the experimental data to validate the mathematical model.

## CHAPTER FIVE

### 5.0 EXPERIMENTAL EVALUATION OF CPH GASIFICATION POWER SYSTEM

#### 5.1 Experimental setup

The experimental set up consist of a blow-type downdraft gasifier, a feeding system, a start-up system, an air supply system, gas cleaning and cooling system, a resistive load, three-phase power generator, PID controller, and a gas analyzer.

A labelled image of the experimental set up is shown in Figure 5.1.

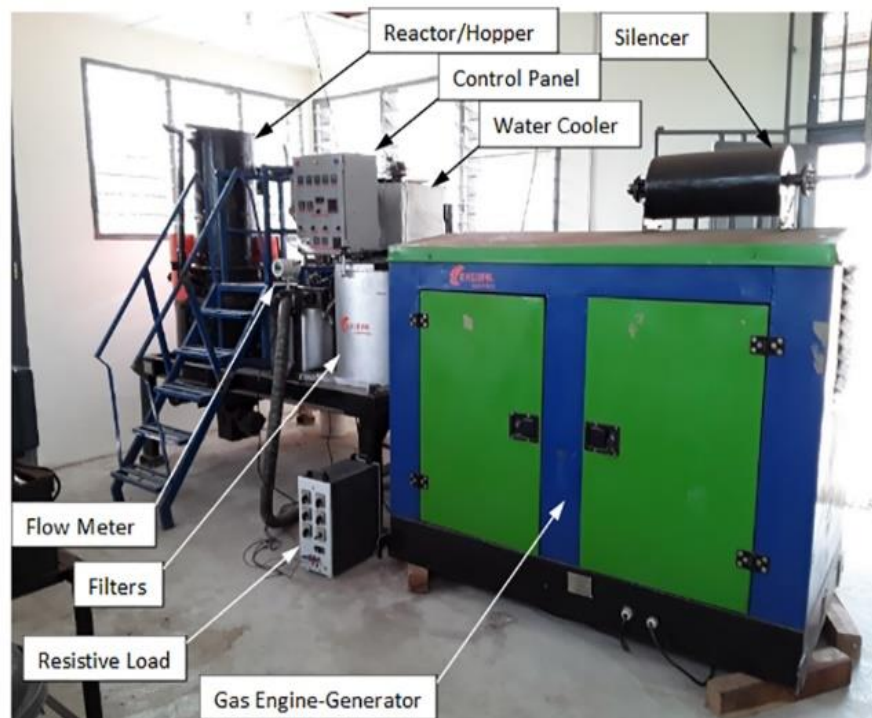


Figure 5.1: 5 kW gasifier-generator set with various compartments labelled.

The gasifier is a cylindrical reactor with an internal diameter of 460 mm and a total height of 900 mm. It is built of carbon steel with an internal coating of refractory material, surrounded by an insulating blanket for safety and also to control heat loss. Biomass is fed into the gasifier through the hopper at the top

of the reactor. An ignition pot and a blower sit at the upper part of the reactor. The blower supplies air to the reactor via the ignition pot and an air valve. An agitator/shaker is mounted at the top of the gasifier to avoid bed bridging during gasifier operation. The agitator/shaker produces mild vibrations at intermittent intervals which ensures continuous downward flow of feedstock into the reactor. The intermittent vibrations also help to remove the ash deposits produced during gasification. At the bottom of the gasifier is a perforated cast iron rotating grate to continuously dispose of ash from the gasifier bed. Six K-type thermocouples are used to measure the temperature distribution inside the gasifier. An electrical load is applied to the generator and the power output from the engine is measured. Electrical parameters such as voltage, current, frequency were measured by a power meter sited on the control panel. A gas flow meter is sited between the final filter and the engine gas inlet. Ultimately, a clean gas pipe links the final filter to the gas engine, where the syngas is burned to generate electricity. The gas engine generator is 4 stroke, 2 cylinder, naturally aspirated and water cooled. The A.C. alternator produces three phase 415V at 1500rpm/50Hz. Figure 5.2 shows the design specification of the gas engine generator. A gas sample point is positioned near the gas inlet point and connected to a wall mounted gas analyzer to measure CO, CO<sub>2</sub>, CH<sub>4</sub> and H<sub>2</sub>.

Make	Enersol Biopower
Fuel Mode	100% producer gas based
No. of Set	1 No.
Capacity	5kVA
Rated Current (Amps/Phase)	26 AMP (Single Phase) & 8 AMP (Three Phase)
No. of cylinders	2
Aspiration	Natural
Phase	Single Phase/Three Phase
Alternator Make	Kirloskar
Governor	Electronic governor
Control Panel	Basic control panel
Frequency	50Hz
Voltage	415 - 420

Figure 5.2: Technical specification of the biomass engine generator

The biomass gasification system for turning biomass into value added product gas is composed of four main compartment – a biomass feeder/hopper, a reactor, a gas cooler, and a gas cleaner. The system also contains a gas engine-generator for converting produced gas into electrical power. Aside the four main parts of the gasification system, biomass feedstock needs to undergo pre-processing such as drying, size reduction, and screening or classification to prepare the feedstock for the gasifier. In the following section, the four main process compartment of a gasification system is considered in more detail.

### ***5.1.1 Hopper***

The biomass hopper is 460 mm in diameter and 900 mm in height and serves as a fuel tank feeding the reactor. The function of the hopper is to convey feedstock from storage to the reactor while preventing the uncontrolled entry of air or the escape of product gas. Biomass feedstock can be fed into the hopper either

manually or by using a conveying system. However, due to the small nature of the system and availability of labour, manual loading of feedstock is more appropriate. Although the hopper is designed to take biomass in any form, feedstock pellets are preferred due to their well-defined shape, mechanical strength and improved calorific value compared to loose materials. Moreover, unlike feedstock pellets, other fuels can complicate the reactor operation by creating large irregularities in the fuel bed. Figure 5.3 shows the gasifier feed column with the various parts well labelled. The use of the shaker attached to the hopper is to produce intermittent vibrations and ensure the constant flow of biomass into the reactor.

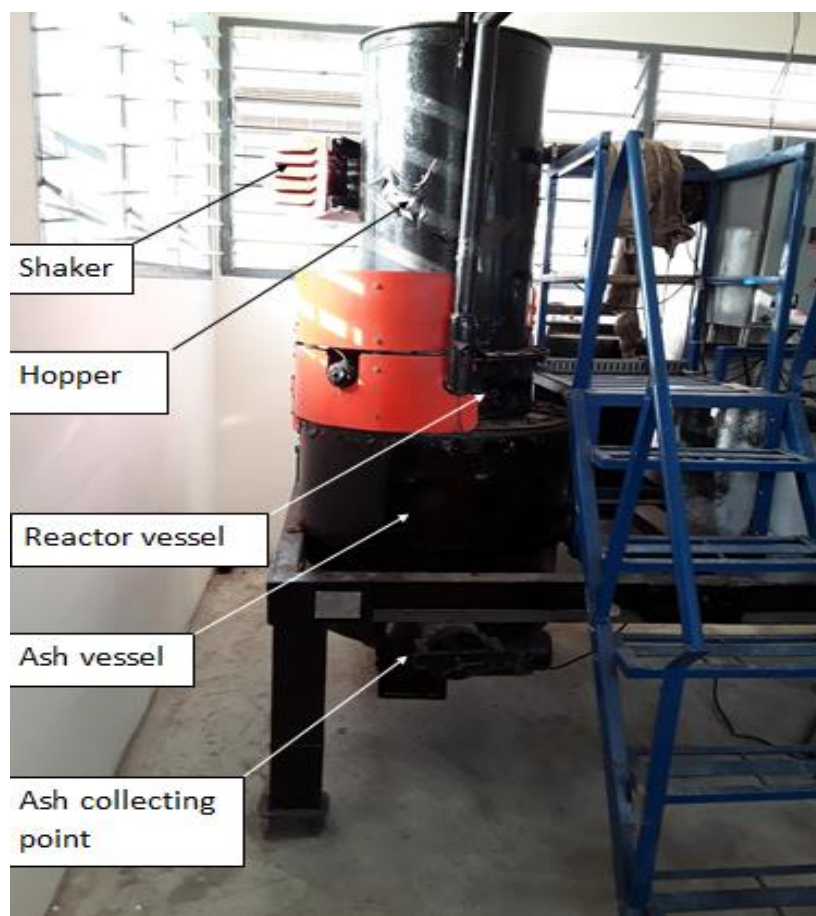


Figure 5.3: Gasifier feeding system

### ***5.1.2 Reactor***

The reactor is where various complex physical and chemical processes take place. It is configured to accommodate the energy balance of the chemical reactions. In gasification system, it is the reactor that binds biomass feedstock with the gasifying agent and also allows reaction to take place.

The reactor is linked to the drying bucket and uses pyrolysis, combustion, and reduction processes to decompose biomass and produce syngas. An ignition port and an air inlet are located at the side of the reactor. When negative pressure is created within the system, the air needed for the combustion is introduced through this inlet. On the other side of the reactor is an exhaust. The gasifier's heart is the reduction bell, which is located inside the bottom reactor chamber, and this is where most of the crucial oxidation and reduction reactions occur.

A charcoal-holding and fine-ash-filtering ash grate is situated beneath the bell. A grate shaker is connected to the ash grate by a stainless steel bar outside the reactor at the lower section. It is activated on a regular basis during gasification. Furthermore, an ash auger located inside the channel between the ash container and the bottom of the reactor chamber can move clockwise and counter-clockwise to draw the remaining ash out of the reactor.

### ***5.1.3 Cooling and Cleaning System***

The gas produced by the gasifier comes out at a high temperature. The hot gas, particularly from the ESB-R series often contains nearly no tar and some amount of fine particles of ash and soot. The temperature of the hot gas is then reduced until ambient temperature is reached. The primary function of gas cooling is to increase the density of the gas in order to maximise the amount of combustible

gas entering the cylinder of the engine at each stroke. Cooling also aids in gas cleaning by preventing the condensation of moisture in the gas after it has been combined with air prior to engine intake. The hot gas passes out of the reactor with pollutants embedded in it and hence requires cleaning to attain the minimum requirements for use in engines. Where ash and tar are generated at all, they need to be handled. The cooling and cleaning system is capable of cooling down all the gas produced by the gasifier in order to condense the moisture and tar, before passing it through a bed of filters. The filtration system is explained below:

#### **5.1.3.1 Filtration System**

Gasifiers have been built with specific throat size and throat nozzle in consideration to provide an intensified hot zone with strong turbulence and mixing to ensure almost complete tar cracking in the gasifier itself. In other words, tar cracking takes place during the operating range of the gasifier thereby leaving the product gas almost tar-free. There is however, some impurities and tar always contained in the raw gas which needs further cleaning. The cleaning sub-system of the gasifier is made up of 1 charcoal filter, 1 cyclone filter, 2 sawdust filters, and a cotton filter (see Figure 5.4).

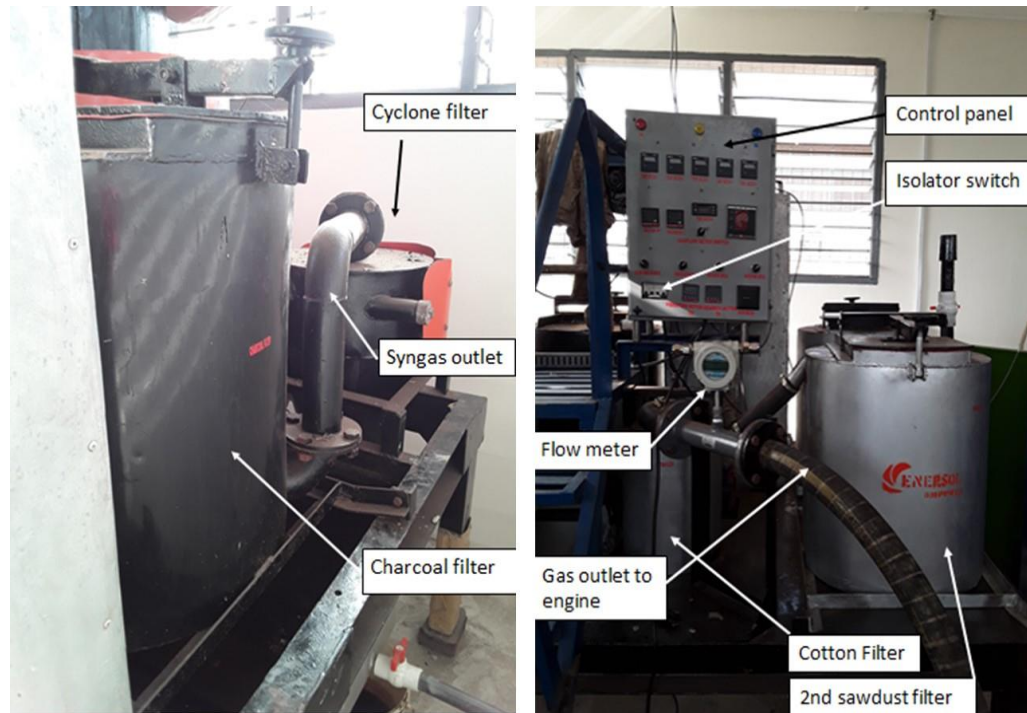


Figure 5.4: Gasifier filters

The charcoal filter is used to ensure that condensed particulates are trapped at this point. Incorporation of such a device allows gasifiers to be coupled to turbo-charged and after-cooled engines for the first time. This filtering system also negates the harmful effect of gas contamination and its associated impacts on engine parts. The cyclone filter cleans and cools the gas coming from the charcoal filter whereas the cotton filter removes both tar and particulates and can also be rejuvenated on line for extended uninterrupted operation.

## 5.2 Materials and methods

The CPH feedstock used in this study was acquired from local plantations within the Ashanti region of Ghana. The CPH feedstock was dried in a solar dryer to reduce the moisture content. On display in Figure 5.5 is an image of the solar dryer used in drying the samples for the gasification process.



Figure 5.5: Solar dryer filled with some cocoa pod husk

A hand-held moisture meter was used to check the moisture level of the samples in the solar dryer at intermittent intervals until moisture content was below 20%. It was then prepared for the gasification experiment by crushing down to a particle size of 10-30 mm using a biomass crusher (see figure 5.6).



Figure 5.6: Biomass Crusher

The moisture content of the crushed feedstock was determined by means of a drying oven before each gasification experiment. A clean container was initially weighed and the balance was zeroed. The container was filled with 30 gram of crushed CPH sample and its weight was recorded as  $W_1$ . The filled container was placed into the oven for 24 hours at a controlled temperature of 105 °C. The container was taken out of the oven after 24 hours and allowed to cool down to room temperature in a desiccator. It was then weighed again and recorded as  $W_2$ . The difference between the dry weight ( $W_2$ ) and the moist weight ( $W_1$ ) was calculated as a percentage of the dry weight ( $W_2$ ) to get the moisture content. The process was repeated before each gasification run.

Due to time constraints and lack of resources, all the 24 samples characterised could not be experimentally evaluated. Since Ashanti region had the most promising energy potential, samples E1, E2, E3, and E4 were used for this section of the analysis. Table 5.1 shows the thermo-physical properties of the study sample.

Table 5.1. Properties of sample materials

Parameter	CPH-1	CPH-2	CPH-3	CPH-4
<i>Proximate analysis (PA) wt.%</i>				
Volatiles	67.3	62.34	63.37	68.65
Fixed carbon	24.83	22.30	20.30	21.37
Ash	7.8	9.54	11.35	9.98
HHV(MJ/kg)	19.21	17.53	16.97	18.18
<i>Ultimate analysis (UA) wt.% (dry basis)</i>				
Carbon	43.81	42.37	41.18	42.32
Hydrogen	5.79	5.73	5.35	5.76
Nitrogen	0.77	1.33	1.68	1.42
Sulfur	0.12	0.16	0.16	0.08
Oxygen	49.52	50.57	51.79	50.43
HHV(MJ/kg)	16.82	16.11	15.08	16.12

---

*Properties*

Average (PA) HHV(MJ/kg) 17.97

Average (UA) HHV(MJ/kg) 16.03

Combined average 17.00

HHV(MJ/kg)

---

### **5.3 Test procedure**

The operation of the gasification system occurs at atmospheric pressure. The reservoir under the gasifier and the circular trough at the top of the gasifier were filled with water for gas cooling and also to prevent gas escape from the gasifier. Fresh charcoal (~ 400 g) was placed on the gasifier bed above the grate up to the level of air nozzles. The charcoal provided the initial heat needed in the reduction zone to start up the gasification process. The hopper of the gasifier was manually loaded with at least 30 kg of feedstock, and the lid was secured. This was done to ensure that the hopper was filled to within about 250 mm of its capacity. The ignition pot at the upper part of the gasifier was filled with some sawdust and about 20 ml of gasoline poured into it to aid ignition and combustion. The gasifier was fired up from the ignition pot and the blower turned on to supply air into the gasifier from central air distribution nozzle and bustle pipes. A flammable gas was generated after about 15 min, which was directed through a number of filters to remove particulates and tars that were capable of damaging the gas engine. After filtration, the producer gas was introduced into the gas

engine and burned. Although it took about 30 min for a steady state gasifier operation (i.e. the temperature in oxidation and reduction zone were nearly constant) to be reached, the start of each run was considered as the time at which a flammable gas was generated and the gas engine generator switched on. A resistive load was applied to the generator and the power output from the engine was measured. A gas flow meter recorded the volume of the producer gas flow rate. Temperatures at various locations around the gasifier were measured by K-type thermocouples every 10 min. Figure 5.7 shows the position of all thermocouples around the gasifier system with T1 located in the gasifier bed, T2 in the gasifier outlet, T3 on the charcoal filter, T4 on the cotton filter, T5 on the sawdust filter and T6 on the water cooler.

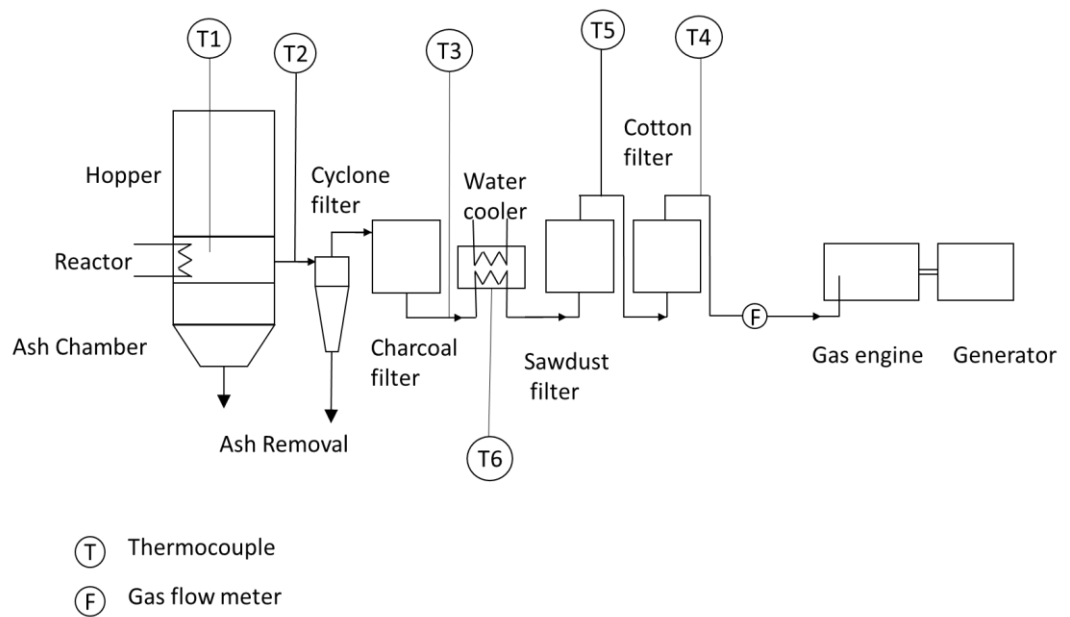


Figure 5.7: Schematic of the CPH gasifier showing the location of all thermocouples

A wall mounted gas analyser connected to the gas engine by syringes was used to sample the producer gas for CO, CO<sub>2</sub>, CH<sub>4</sub> and H<sub>2</sub> at 10 min intervals.

Figure 5.8 is an image of the gas analyser that was used for monitoring and sampling gases from the gasifier.

Electrical parameters like voltage, current and frequency were also recorded at 10 min intervals. Mass consumption rate of the biomass fuel was determined by measuring the level of biomass in the hopper at the start of the experiment, then checking the level at the end of the experiment.

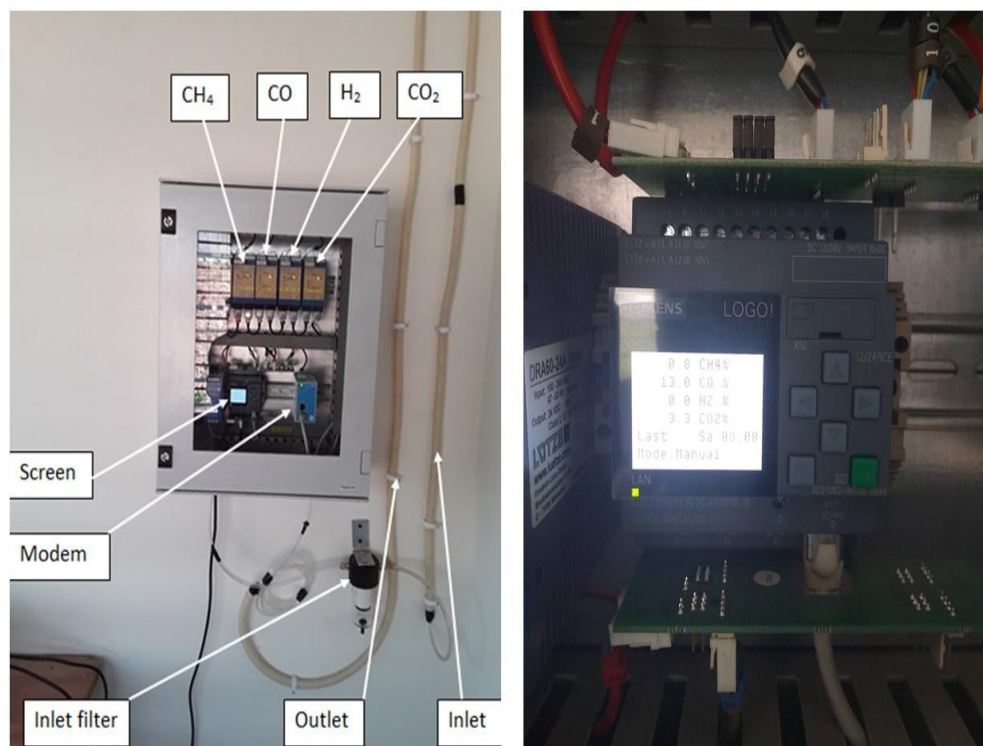


Figure 5.8: Syngas analyser for gas sampling

#### 5.4 Calculation of the experimental results

In order to evaluate the performance of the CPH gasifier, key performance indicators such as calorific value, cold gas efficiency, carbon conversion efficiency, electrical power, engine efficiency and overall efficiency were determined using the equations described below; The higher heating value

(HHV) was calculated from the composition of the CPH using the results of the PA and UA as shown in equations 5.1 and 5.2 respectively.

For PA;

$$HHV = 0.3536FC + 0.1559VM - 0.0078ASH \quad 5.1$$

Where FC is the fixed carbon and VM is the volatile matter

For UA;

$$HHV = 0.3491C + 1.1783H + 0.105S - 0.1034O - 0.0151N - 0.0211ASH \quad 5.2$$

Where C, H, S, O, and N are Carbon, Hydrogen, Sulphur, Oxygen, and Nitrogen respectively.

The energy available in the CPH ( $Q_{fuel}$ ) is expressed in equation 5.3;

$$Q_{fuel} = m_{fuel} * HHV \quad 5.3$$

Where  $m_{fuel}$  is the mass consumption rate of CPH

The energy available in the combustible gas ( $Q_{cg}$ ) is calculated from equation 5.4.

$$Q_{cg} = V_{gas} * (Y_{CO} * LHV_{CO} + Y_{CH_4} * LHV_{CH_4} + Y_{H_2} * LHV_{H_2}) \quad 5.4$$

Where  $V_{gas}$  is the gas flow rate, Y is the volumetric concentration of the individual gases and LHV is the lower heating value. The values for HHV,  $LHV_{CO}$ ,  $LHV_{CH_4}$  and  $LHV_{H_2}$  used in equations 5.3 and 5.4, were taken as 17 MJ/kg, 11.6 MJ/Nm<sup>3</sup>, 32.8 MJ/Nm<sup>3</sup> and 9.9 MJ/Nm<sup>3</sup>, respectively.

Cold gas efficiency (CGE) is defined as;

$$CGE = Q_{cg}/Q_{fuel} \quad 5.5$$

The engine conversion efficiency is calculated from equation 5.6.

$$\eta_{conv} = W_{elec}/Q_{cg} \quad 5.6$$

Where  $W_{elec}$  is electrical power which can be calculated using equation 5.7

$$W_{elec} = I * V * \sqrt{3} \quad 5.7$$

I is current and V is voltage

The overall efficiency of the biomass gasifier system ( $\eta_{ov}$ ) is given as

$$\eta_{ov} = W_{elec}/Q_{fuel} \quad 5.8$$

The lower heating value (LHV) of the producer gas in MJ/m<sup>3</sup> can be estimated from the gas composition as follow;

$$LHV = [(10.79 * H_2) + (12.636 * CO) + (35.82 * CH_4)] \quad 5.9$$

Where H<sub>2</sub>, CO, and CH<sub>4</sub> are the volumetric concentrations of the components in the producer gas.

Carbon conversion efficiency (CCE) can be calculated as follow;

$$CCE = \frac{12*(CO+CO_2+CH_4)}{22.4*C} * V_g * 100\% \quad 5.10$$

Where C is the mass fraction of carbon in the biomass, from the ultimate analysis and  $V_g$  is the volume of the producer gas per unit weight of CPH (m<sup>3</sup>/kg).

$V_g$  which is also the gas yield (m<sup>3</sup>/kg) can be calculated using the gas flow rate ( $V_{gas}$ ) and the mass consumption as follows.

$$Vg = V_{gas}/m_{fuel}$$

5.11

## **5.5 Results and discussion**

The experimental results on CPH gasifier system are presented and analysed. The performance of the CPH-fed gasifier system is determined using parameters such as gas yield, cold gas efficiency, overall efficiency, and engine efficiency. The gas flow rate, and the producer gas composition are also analysed. The calorific value of the producer gas is determined based on the gas analysis. The mass consumption rate of CPH is calculated and the temperature profile at various zones within the gasifier studied.

### ***5.5.1 Temperature distribution in the gasifier***

The thermal efficiency of the CPH gasifier system like other thermochemical processes is temperature dependent [170]. There are four main reaction zones in the CPH downdraft gasifier: drying/moisture evaporation, pyrolysis, oxidation and reduction zones which are all influenced by temperature [171]. Figures 5.8 shows the bed temperature distribution at different points around the gasifier. It is also clear from Figures 5.8 that temperature measured at point T2 was always the highest. Since the hottest region in a downdraft gasifier is the partial oxidation zone [172], it can be deduced that the temperature measuring point of T2 may be located in the partial oxidation zone of the CPH gasifier system. Looking closely at Figures 5.8, it is highly likely that measuring point T1 is also located in the oxidation zone with T2. The high temperature in the oxidation zone helps in tar cracking to improve the calorific value of the producer gas [52]. Subsequently, temperature measuring point T6 may be located in the drying

zone, T5 and T4 in the pyrolysis zone, and T3 in the reduction zone. Nonetheless, it is not an easy task differentiating the four distinct zones of a downdraft gasifier [172].

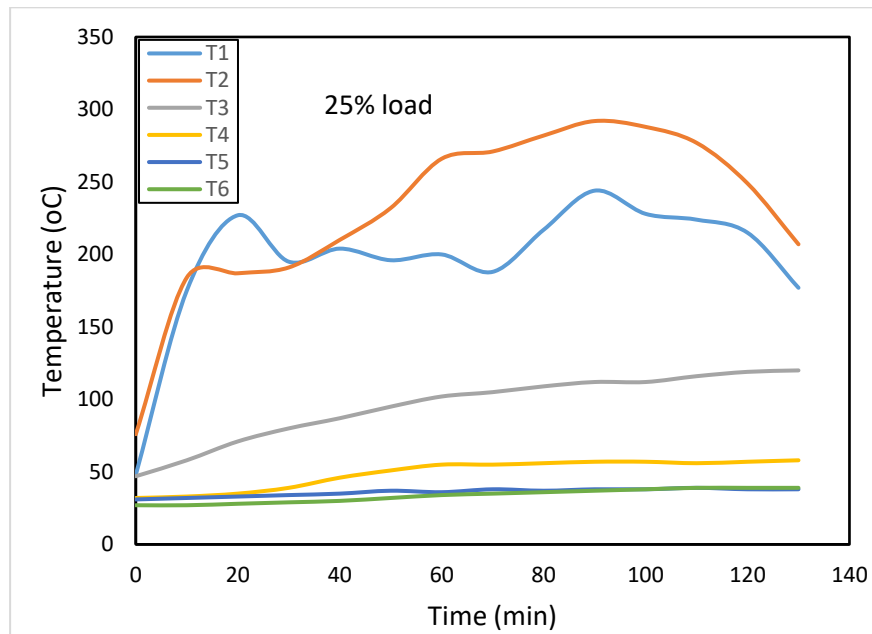


Figure 5.9a

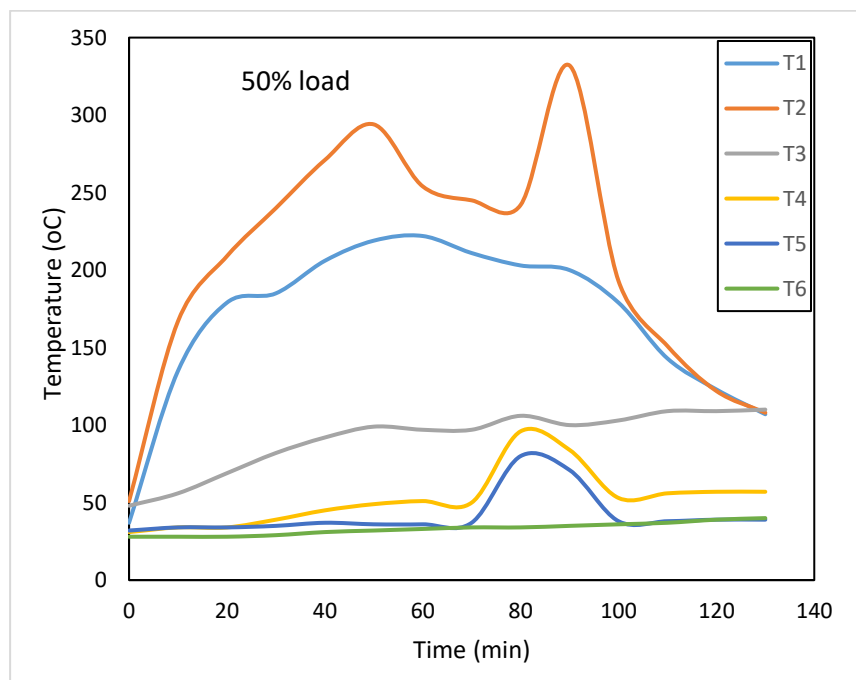


Figure 5.9b

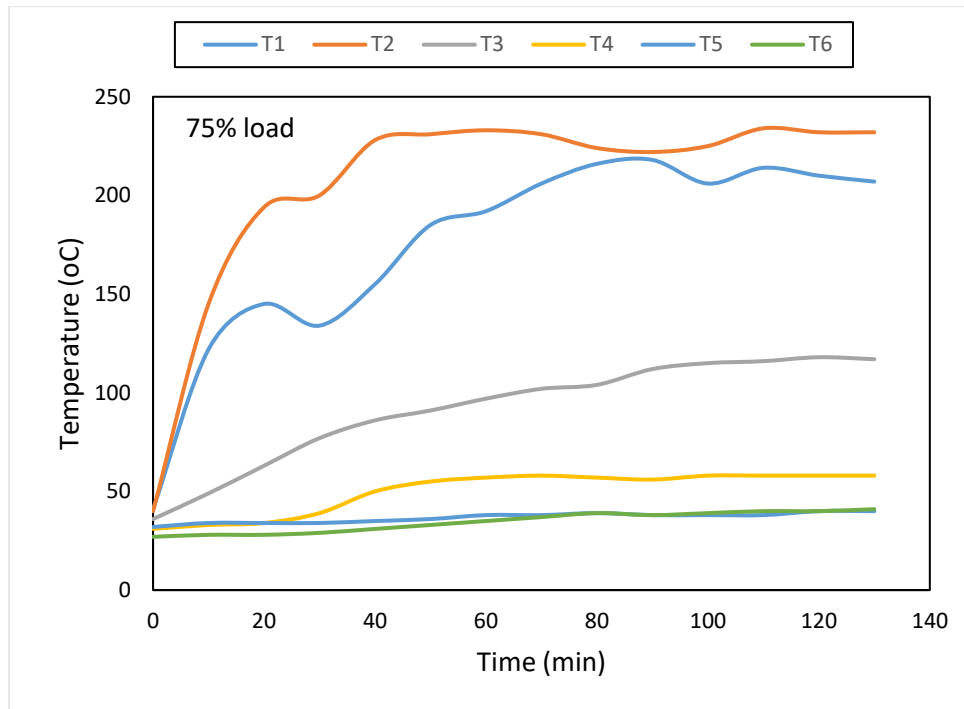


Figure 5.9c

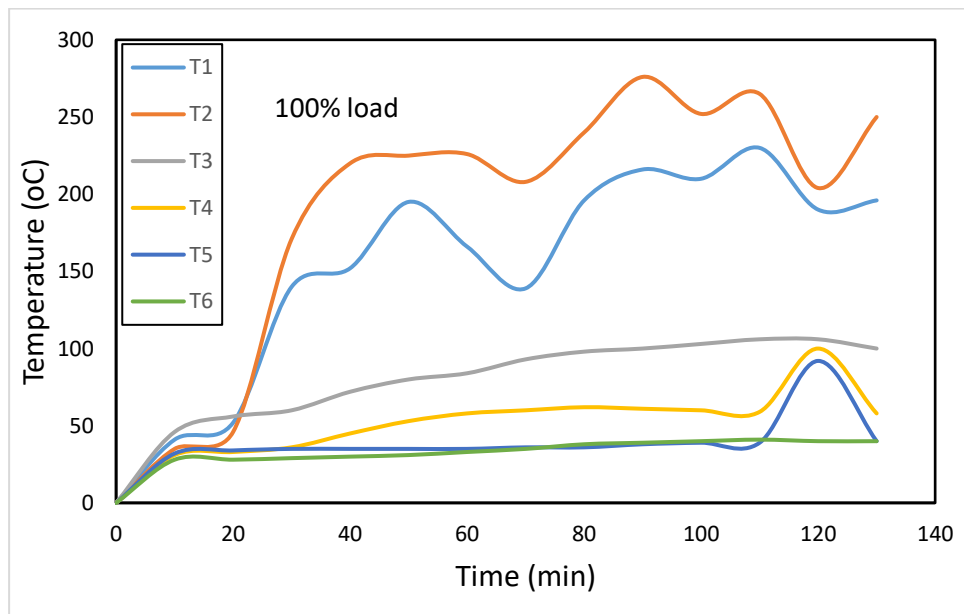


Figure 5.9d

Figure 5.9: Variation of temperature ( $^{\circ}\text{C}$ ) with time at different loads

### ***5.5.2 Composition of producer gas and electrical power***

Samples of producer gas from the CPH gasification were collected at ten minutes intervals and sampled for methane, carbon monoxide, carbon dioxide, and hydrogen. The composition of producer gas was analysed using an installed gas analyzer connected to the gasifier via syringes. Figure 5.10 shows the variation of combustible gas components in dynamic proportions with the electrical energy potential of the producer gas. The composition of CO<sub>2</sub> is also plotted to help explain the gasifier behaviour during operation. It can be seen from Figure 5.10 that the CO component of the producer gas was the highest in terms of percentage whereas H<sub>2</sub> gas recorded the lowest percentage composition. Although the percentage of H<sub>2</sub> gas in the producer gas was quite low, the percentage composition of CH<sub>4</sub> in the producer gas was substantially high (6.1-7.6%) compared to similar biomass resources. It is worth noting that the percentage composition of CO<sub>2</sub> in the producer gas was similar to that of CH<sub>4</sub>. It can be observed that the volumetric concentration of H<sub>2</sub> peaked during the first 15-25 min and then gradually reduced as time progressed for most of the runs. The low volumetric concentration of H<sub>2</sub> may be attributed to the very reactive and light nature of H<sub>2</sub>. In like manner, H<sub>2</sub> has a high dependency on water provided by the drying and pyrolysis zone, hence once evaporation of the moisture in the feed was completed in the first few minutes of the gasification process, it dwindled. The lower temperatures in the CPH gasification process may have also resulted in the incomplete destruction of tar constituents which contain huge proportions of hydrocarbons. It quite clear from Figure 5.10 that an increase in H<sub>2</sub> is always complemented by a decrease in CO and an increase in CO<sub>2</sub>.

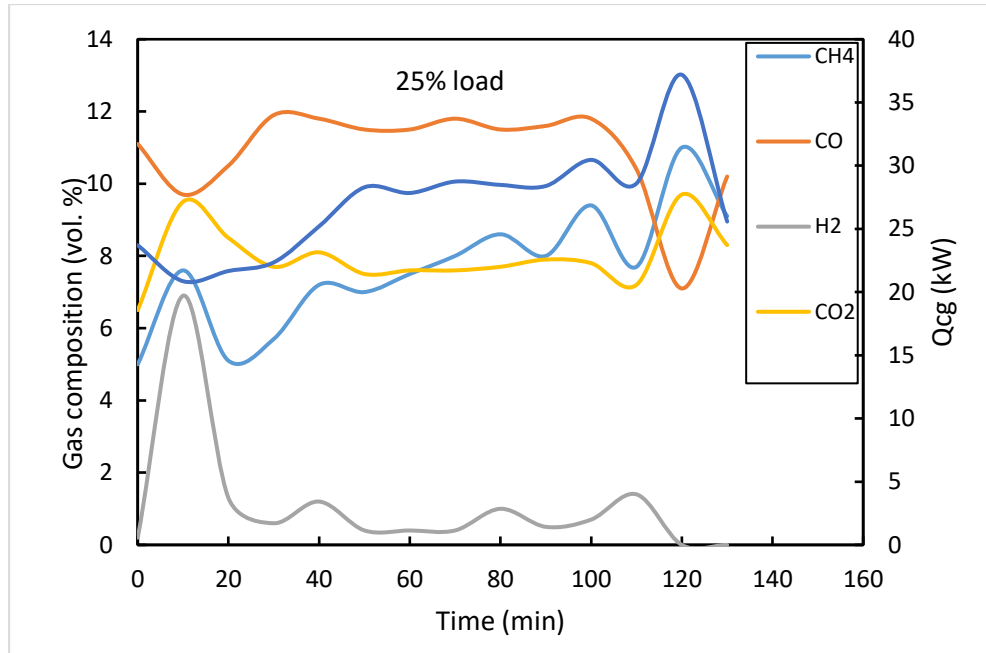


Figure 5.10a

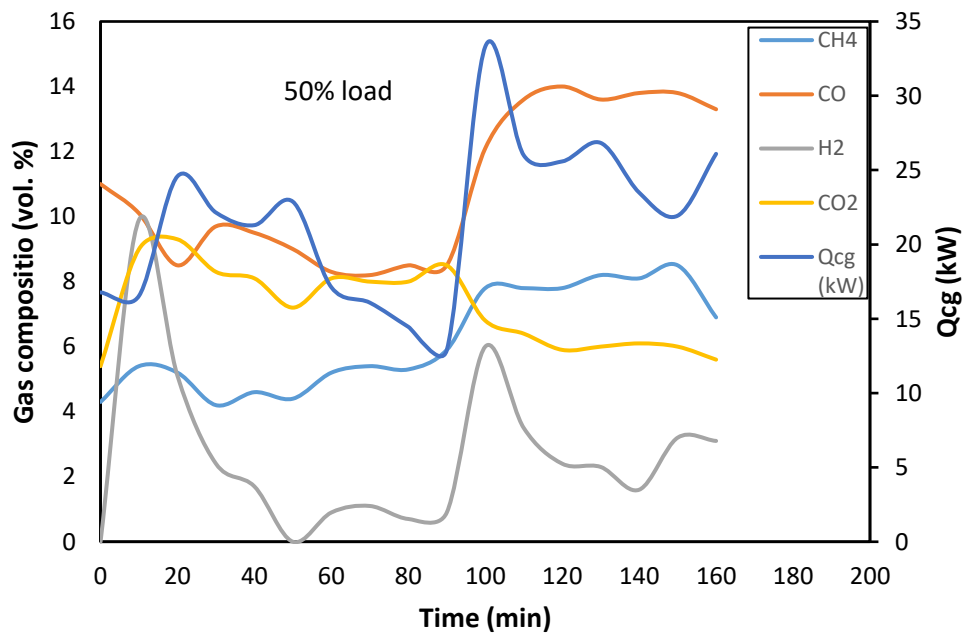


Figure 5.10b

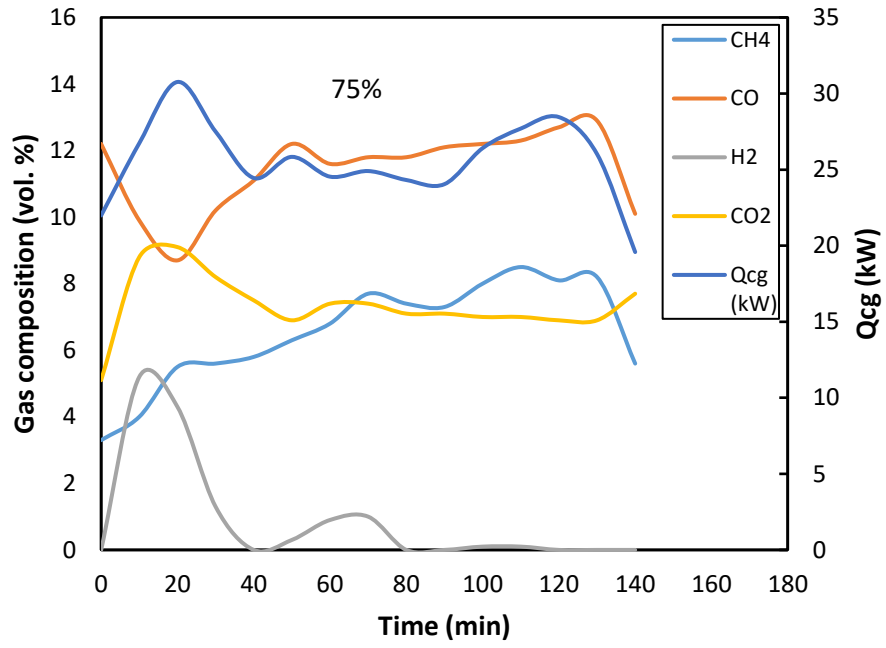


Figure 5.10c

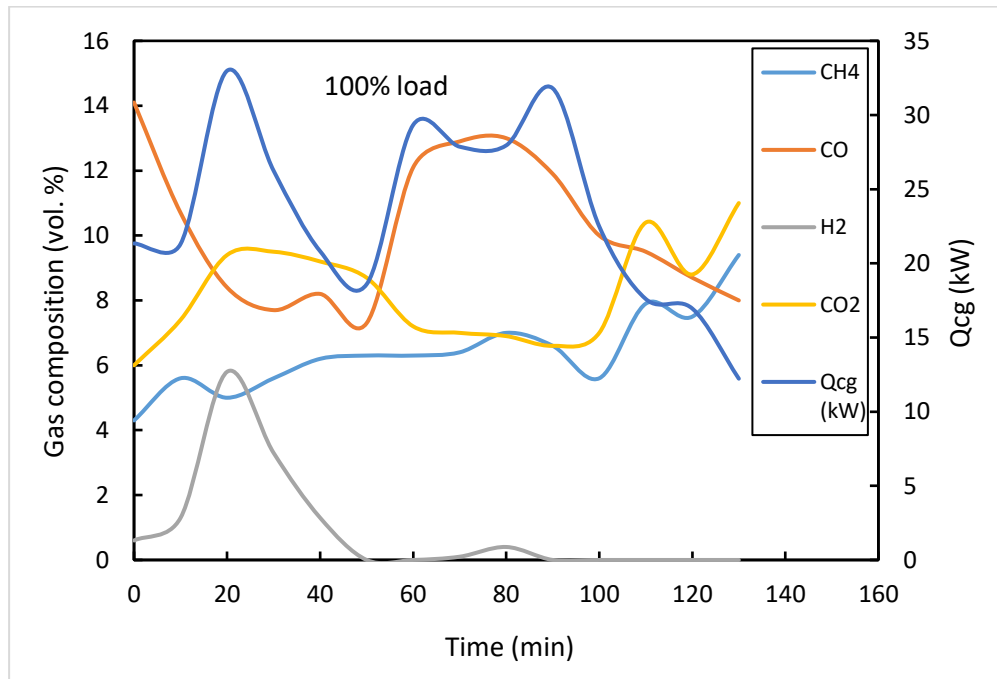


Figure 5.10d

Figure 5.10: Variation in gas composition and power generation potential of producer gas ( $Q_{cg}$ )

The variation in electrical energy of the producer gas with gas composition and time is presented in Figure 5.10. The electrical energy was calculated using the producer gas composition. CO, H<sub>2</sub> and CH<sub>4</sub> are the main components of the producer gas and hence responsible for the energy density, however low or high it may be. There is a similar variation trend in the calculated electrical energy of the producer gas and that of the gas composition. Generally, CH<sub>4</sub> has a higher calorific value than CO and H<sub>2</sub>, hence, its variation has a more significant impact on the electrical energy of the producer gas, although the higher volumetric concentration of CO also played an effective role. This is evident in Figure 5.10, as CH<sub>4</sub> concentration increases, electrical energy of the producer gas mostly increases.

### ***5.5.3 Fuel consumption and moisture content***

The mean CPH consumption for this experimental study was about 11.7 kg/h. The gas engine is rated at 5kW maximum over short periods but continuous maximum load of 4kW. At 1kW, consumption rate was 11.16 kg/h and at 4 kW, consumption rate was 11.25 kg/h. For 2 kW and 3 kW load, consumption rate was 10.73 kg/h and 13.46 kg/h respectively. Thus, the highest consumption rate was recorded at 3 kW load. This may be due to the comparatively low moisture content of the CPH feedstock used at that load, since the lower moisture content requires less energy for drying and therefore accelerates pyrolysis. Figure 5.11 gives a clear picture of the relationship between moisture content and mass consumption. It was observed that with the exception of one odd run at 2 kW load where a low consumption rate was recorded for a low moisture content, there was a general trend in which high moisture content reduced the

consumption and feeding rate of the CPH. This is in agreement with other studies such as Sharma and Sheth [173].

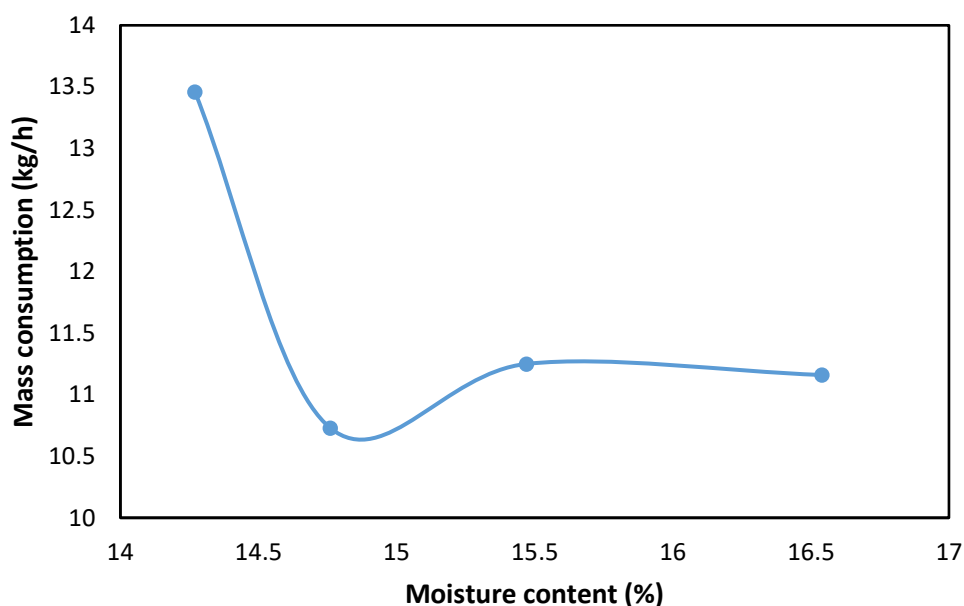


Figure 5.11: Variation in mass consumption with moisture content

#### ***5.5.4 Cold gas efficiency, carbon conversion efficiency, and gas yield***

Cold gas efficiency (CGE) is the ratio of energy in the producer gas per unit weight of biomass to the energy in the biomass material, whereas carbon conversion efficiency (CCE) is the measure of the amount of carbon in the feedstock that gets converted into producer gas. On the contrary, gas yield ( $V_g$ ) is the ratio of the volume of producer gas to the mass of feedstock supplied to the system. The gas yield was calculated from the fuel consumption and gas flow rate. The gas flow rate was between  $10.9 \text{ m}^3/\text{h}$  and  $37.24 \text{ m}^3/\text{h}$  while the average consumption rate was  $11.7 \text{ kg/h}$ . It was observed that the gas yield showed average values of  $1.95\text{-}2.25 \text{ m}^3/\text{kg}$ . Figure 5.12 shows the relationship between cold gas efficiency, carbon conversion efficiency, and gas yield.

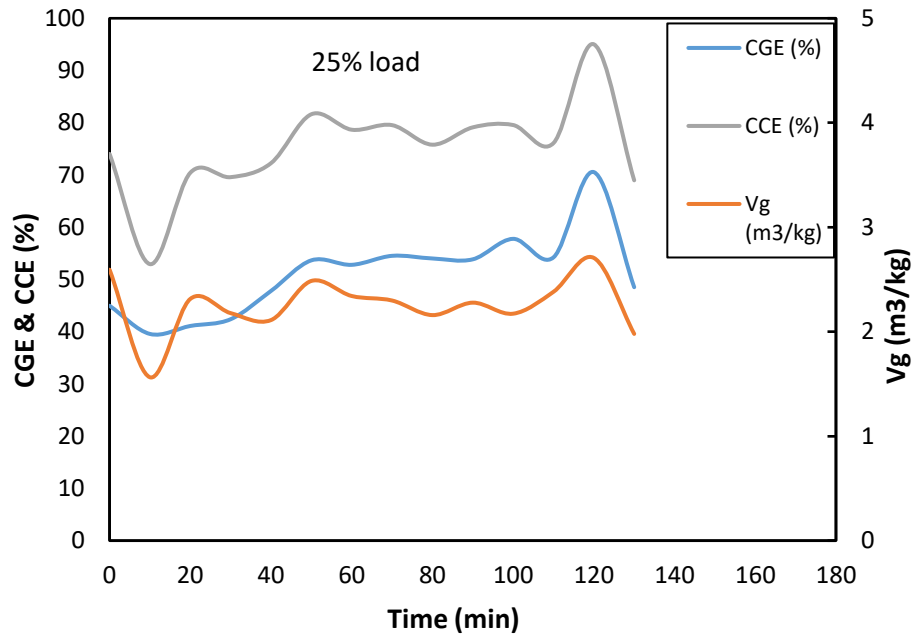


Figure 5.12a

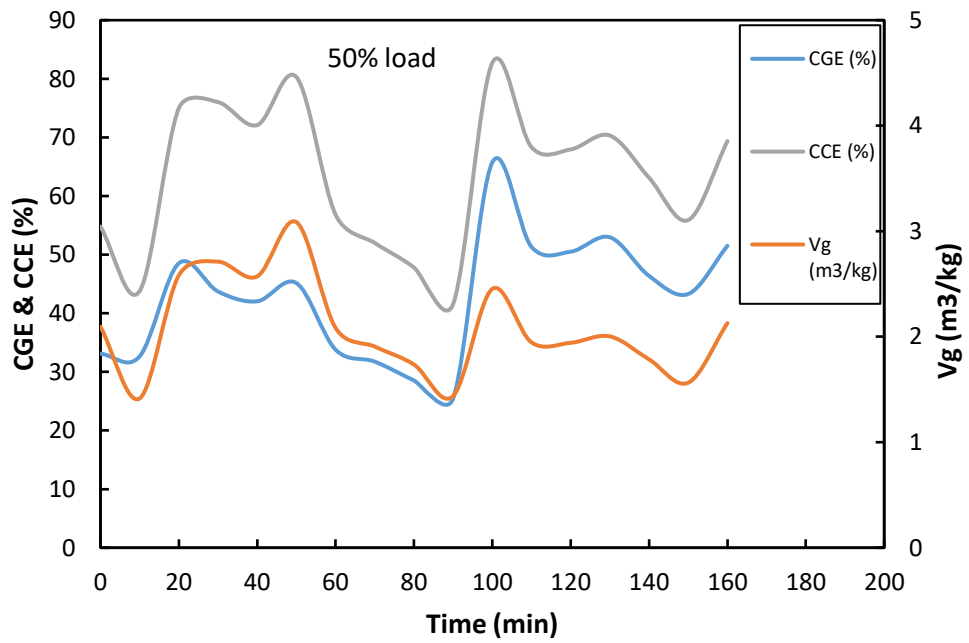


Figure 5.12b

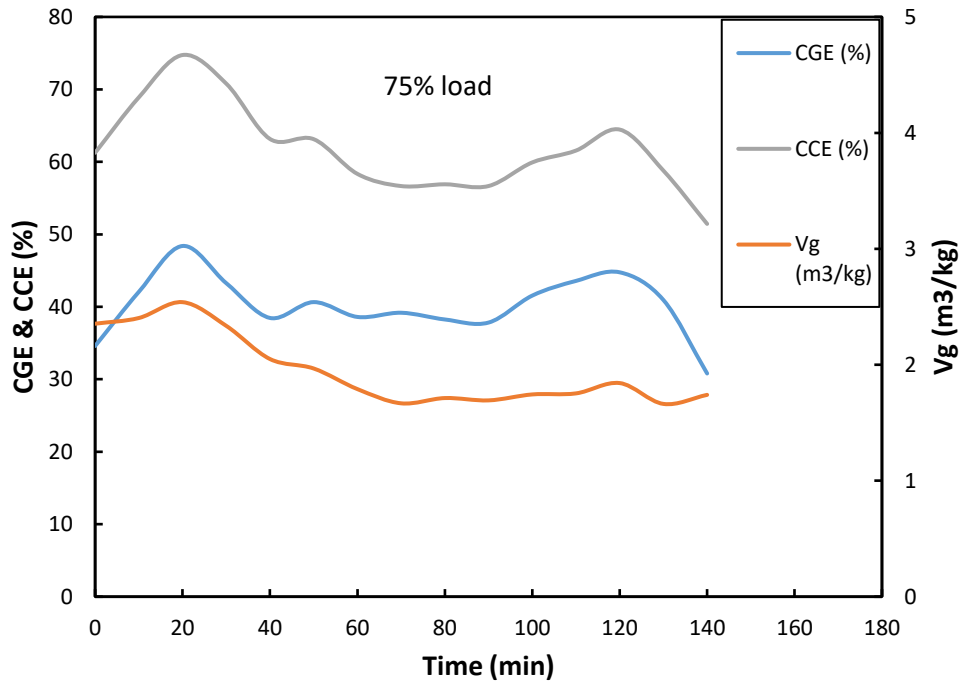


Figure 5.12c

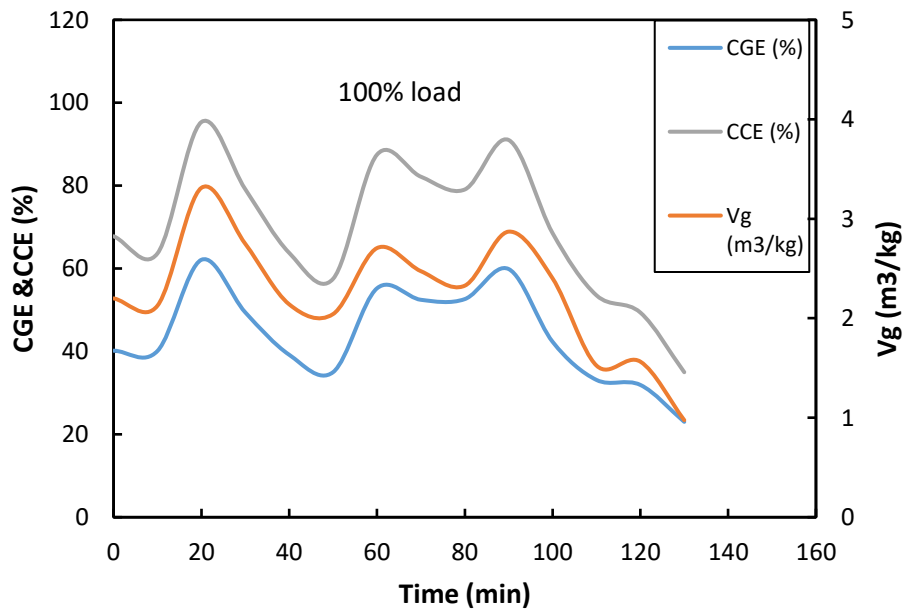


Figure 5.12d

Figure 5.12: Variation in CGE, CCE and Vg at different loads

The gas yield trend line is the same as the cold gas efficiency trend line. As the gas yield increases, the cold gas efficiency also increases and vice versa. Carbon conversion efficiency also follows the same natural trajectory as gas yield, and cold gas efficiency. Hence, an increase or decline in carbon conversion efficiency invariably affects the gas yield and the cold gas efficiency.

#### ***5.5.5 Carbon conversion efficiency, cold gas efficiency, and electrical power***

Figure 5.13 depicts the relationship between carbon conversion efficiency, cold gas efficiency, and the power generation potential of the producer gas ( $Q_{cg}$ ). It was observed that an increase in carbon conversion efficiency was always complemented by an increase in cold gas efficiency and the power generation potential of the producer gas. Therefore, it can be deduced that cold gas efficiency has a direct correlation with both carbon conversion efficiency and the power generation potential of the producer gas. This is consistent with other findings reported in literature like [171] and [174].

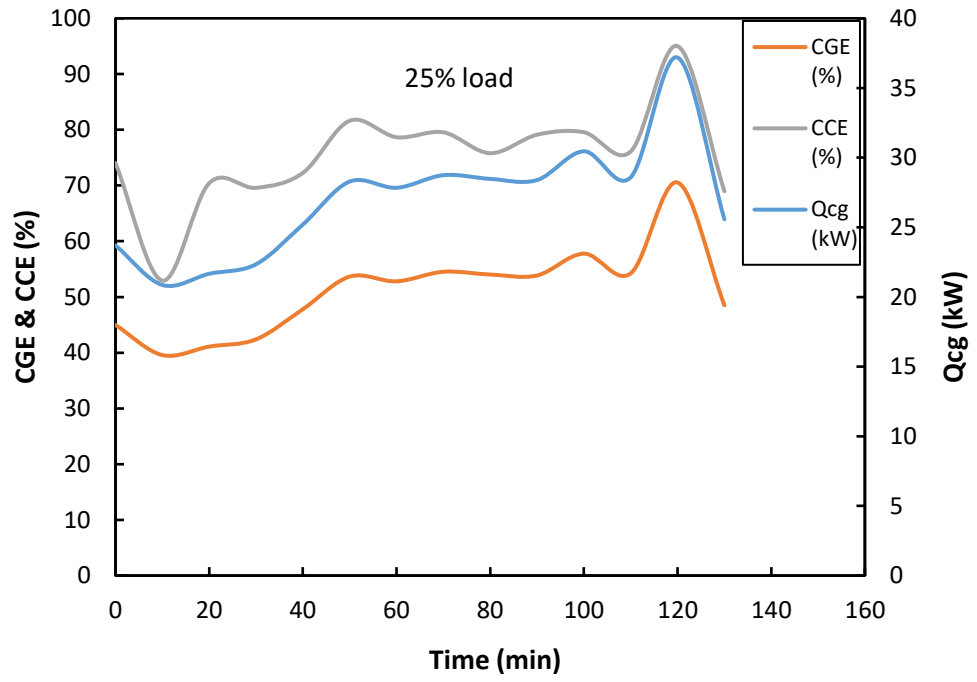


Figure 5.13a

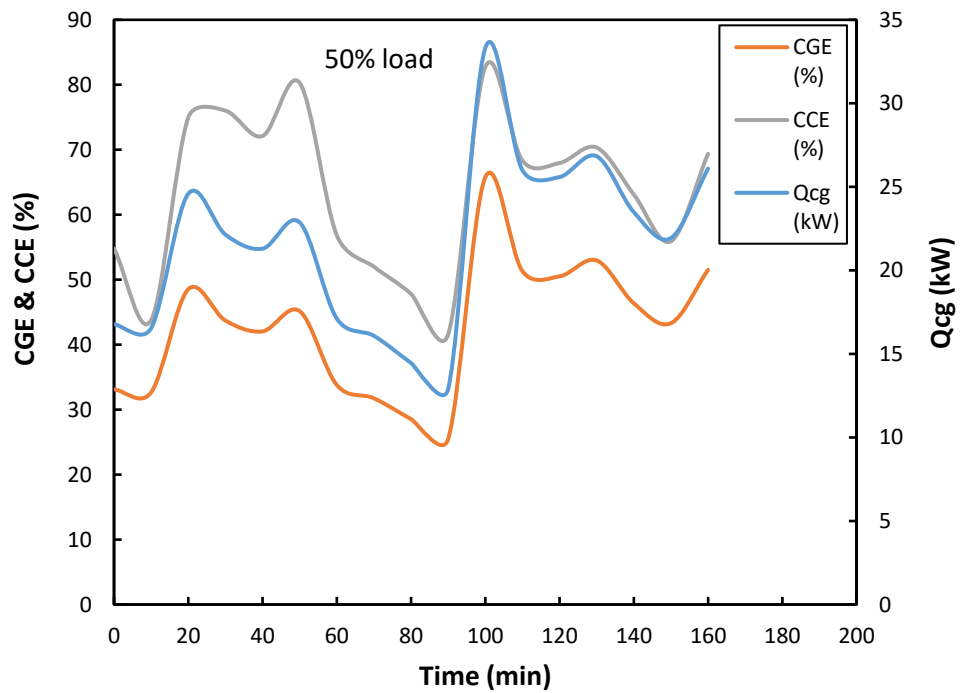


Figure 5.13b

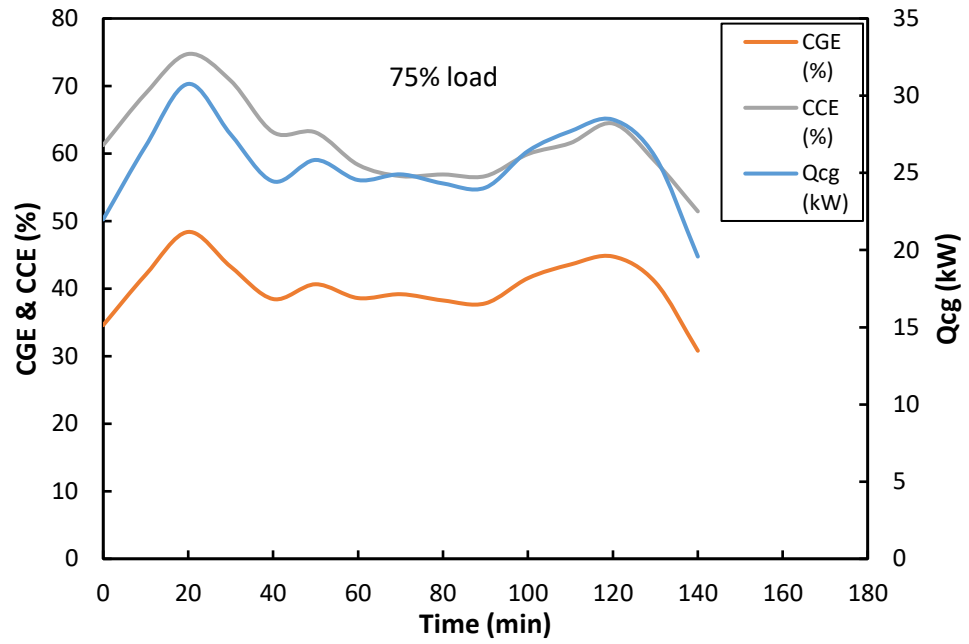


Figure 5.13c

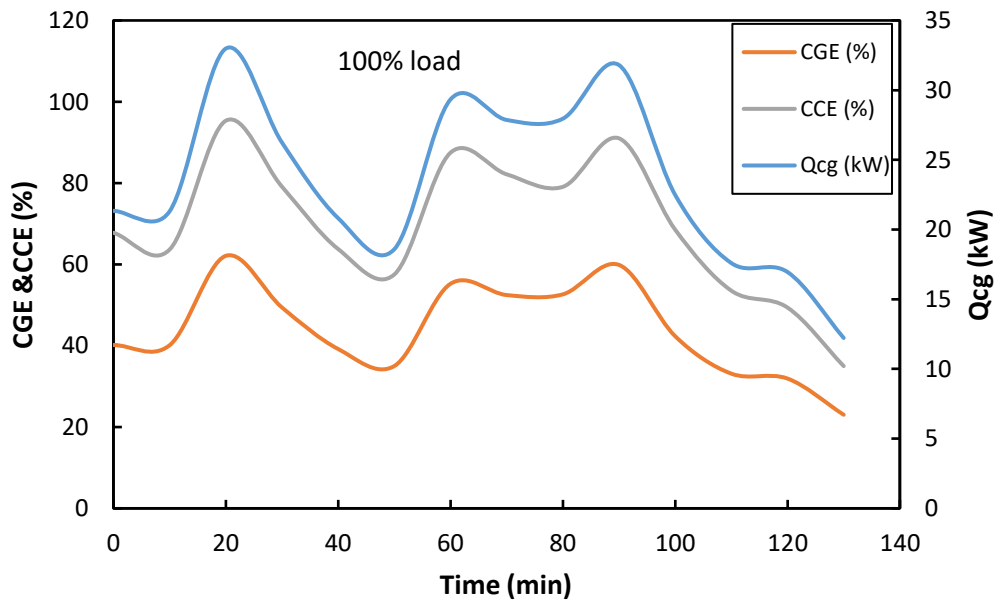


Figure 5.13d

Figure 5.13: Variation in CGE, CCE and Qcg at different loads

### 5.5.6 Engine efficiency and overall efficiency

Figure 5.14 shows the effect of electrical load on engine efficiency and overall efficiency.

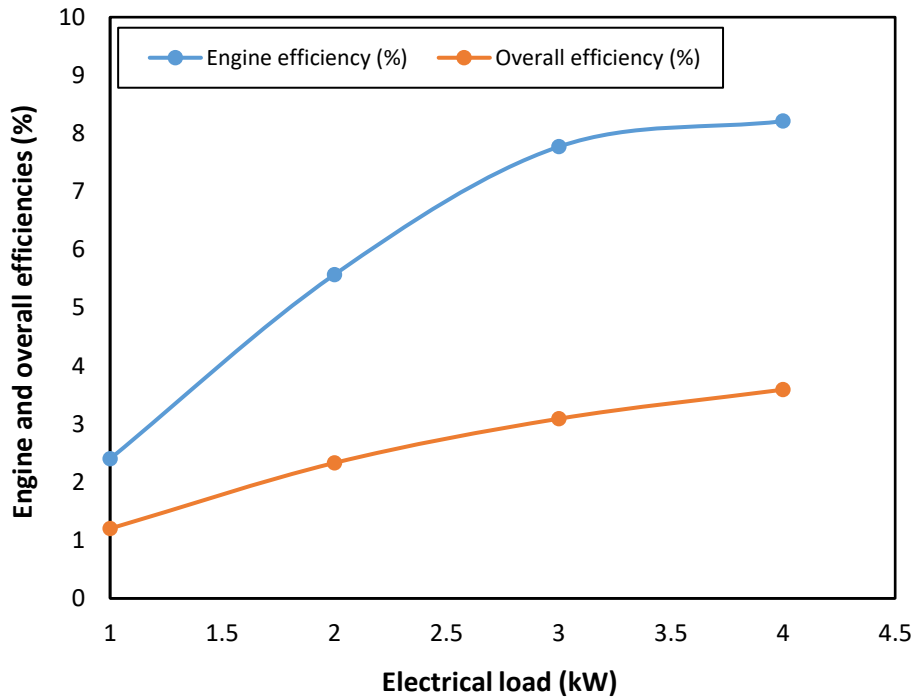


Figure 5.14: Variation in engine efficiency and overall efficiency with electrical load

It was observed that as electrical load increases, engine efficiency also increases, thereby causing a further increase in the overall efficiency of the CPH gasifier system. This is because most engines have been designed to run at 50% to 100% of rated load, with maximum efficiency usually around 75% of rated load. As a result, engine efficiency drops precipitously below about 50% load. Furthermore, a high engine load improves combustion due to increased in-cylinder temperature after multiple runs at this load. This enhances fuel atomization and evaporation processes, as well as fuel air mixing. Consequently, a better fuel mix will result in better power delivery when combusted. It is

therefore recommended that higher electrical loads be used during the operation of the CPH gasifier system for best results.

### 5.5.6 Performance of the CPH gasifier system in summary

Table 5.2 provides an overview of the performance of the CPH gasifier system.

Table 5.2. Performance of CPH gasifier system

Ru n	Power input into the gasifi er (kW)	Power output from the gasifie r (kW)	Carbon conversi on efficienc y (%)	Efficien cy of the gasifier (%)	Engine efficienc y (%)	Overall efficienc y of the CPH gasifier system (%)	CPH consumpti on rate (kg/h)
1	52.71	26.95	75.26	51.13	2.40	1.20	11.16
2	50.66	21.65	63.40	42.73	5.57	2.33	10.73
3	63.56	25.55	61.78	40.20	7.77	3.09	13.46
4	53.11	23.39	69.52	44.04	8.21	3.59	11.25

At an applied load of 1 kWe, the gasifier system consumed CPH at a rate of 11.16 kg/h to produce combustible gas with a power potential of 26.95 kW from an energy input of 52.71 kW, which is equivalent to about 51% conversion efficiency. 2.4% of the produced gas was converted to electricity, giving the CPH gasifier-engine-generator system an overall efficiency of 1.2%. The performance indicators after running the system at the different electrical loads are all shown in Table 5.2.

The average efficiency of the biomass gasifier was 44.52%, with a maximum efficiency of 51.13% at peak performance. The average engine efficiency was 5.99%, with a high peak of 8.21%, and the average overall efficiency was 2.55%, with a high peak of 3.59%.

In summary, gasification of cocoa pod husks into syngas was successful, taking into consideration a carbon conversion efficiency of 61%-75% and a gasifier efficiency of 40%-51%. However, the conversion of syngas into electrical energy was unsuccessful due to low engine efficiency (2%-8%). It is likely that the gas engine-generator may not be fit for purpose, and hence the syngas may be burned directly for cooking and heating. Alternatively, a better internal combustion gas engine generator could complement the gasifier and give a better electrical power output.

The energy flow of the entire system is depicted in Figure 5.15 as a Sankey diagram to illustrate the conversion of biomass energy input into useful energy output (producer gas and power) and to account for system energy losses. In the first phase, the cocoa pod husk's inherent chemical energy was converted into producer gas by gasification, with an overall efficiency of 40-51%. A fraction of the thermal energy within the biomass material (20-25%) was recovered as low-grade heat in the form of sensible heat and used for gas cooling. Energy losses in the gasifier through wall and ash and the gas clean-up process account for about 29-35% of the biomass energy input. In the second phase, the producer gas is converted into electricity with an electrical efficiency of 2-8% using the gas engine-generator set. 92-98% of the producer gas energy input is lost as thermal energy in the gas engine-generator's power train and flue gas stream.

Considering the energy losses and the significant thermal energy that the system produces, a cogeneration system may be more efficient.

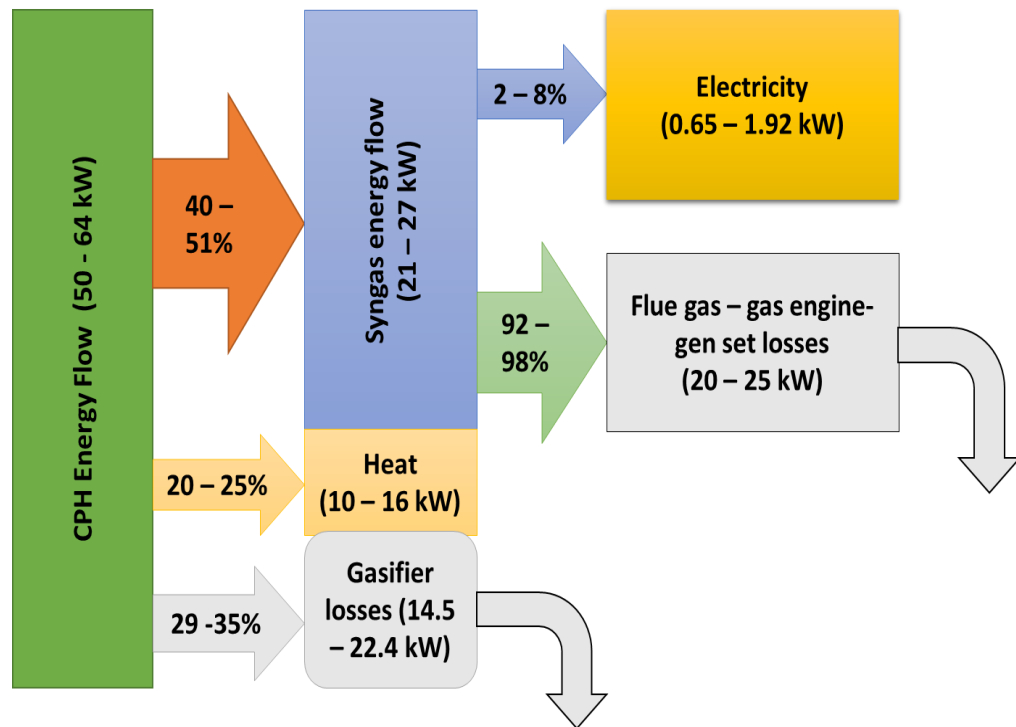


Figure 5.15: Energy flow diagram (Sankey chart) of the cocoa pod husk gasifier engine-gen set

## 5.6 Model Validation

The developed thermodynamic equilibrium model in the present study was validated by comparing its results with the experimental data of a 5 kW<sub>e</sub> downdraft biomass gasifier fed with CPH. A fixed temperature setting of 1100K and ER of 0.3 were used in line with the experimental results reported by both Jarunthammachote and Dutta [145] and Jayah et al [169]. The root mean square (RMS) error was used as a measure of the extent of deviation of the theoretical values from the experimental results and was calculated by the following relation:

$$RMS = \sqrt{\frac{\sum(X_e - X_p)^2}{N}} \quad (5.12)$$

Where  $X_e$ ,  $X_p$ , and  $N$  are experimental data, predicted model and number of observations, respectively.

Figure 5.16 compares the results of the numerical model to the experimental data.

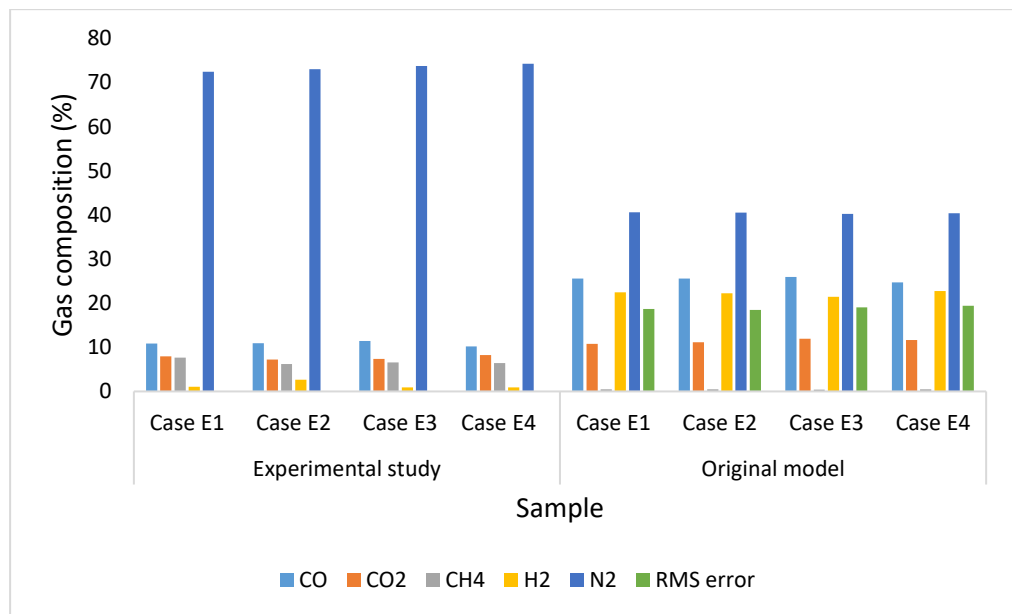


Figure 5.16: Comparison of the developed model with experimental results

The comparison in Figure 5.16 illustrates a model trend that overestimate hydrogen and carbon monoxide and underestimate methane. This is common with thermodynamic equilibrium models due to the assumptions defined in order to simplify the model, such as that all gases are assumed to be ideal, there is no residue formation, there is no tar, etc. In the equilibrium models in the literature, such as [145], [164], [167], [168], and [175], higher concentrations of hydrogen and lower amounts of methane were predicted than the measured data from

experiments. In the case of methane, the predicted concentration by the developed model was low as expected because the equilibrium constant of methane reaction for all equilibrium models tends to be zero at elevated temperatures. Additionally, in a real gasifier, devolatilization of fuel releases high amounts of methane and higher hydrocarbons, which do not undergo full reaction with the equilibrium concentrations of carbon monoxide, carbon dioxide, and hydrogen gas. Thus, in an experimental setting, equilibrium state is never reached and hence the high amount of methane detection [161].

### **5.7 Model Modification**

Thermodynamic models are developed based on assumptions. One of those assumptions is that the gasification system is in a state of thermodynamic equilibrium and hence the presence of non-equilibrium phenomenon is not considered in the model. This brings about a deviation in results between the developed model and the experimental data since equilibrium is never reached in actual conditions [168], [176]. To improve the accuracy of the theoretical model, it was necessary to carry out some basic modifications. Different modification techniques have been used by other researchers. Some modifications in literature have considered carbon conversion and tar formation with reasons that not all the carbon content of biomass is converted in actual conditions but equilibrium models overestimate the carbon conversion efficiency. In addition, the producer gas in equilibrium models are tar free whereas under actual conditions in a gasifier, tars are produced. Other researchers such as Jarunghammachote et al [145] and Barman et al [164] have considered the use of a correction factor to better their equilibrium models.

Jarungthammachote et al [145] multiplied the equilibrium constant of the methane reaction ( $K_2$ ) and the equilibrium constant of the water gas shift reaction ( $K_1$ ) by a coefficient of 11.28 and 0.91 respectively. Barman et al [164] on the other hand multiplied the equilibrium constant of the methane reaction by a coefficient of 3.5. To overcome the limitations of the present model and increase the accuracy of the predicted results, a correction factor (A) was introduced to the equilibrium constant equations.

$$A \times K_1 = \frac{n_{CO_2} \times n_{H_2}}{n_{CO} \times n_{H_2O}} \quad 5.13$$

$$A \times K_2 = \frac{n_{CH_4} \times n_{total}}{(n_{H_2})^2} \quad 5.14$$

A coefficient of 90 was multiplied with the equilibrium constant ( $K_2$ ) of the methanation reaction while the equilibrium constant of the water gas shift reaction ( $K_1$ ) was multiplied by a coefficient of 0.43. The coefficient of  $K_1$  was obtained by finding the average value of the ratio of CO from the experimental data to CO calculated from the developed model. The coefficient of  $K_2$  was obtained the same way as finding the coefficient for  $K_1$  based on the amount of  $CH_4$ . However, due to the tendency of the methane reaction to deviate from equilibrium, the predicted  $CH_4$  levels were extremely low, even after modification, and had to be progressively increased by increasing the coefficient to normalise the results. Barman et al [164] applied a similar modification to their equilibrium model in order to match experimental data.

Figure 5.17 compares the results of the modified model with the experimental data obtained from the CPH downdraft gasifier.

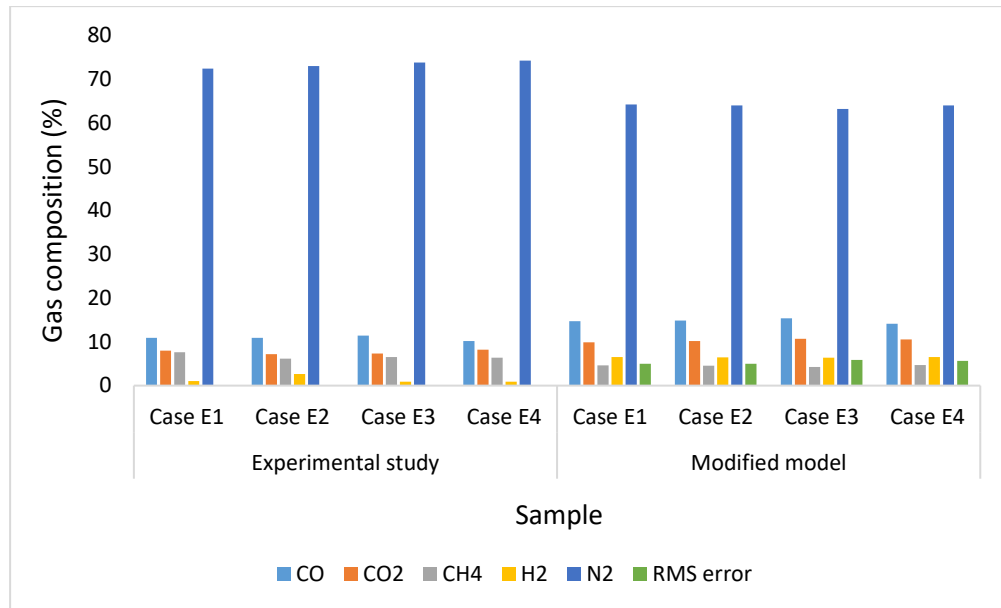


Figure 5.17: Comparison of modified model with experimental results.

It was observed that modifying the model leads to better agreement between the model's predictions and the experimental results. Hydrogen was drastically reduced, while methane was significantly increased, in order to provide a better comparison to the experimental results. This is further evident in the RMS errors, which also decreased significantly.

## 5.8 Concluding Remarks

This chapter investigated the performance of a 5 kWe downdraft biomass gasifier-generator set fed with cocoa pod husks from local plantations. The main conclusions of this study can be summarized as follows:

- Biomass consumption rate increases as moisture content of the feedstock decreases. This is due to the less energy need for the drying stage of the gasification process when moisture content is low, thereby speeding up pyrolysis.

- The producer gas flow rate fluctuated with time during operation. The rate of gas flow increases with temperature. This is so that in thermal gasification, the exothermic heat created in the oxidation zone, which is increased by high oxygen levels, supplies the gasifier system with the heat it needs to operate. Since the carbon monoxide-producing water gas reaction is endothermic, gasification is more favourable at higher temperatures. Nonetheless, the exothermic nature of the reactions that produce methane during methanation and steam reforming favours their occurrence at low temperatures. Thus, depending on the kind of reaction taking place at each time during the gasification, there were steady increases and decreases. Thus, depending on the type of reaction occurring at each stage of the gasification, there were consistent increases and decreases in gas flow rate.
- The volumetric concentration of hydrogen gas in the producer gas was very low compared to the other combustible gases. The very light and reactive nature of hydrogen may have contributed to this behaviour. Notwithstanding, hydrogen gas was at peak production during the first 25 min of gasification.

The gas yield varied between 1.95 Nm<sup>3</sup>/kg and 2.25 Nm<sup>3</sup>/kg whereas the mean lower heating value, cold gas efficiency, and carbon conversion efficiency were 3.92 MJ/Nm<sup>3</sup>, 44.5% and 67.5% respectively. At peak performance, the efficiency of the gasifier was approximately 51% and carbon conversion efficiency was 75%. The efficiency of the gas engine was 6% and the overall

efficiency of the CPH gasifier system was 2.6%, although they were both better with higher electrical load.

On the whole, CPH gasification was successful, although the secondary conversion of the producer gas into electricity was ineffective due to poor gas engine performance. CPH gasification may therefore be useful in rural settings, considering the versatility of producer gas as a fuel source for small-scale bioenergy applications.

## CHAPTER SIX

### 6.0 CONCLUSION AND RECOMMENDATIONS

The purpose of this chapter is to draw conclusions and give recommendations based on the objectives of the study. The relevance and implication of the individual chapters' outcomes are discussed.

#### 6.1 Conclusions

This thesis aimed to achieve the following four primary objectives:

1. Examine different types of biomass materials and energy conversion technologies to identify potential materials and technologies for the proposed bio-rural energy project.
2. Use proximate and ultimate analyses to characterise various types of selected CPH materials for their thermochemical properties.
3. Build a mathematical model to determine the thermal performance of a particular CPH energy conversion system.
4. Test the efficiency of a CPH-fed power plant.

##### *6.1.1 Review of biomass types and their conversion processes*

This thesis has reviewed biomass resources, bioenergy conversion technologies, and bioenergy production potential for rural development. Ghana has a significant potential for bioenergy production due to the sheer amount of biomass the country produces. Agricultural crop residues have the largest energy potential at 728.43 PJ, whereas animal production has a total energy potential of 76.72 PJ, based on 2020 production. While most rural communities in Ghana remain remote and isolated with no access to electricity due to the high cost of

grid extension, residual biomass could be used to support decentralised bio-power production on a sustainable basis since agriculture is the primary source of income for the majority of rural inhabitants.

Compared to other renewable energy sources, biomass has the most promising socio-economic potential since the development of bioenergy in rural Ghana may provide modern energy services, create jobs, reduce poverty, and increase food production. The cultivation of biodiesel-producing energy crops, such as jatropha, could also revive marginal lands on the verge of destruction. The findings of this review indicate that the choice of conversion technology is determined by the end-use application and the kind and features of the available biomass feedstock. Generally, a combination of conversion technologies would permit the simultaneous generation of electricity and other fuels. Despite this, evidence from literature demonstrates that biomass gasification is the most effective technology for supplying rural populations in Ghana with the power they require for basic necessities. Unlike other conversion processes, gasification has variable feedstock requirements and transforms the full carbon content of feedstock, resulting in a greater calorific value output with improved energy capture.

Cocoa is one of the most common crops in rural Ghana, with an estimated annual production of over 850,000 metric tonnes. Through gasification, CPH may be used to generate electric power. CPH is a good source of energy due to its comparatively high calorific value. The use of CPH pellets for power generation by gasification would be a sustainable method of increasing energy availability to rural populations in Ghana. CPH pellets may potentially be used as cooking fuel due to their superior energy density. Additionally, CPH pellets can give

people in rural areas an extra source of income, which can improve their standard of living. It is however suggested that research on CPH gasification in rural Ghana be intensified.

### ***6.1.2 Characterization and evaluation of CPH***

Locally sourced CPH from all cocoa growing regions in Ghana were characterised by ultimate and proximate analysis. The thesis has revealed that CPH has a higher heating value of 14.44-19.21 MJ/kg which could be useful for electricity production. The moisture content recorded were generally below 15% and hence suitable for a trouble-free thermochemical conversion. The volatile matter content of CPH were rather high, making them suitable feedstock for combustion, gasification, and pyrolysis. Due to its high volatile content, CPH would be easy to ignite, possess greater flame stability, and experience little carbon loss during combustion. Although thermochemical processes such as combustion, gasification, and pyrolysis are suitable technologies, the high ash content (11% on average) of CPH could be a potential hindrance that needs to be managed in order to reduce power plant maintenance cost and improve CPH fuel quality and yield. Gasification appears to be the best technique for converting CPH to electricity, as it converts the entire carbon content of the feedstock and provides a better energy capture with lower emissions than other conversion technologies. The gasification of CPH would thus result in cleaner combustion and more environmentally friendly electricity. The concept of utilising CPH to generate power in Ghana's rural areas is technologically advanced, yet its significance cannot be overstated. The use of carbonised and pelletized CPH in gasifiers may potentially generate a secondary market and give

farmers an additional source of revenue. The production of electricity from CPH may significantly improve the quality of life of rural residents by fostering economic growth and alleviating poverty. Additionally, the burnt CPH and excess ash can be repurposed as fertiliser to facilitate agricultural development.

There were variations in the material characteristics of the CPH samples; however, differences in location, soil pollution, soil type, nutrient deficiency, toxicity, cultivation techniques, climate, and storage conditions may have accounted for variations in thermal properties across cocoa pod husk samples. Overall, Amelonado from the Ashanti region of Ghana had the greatest energy potential at 19.21 MJ/kg and the least amount of ash. The Ashanti region can perhaps be prioritised for any future bio-energy plant demonstrations.

### ***6.1.3 Thermodynamic equilibrium model***

A thermodynamic equilibrium model for downdraft biomass gasifiers was developed in order to calculate the composition of producer gas generated by CPH gasification. The developed model was then used to simulate the CPH gasification process. It was discovered that the outcomes anticipated by this model were identical to those expected by other researchers who had constructed conceptually equivalent models. In addition, the effects of equivalence ratio, moisture content, and gasification temperature on the output of producer gas were also analysed. When the equivalence ratio was raised, the CO, H<sub>2</sub>, and CH<sub>4</sub> levels of the producer gas, which collectively make up the gas's major component, decreased. As expected, when the equivalence ratio increased, both the heating value of syngas and the efficiency of cold gas declined. In contrast,

a rise in the equivalence ratio increased the mass fraction of nitrogen gas and carbon dioxide.

As the moisture content rose, the percentage composition of methane and nitrogen gas remained rather consistent, with very minor fluctuations. The mass fractions of hydrogen and carbon dioxide in the producing gas increased as the quantity of moisture increased. In the majority of instances, a rise in the moisture content of the production gas led to a drop in the carbon monoxide concentration. When the temperature of the gasification process was raised, the proportion of carbon monoxide and hydrogen gas in the product gas also rose. However, the quantities of methane, carbon dioxide, and nitrogen gas in the product gas were reduced. As the temperature of gasification increased, so did the heating value and efficiency of cold gas. At a temperature of 1050 degrees Celsius, the gasification process attained its maximum efficiency.

#### ***6.1.4 Analysis of gasifier performance***

The study evaluated the performance of a 5 kWe downdraft CPH gasifier-generator for electricity production. The study revealed that the rate of biomass consumption increases as feedstock moisture content drops. This is because the drying phase of the gasification process requires less energy when moisture levels are low, hence facilitating pyrolysis. Compared to other flammable gases, the volumetric concentration of hydrogen gas in producer gas was extremely low. Hydrogen's very light and reactive nature may have led to this behaviour. Despite this, hydrogen gas production peaked during the first 25 minutes of the experiment. The gas yield was between 1.95 Nm<sup>3</sup>/kg and 2.25 Nm<sup>3</sup>/kg while the average lower heating value, cold gas efficiency, and carbon conversion

efficiency were 3.92 MJ/Nm<sup>3</sup>, 44.5%, and 67.5%, respectively. At peak performance, the gasifier's efficiency was roughly 51%, and the carbon conversion efficiency was 75%. The efficiency of the gas engine was 6%, while the total efficiency of the CPH gasifier system was 2.6%. With a larger electrical load, however, both the gas engine efficiency and overall efficiency were improved.

Based on the results of this experimental study and biomass resource availability, it can be concluded that gasification of cocoa pod husk has a significant potential to provide modern energy for cooking and bio-power generation in rural communities, especially the cocoa growing communities with limited or no access to modern energy services. Ghana may be able to expand its electricity coverage in rural areas by making good use of the plenitude of CPH resources available at its disposal. The study revealed that the efficiency of the gas engine-generator set was very low due to poor performance. However, the potential still remains since system efficiency can be improved.

In conclusion, the gasification of cocoa pod husks into syngas was successful, with a carbon conversion efficiency of 61%-75% and a gasifier efficiency of 40%-51%. However, due to low engine efficiency (2%-8%), the conversion of syngas into electrical energy proved ineffective. As a result, the gas engine generator is unlikely to be fit for purpose; the syngas may be used directly for heating and cooking purposes. Alternatively, a more powerful internal combustion engine generator might enhance the gasifier and provide more electrical power. Furthermore, considering the energy losses and the significant amount of thermal energy that the system produces, a cogeneration system with heat recovery may be more efficient.

## **6.2 Contribution to knowledge**

This research study is timely because it tackles contemporary global concerns such as global warming, energy security, and affordability in Ghana through the development of low-carbon technologies. This thesis conducted a thorough and exhaustive assessment of the creation and implementation of a bio-rural energy strategy for Ghana. Therefore, the study has significantly contributed to the evaluation of bio-rural energy development in Ghana. It has been demonstrated that Ghana has a significant technical capacity to support the development of a bio-rural energy scheme that can be produced without the use of agricultural lands, a situation that has the potential to generate conflict with farmers and affect the country's food production.

For the first time in Ghana, all four different varieties of cocoa pod husk produced in the country have been thermo-chemically characterized and their energy potential determined. Previous research efforts have not examined cocoa pod husks at this level of detail; instead, they have merely characterised cocoa pod husks without examining the varieties. Furthermore, no known study has gone beyond the characterization of cocoa pod husks to demonstrate how geographical location, climate, soil type, cultivation methods, and storage conditions influence thermochemical properties and energy potential.

Additionally, this thesis has proven both theoretically and practically that cocoa pod husks can be converted into biofuel by gasification and then to electrical energy via an internal combustion gas engine-generator set, a hitherto unexplored field. This project's conceptual framework is a master stroke, providing a baseline of knowledge that could benefit Ghana's decision-making process regarding bio-rural energy development. In overall terms, the research

project embraces creativity and innovation that can only advance the field of research on biomass as a low-carbon alternative energy source.

### **6.3 Recommendations for future work**

The following recommendations have been suggested:

1. Future studies may use relevant GIS technologies to identify potential sites for locating biomass conversion plants. This will ensure that there is sustainable feedstock supply all year round.
2. This thesis was mainly focused on the theoretical and technical potential of cocoa pod husk as a fuel source for electricity generation via gasification. The application of CPH in a more efficient manner as a bioenergy source could result in environmental and economic trade-offs. However, a complete economic and environmental assessment is needed in order to provide a comprehensive understanding and facilitate its commercialization.
3. Future modelling of CPH gasification process may need to account for tar formation to increase the accuracy of expected outcomes.
4. The inefficiency of the gas engine-gen set contributed to the low overall efficiency of the system. More practical experiments, including gas engine tests and cogeneration with heat recovery, are imperative to gain more insight on how to maximise overall efficiency.
5. To ensure the continuity of research and development, future studies may pilot cocoa pod husk gasification for power generation in cocoa growing communities without grid access.

## REFERENCES

- [1] F. Kemausuor, I. Nygaard, and G. Mackenzie, “Prospects for bioenergy use in Ghana using Long-range Energy Alternatives Planning model,” *Energy*, vol. 93, pp. 672–682, 2015.
- [2] G. Serwaa Mensah, F. Kemausuor, and A. Brew-Hammond, “Energy access indicators and trends in Ghana,” *Renew. Sustain. Energy Rev.*, vol. 30, no. 2014, pp. 317–323, 2014.
- [3] S. Gyamfi, M. Modjinou, and S. Djordjevic, “Improving electricity supply security in Ghana - The potential of renewable energy,” *Renew. Sustain. Energy Rev.*, vol. 43, pp. 1035–1045, 2015.
- [4] IEA Ghana, “The Most Important Problems Confronting Ghana: A Presentation And Discussion Of IEA’s Survey Results,” 2016. [Online]. Available: <http://ieagh.org/iea-event/presentation-and-discussion-of-iea-survey-results-on-the-most-important-problems-confronting-ghana/#>. [Accessed: 30-May-2019].
- [5] E. Cooke, S. Hague, and A. McKay, “The Ghana Poverty and Inequality Report,” 2016.
- [6] Y. S. Mohammed, A. S. Mokhtar, N. Bashir, and R. Saidur, “An overview of agricultural biomass for decentralized rural energy in Ghana,” *Renew. Sustain. Energy Rev.*, vol. 20, pp. 15–22, 2013.
- [7] F. Kemausuor, A. Kamp, S. T. Thomsen, E. C. Bensah, and H. Stergård, “Assessment of biomass residue availability and bioenergy yields in Ghana,” *Resour. Conserv. Recycl.*, vol. 86, pp. 28–37, 2014.

- [8] E. A. Ayamga, F. Kemausuor, and A. Addo, “Technical analysis of crop residue biomass energy in an agricultural region of Ghana,” *Resour. Conserv. Recycl.*, vol. 96, pp. 51–60, 2015.
- [9] F. Kemausuor, G. Y. Obeng, A. Brew-Hammond, and A. Duker, “A review of trends, policies and plans for increasing energy access in Ghana,” *Renew. Sustain. Energy Rev.*, vol. 15, no. 9, pp. 5143–5154, 2011.
- [10] M. Sakah, F. Amankwah, R. Katzenbach, and S. Gyam, “Towards a sustainable electrification in Ghana : A review of renewable energy deployment policies,” *Renew. Sustain. Energy Rev.*, vol. 79, pp. 544–557, 2017.
- [11] E. N. Kumi, “The Electricity Situation in Ghana: Challenges and Opportunities,” CGD Policy Paper, Washington DC, 2017.
- [12] W. Gboney, “Policy and regulatory framework for renewable energy and energy efficiency development in Ghana,” *Clim. Policy*, vol. 9, no. 5, pp. 508–516, 2009.
- [13] A. Ahmed, B. B. Champion, and A. Gasparatos, “Biofuel development in Ghana: policies of expansion and drivers of failure in the jatropha sector,” *Renewable and Sustainable Energy Reviews*, vol. 70. Elsevier Ltd, pp. 133–149, 01-Apr-2017.
- [14] FAOSTAT, “Crops production Ghana,” *Food and Agriculture Organisation of the UN*, 2020. .
- [15] R. Campos-Vega, K. H. Nieto-Figueroa, and B. D. Oomah, “Cocoa

(*Theobroma cacao* L.) pod husk: Renewable source of bioactive compounds,” *Trends Food Sci. Technol.*, vol. 81, pp. 172–184, 2018.

- [16] Parliament of Ghana, “Highlights of budget statement for 2018,” 2017. [Online]. Available: <https://www.parliament.gh/news?CO=26>. [Accessed: 11-May-2020].
- [17] M. Syamsiro, H. Saptoadi, B. H. Tambunan, and N. A. Pambudi, “A preliminary study on use of cocoa pod husk as a renewable source of energy in Indonesia,” *Energy Sustain. Dev.*, vol. 16, no. 1, pp. 74–77, 2012.
- [18] C. H. Tsai, W. T. Tsai, S. C. Liu, and Y. Q. Lin, “Thermochemical characterization of biochar from cocoa pod husk prepared at low pyrolysis temperature,” *Biomass Convers. Biorefinery*, vol. 8, no. 2, pp. 237–243, 2018.
- [19] M. Adjin-Tetteh, N. Asiedu, D. Dodoo-Arhin, A. Karam, and P. N. Amaniampong, “Thermochemical conversion and characterization of cocoa pod husks a potential agricultural waste from Ghana,” *Ind. Crops Prod.*, vol. 119, pp. 304–312, 2018.
- [20] H. P. S. Abdul Khalil *et al.*, “The role of soil properties and it’s interaction towards quality plant fiber: A review,” *Renew. Sustain. Energy Rev.*, vol. 43, pp. 1006–1015, 2015.
- [21] T. Chatzistathis and I. Therios, “How Soil Nutrient Availability Influences Plant Biomass and How Biomass Stimulation Alleviates Heavy Metal Toxicity in Soils: The Cases of Nutrient Use Efficient Genotypes and Phytoremediators, Respectively,” *Biomass Now - Cultiv.*

*Util.*, pp. 427–448, 2013.

- [22] S. Clarke and F. Preto, “Biomass Burn Characteristics,” *Minist. Agric. Food Rural Aff.*, vol. 11, no. 33, pp. 1–6, 2011.
- [23] European Commission, “Directive of the European parliament and of the Council on the promotion of the use of energy from renewable sources,” *Off. J. Eur. Union*, pp. 16–62, 2009.
- [24] T. V. Ramachandra, G. Kamakshi, and B. V. Shruthi, “Bioresource status in Karnataka,” *Renew. Sustain. Energy Rev.*, vol. 8, no. 1, pp. 1–47, 2004.
- [25] EIA, “Biomass Explained.” [Online]. Available: [https://www.eia.gov/energyexplained/?page=biomass\\_home](https://www.eia.gov/energyexplained/?page=biomass_home). [Accessed: 16-Oct-2018].
- [26] BioEnergy Consult, “Biomass as Renewable Energy Resource,” 2018. [Online]. Available: <https://www.bioenergyconsult.com/tag/types-of-biomass/>. [Accessed: 19-Nov-2018].
- [27] EERE, “Biomass Resources,” 2018. .
- [28] R. E. H. Sims, A. Hastings, B. Schlamadinger, G. Taylor, and P. Smith, “Energy crops: Current status and future prospects,” *Glob. Chang. Biol.*, vol. 12, no. 11, pp. 2054–2076, 2006.
- [29] U. K. Mirza, N. Ahmad, and T. Majeed, “An overview of biomass energy utilization in Pakistan,” *Renew. Sustain. Energy Rev.*, vol. 12, no. 7, pp. 1988–1996, 2008.
- [30] P. McKendry, “Energy production from biomass (part 2): Conversion

- technologies,” *Bioresour. Technol.*, vol. 83, no. 1, pp. 47–54, 2002.
- [31] P. Adams, T. Bridgwater, A. Lea-Langton, A. Ross, and I. Watson, “Chapter 8 - Biomass Conversion Technologies,” *Greenh. Gas Balanc. Bioenergy Syst.*, pp. 107–139, 2018.
- [32] F. Corona, D. Hidalgo, D. Díez-Rodríguez, and A. Urueña, “Thermochemical Conversion as the Key Step for the Production of Value-Added Products from Waste,” *Biofuels*, pp. 1–26, 2016.
- [33] World Energy Council, “World Energy Resources Waste to Energy | 2016,” *Waste-To-Energy*, pp. 1–76, 2016.
- [34] BioEnergy Consult, “Summary of Biomass Combustion Technologies,” 2018. [Online]. Available: <https://www.bioenergyconsult.com/tag/biomass-combustion-process/>. [Accessed: 06-Dec-2018].
- [35] A. Demirbas, “Combustion characteristics of different biomass fuels,” *Prog. Energy Combust. Sci.*, vol. 30, no. 2, pp. 219–230, 2004.
- [36] Alberta Agriculture and Forestry, “Biomass Combustion Basics,” 2015. [Online]. Available: [https://www1.agric.gov.ab.ca/\\$department/deptdocs.nsf/all/eng15548](https://www1.agric.gov.ab.ca/$department/deptdocs.nsf/all/eng15548). [Accessed: 10-Dec-2018].
- [37] C. S. Park, P. S. Roy, and S. H. Kim, “Current Developments in Thermochemical Conversion of Biomass to Fuels and Chemicals,” *Intech open*, vol. 2, pp. 19–41, 2018.
- [38] Yokogawa South Africa (Pty.) Ltd., “Biomass Power,” 2022. [Online].

Available: <https://www.yokogawa.com/za/industries/renewable-energy/biomass-power/#Challenges>. [Accessed: 21-Oct-2022].

- [39] P. McKendry, “Energy production from biomass (part 3): gasification technologies,” *Bioresour. Technol.*, vol. 83, no. 1, pp. 55–63, Jul. 2002.
- [40] UEMOA, “Biomass Conversion Technologies,” 2008.
- [41] S. Guran, *Sustainable Waste-to-Energy Technologies: Gasification and Pyrolysis*. Elsevier Inc., 2018.
- [42] National Energy Technology Laboratory, “Gasification Introduction,” 2022. [Online]. Available: <https://netl.doe.gov/research/Coal/energy-systems/gasification/gasifipedia/intro-to-gasification>. [Accessed: 21-Oct-2022].
- [43] B. Digman, H. S. Joo, and D.-S. Kim, “Recent Progress in Gasification/Pyrolysis Technologies for Biomass Conversion to Energy,” *Environ. Prog. Sustain. Energy*, vol. 28, no. 1, pp. 47–51, 2009.
- [44] A. Kumar, D. D. Jones, and M. A. Hanna, “Thermochemical biomass gasification: A review of the current status of the technology,” *Energies*, vol. 2, no. 3, pp. 556–581, 2009.
- [45] CapitalEnergy, “Downstream processing of gasification,” 2019. [Online]. Available: <http://capitalenergy.biz/?p=6718>. [Accessed: 25-Jun-2019].
- [46] S. Pang, “Advances in thermochemical conversion of woody biomass to energy ,fuels and chemicals,” *Biotechnol. Adv.*, pp. 1–9, 2018.
- [47] M. L. Valderrama Rios, A. M. González, E. E. S. Lora, and O. A.

- Almazán del Olmo, “Reduction of tar generated during biomass gasification: A review,” *Biomass and Bioenergy*, vol. 108. Elsevier Ltd, pp. 345–370, 01-Jan-2018.
- [48] U. Henriksen *et al.*, “The design, construction and operation of a 75 kW two-stage gasifier,” *Energy*, vol. 31, no. 10–11, pp. 1542–1553, 2006.
- [49] A. Gómez-Barea, B. Leckner, A. Villanueva Perales, S. Nilsson, and D. Fuentes Cano, “Improving the performance of fluidized bed biomass/waste gasifiers for distributed electricity: A new three-stage gasification system,” in *Applied Thermal Engineering*, 2013, vol. 50, no. 2, pp. 1453–1462.
- [50] E. J. Leijenhurst, W. Wolters, B. Van De Beld, and W. Prins, “Staged Biomass Gasification by Autothermal Catalytic Reforming of Fast Pyrolysis Vapors,” *Energy and Fuels*, vol. 29, pp. 7395–7407, 2015.
- [51] S. Heidenreich and P. U. Foscolo, “New concepts in biomass gasification,” *Progress in Energy and Combustion Science*, vol. 46. Elsevier Ltd, pp. 72–95, 01-Feb-2015.
- [52] L. Devi, K. J. Ptasiński, and F. J. J. G. Janssen, “A review of the primary measures for tar elimination in biomass gasification processes,” *Biomass and Bioenergy*, vol. 24, pp. 125–140, 2003.
- [53] M. H. Duku, S. Gu, and E. Ben Hagan, “A comprehensive review of biomass resources and biofuels potential in Ghana,” *Renew. Sustain. Energy Rev.*, vol. 15, no. 1, pp. 404–415, 2011.
- [54] W. Ahiataku-Togobo and A. Ofori-Ahenkorah, “Bioenergy Policy

- Implementation in Ghana,” in *COMPETE International Conference*, 2009.
- [55] S. K. Sansaniwal, M. A. Rosen, and S. K. Tyagi, “Global challenges in the sustainable development of biomass gasification: An overview,” *Renew. Sustain. Energy Rev.*, vol. 80, pp. 23–43, 2017.
- [56] P. V. Ramamurthi, M. C. Fernandes, P. S. Nielsen, and C. P. Nunes, “Utilisation of rice residues for decentralised electricity generation in Ghana: An economic analysis,” *Energy*, vol. 111, pp. 620–629, Sep. 2016.
- [57] Carbon Trust, “Biomass heating: A practical guide for potential users,” UK, 2009.
- [58] X. Shi, F. Ronsse, and J. G. Pieters, “Finite element modeling of intraparticle heterogeneous tar conversion during pyrolysis of woody biomass particles,” *Fuel Process. Technol.*, vol. 148, pp. 302–316, 2016.
- [59] R. L. Bain, “An Introduction to Biomass Thermochemical Conversion,” *DOE/NASLUGC Biomass Sol. Energy Work.*, pp. 1–77, 2004.
- [60] R. T. Dilks, F. Monette, and M. Glaus, “The major parameters on biomass pyrolysis for hyperaccumulative plants - A review,” *Chemosphere*, vol. 146, pp. 385–395, 2016.
- [61] P. Basu, *Biomass gasification, pyrolysis and torrefaction : practical design and theory*, 3rd ed. London: Academic Press.
- [62] D. Mohan, C. U. Pittman, and P. H. Steele, “Pyrolysis of wood/biomass for bio-oil: A critical review,” *Energy and Fuels*, vol. 20, no. 3. pp. 848–

889, May-2006.

- [63] V. Dhyani and T. Bhaskar, “A comprehensive review on the pyrolysis of lignocellulosic biomass,” *Renew. Energy*, vol. 129, pp. 695–716, 2018.
- [64] R. E. Guedes, A. S. Luna, and A. R. Torres, “Operating parameters for bio-oil production in biomass pyrolysis: A review,” *Journal of Analytical and Applied Pyrolysis*, vol. 129. Elsevier B.V., pp. 134–149, 01-Jan-2018.
- [65] Y. Chhiti and M. Kemiha, “Thermal Conversion of Biomass, Pyrolysis and Gasification : A Review,” *Int. J. Eng. Sci.*, vol. 2, no. 3, pp. 75–85, 2013.
- [66] K. Im-orb, W. Wiyaratn, and A. Arpornwichanop, “Technical and economic assessment of the pyrolysis and gasification integrated process for biomass conversion,” *Energy*, vol. 153, pp. 592–603, 2018.
- [67] M. Ni, D. Y. C. Leung, M. K. H. Leung, and K. Sumathy, “An overview of hydrogen production from biomass,” *Fuel Process. Technol.*, vol. 87, no. 5, pp. 461–472, 2006.
- [68] A. V. Bridgwater, “The production of biofuels and renewable chemicals by fast pyrolysis of biomass,” *Int. J. Glob. Energy Issues*, vol. 27, no. 2, p. 160, 2007.
- [69] M. H. Duku, S. Gu, and E. Ben Hagan, “Biochar production potential in Ghana - A review,” *Renew. Sustain. Energy Rev.*, vol. 15, no. 8, pp. 3539–3551, 2011.
- [70] C. Paenpong and A. Pattiya, “Effect of pyrolysis and moving-bed

- granular filter temperatures on the yield and properties of bio-oil from fast pyrolysis of biomass,” *J. Anal. Appl. Pyrolysis*, vol. 119, pp. 40–51, 2016.
- [71] M. S. Abu Bakar and J. O. Titiloye, “Catalytic pyrolysis of rice husk for bio-oil production,” in *Journal of Analytical and Applied Pyrolysis*, 2013, vol. 103, pp. 362–368.
- [72] J. Park, Y. Lee, C. Ryu, and Y. Park, “Slow pyrolysis of rice straw : Analysis of products properties , carbon and energy yields,” *Bioresour. Technol.*, vol. 155, pp. 63–70, 2014.
- [73] D. Mansur, T. Tago, T. Masuda, and H. Abimanyu, “Conversion of cacao pod husks by pyrolysis and catalytic reaction to produce useful chemicals,” *Biomass and Bioenergy*, vol. 66, pp. 275–285, 2014.
- [74] S. B. Atakora, “Biomass technologies in Ghana,” in *The ninth biennial bioenergy conference 2000*, 2000.
- [75] W. L. Filho and D. Surroop, *The Nexus: Energy, Environment and Climate Change*. Springer, 2017.
- [76] A. Demirbas, “Mechanisms of liquefaction and pyrolysis reactions of biomass,” *Energy Convers. Manag.*, vol. 41, pp. 633–646, 2000.
- [77] H. J. Huang, X. Z. Yuan, B. T. Li, Y. D. Xiao, and G. M. Zeng, “Thermochemical liquefaction characteristics of sewage sludge in different organic solvents,” *J. Anal. Appl. Pyrolysis*, vol. 109, pp. 176–184, Sep. 2014.
- [78] A. Koriakin, S. Moon, D. Kim, and C. Lee, “Liquefaction of oil palm

empty fruit bunch using sub- and supercritical tetralin , n -dodecane , and their mixture,” *Fuel*, vol. 208, pp. 184–192, 2017.

- [79] J. A. Ramirez, R. J. Brown, and T. J. Rainey, “A review of hydrothermal liquefaction bio-crude properties and prospects for upgrading to transportation fuels,” *Energies*, vol. 8, no. 7, pp. 6765–6794, 2015.
- [80] D. C. Elliott, P. Biller, A. B. Ross, A. J. Schmidt, and S. B. Jones, “Hydrothermal liquefaction of biomass: Developments from batch to continuous process,” *Bioresour. Technol.*, vol. 178, pp. 147–156, 2015.
- [81] ETA Florence Renewable Energies, “Hydrothermal Liquefaction in the Green Energy Transition,” 2021. [Online]. Available: [https://issuu.com/besustainablemagazine/docs/besustainable\\_magazine\\_issue\\_12\\_-\\_april\\_2021/s/12150137](https://issuu.com/besustainablemagazine/docs/besustainable_magazine_issue_12_-_april_2021/s/12150137). [Accessed: 21-Oct-2022].
- [82] A. R. K. Gollakota, N. Kishore, and S. Gu, “A review on hydrothermal liquefaction of biomass,” *Renew. Sustain. Energy Rev.*, vol. 81, pp. 1378–1392, 2018.
- [83] Z. Shuping, W. Yulong, Y. Mingde, I. Kaleem, L. Chun, and J. Tong, “Production and characterization of bio-oil from hydrothermal liquefaction of microalgae *Dunaliella tertiolecta* cake,” *Energy*, vol. 35, no. 12, pp. 5406–5411, 2010.
- [84] Y. H. Chan, A. T. Quitain, S. Yusup, Y. Uemura, M. Sasaki, and T. Kida, “Liquefaction of palm kernel shell in sub- and supercritical water for bio-oil production,” *J. Energy Inst.*, vol. 91, no. 5, pp. 721–732, 2018.

- [85] X. Z. Ā. Yuan, H. Li, G. M. Zeng, J. Y. Tong, and W. Xie, “Sub- and supercritical liquefaction of rice straw in the presence of ethanol – water and 2-propanol – water mixture,” *Energy*, vol. 32, pp. 2081–2088, 2007.
- [86] A. Dimitriadis and S. Bezergianni, “Hydrothermal liquefaction of various biomass and waste feedstocks for biocrude production\_ A state of the art review,” *Renew. Sustain. Energy Rev.*, vol. 68, pp. 113–125, 2017.
- [87] F. Behrendt, Y. Neubauer, M. Oevermann, B. Wilmes, and N. Zobel, “Direct Liquefaction of Biomass,” *Chem. Eng. Technol.*, vol. 31, no. 5, pp. 667–677, 2008.
- [88] J. Akhtar and N. A. S. Amin, “A review on process conditions for optimum bio-oil yield in hydrothermal liquefaction of biomass,” *Renewable and Sustainable Energy Reviews*, vol. 15, no. 3, pp. 1615–1624, Apr-2011.
- [89] M. Kumar, A. Olajire Oyedun, and A. Kumar, “A review on the current status of various hydrothermal technologies on biomass feedstock,” *Renew. Sustain. Energy Rev.*, vol. 81, pp. 1742–1770, Jan. 2018.
- [90] C. Xu and J. Lancaster, “Conversion of secondary pulp/paper sludge powder to liquid oil products for energy recovery by direct liquefaction in hot-compressed water,” *Water Res.*, vol. 42, pp. 1571–1582, Mar. 2008.
- [91] X. Yuan, J. Wang, G. Zeng, H. Huang, X. Pei, and H. Li, “Comparative studies of thermochemical liquefaction characteristics of microalgae using different organic solvents,” *Energy*, vol. 36, no. 11, pp. 6406–

6412, 2011.

- [92] V. P. Soudham, “Biochemical conversion of biomass to biofuels,” Umeå University, Sweden, 2015.
- [93] FAO, “Unified Bioenergy Terminology,” Rome, Italy, 2004.
- [94] Y. Lin and S. Tanaka, “Ethanol fermentation from biomass resources: Current state and prospects,” *Appl. Microbiol. Biotechnol.*, vol. 69, no. 6, pp. 627–642, 2006.
- [95] S. I. Mussatto and J. A. Teixeira, “Lignocellulose as raw material in fermentation processes.,” *Curr. Res. Technol. Educ. Top. Appl. Microbiol. Microb. Biotechnol.*, pp. 897–907, 2010.
- [96] V. P. Soudham, D. G. Raut, I. Anugwom, T. Brandberg, C. Larsson, and J. P. Mikkola, “Coupled enzymatic hydrolysis and ethanol fermentation: ionic liquid pretreatment for enhanced yields,” *Biotechnol. Biofuels*, vol. 8, no. 135, pp. 1–13, 2015.
- [97] J. C. Martínez-Patiño, E. Ruiz, C. Cara, I. Romero, and E. Castro, “Advanced bioethanol production from olive tree biomass using different bioconversion schemes,” *Biochem. Eng. J.*, vol. 137, pp. 172–181, 2018.
- [98] M. M. El-Dalatony *et al.*, “Whole conversion of microalgal biomass into biofuels through successive high-throughput fermentation,” *Chem. Eng. J.*, vol. 360, pp. 797–805, 2019.
- [99] J. Malça and F. Freire, “Renewability and life-cycle energy efficiency of bioethanol and bio-ethyl tertiary butyl ether (bioETBE): Assessing the

implications of allocation,” *Energy*, vol. 31, no. 15, pp. 3362–3380, 2006.

- [100] M. Koç, Y. Sekmen, T. Topgül, and H. S. Yücesu, “The effects of ethanol-unleaded gasoline blends on engine performance and exhaust emissions in a spark-ignition engine,” *Renew. Energy*, vol. 34, no. 10, pp. 2101–2106, 2009.
- [101] M. Al-Hasan, “Effect of ethanol-unleaded gasoline blends on engine performance and exhaust emission,” *Energy Convers. Manag.*, vol. 44, no. 9, pp. 1547–1561, 2003.
- [102] W.-D. Hsieh, R.-H. Chen, T.-L. Wu, and T.-H. Lin, “Engine performance and pollutant emission of an SI engine using ethanol–gasoline blended fuels,” *Atmos. Environ.*, vol. 36, pp. 403–410, 2002.
- [103] J. Wang and Y. Yin, “Fermentative hydrogen production using various biomass-based materials as feedstock,” *Renew. Sustain. Energy Rev.*, vol. 92, pp. 284–306, 2018.
- [104] C. S. Mbajiuka, A. C. Ifediora, C. E. Onwuakor, and L. I. Nwokoji, “Fermentation of pods of cocoa (*Theobroma cacao* L) using palm wine yeasts for the production of alcohol and biomass,” *Am. J. Microbiol. Res.*, vol. 3, no. 2, pp. 80–84, 2015.
- [105] M. M. S. Cabral, A. K. de S. Abud, C. E. de F. Silva, and R. M. R. G. Almeida, “Bioethanol production from coconut husk fiber,” *Ciência Rural*, vol. 46, no. 10, pp. 1872–1877, 2016.
- [106] M. N. Uddin *et al.*, “Prospects of Bioenergy Production From Organic

- Waste Using Anaerobic Digestion Technology: A Mini Review,” *Front. Energy Res.*, vol. 9, 2021.
- [107] S. Harirchi *et al.*, “Microbiological insights into anaerobic digestion for biogas, hydrogen or volatile fatty acids (VFAs): a review,” *Bioengineered*, vol. 13, no. 3, pp. 6521–6557, 2022.
- [108] A. Donoso-Bravo and F. Mairet, “Determining the limiting reaction in anaerobic digestion processes. How has this been tackled?,” *J. Chem. Technol. Biotechnol.*, vol. 87, no. 10, pp. 1375–1378, 2012.
- [109] X. Li *et al.*, “Anaerobic digestion using ultrasound as pretreatment approach: Changes in waste activated sludge, anaerobic digestion performances and digestive microbial populations,” *Biochem. Eng. J.*, vol. 139, pp. 139–145, 2018.
- [110] Darwin, J. J. Cheng, Z. Liu, and J. Gontuphil, “Anaerobic co-digestion of cocoa husk with digested swine manure: Evaluation of biodegradation efficiency in methane productivity,” *Agric. Eng. Int. CIGR J.*, vol. 18, no. 4, pp. 147–156, 2016.
- [111] Nexus PMG, “Anaerobic Digestion,” 2022. [Online]. Available: <https://nexuspmg.com/anaerobic-digestion/>. [Accessed: 28-Oct-2022].
- [112] F. Kemausuor, M. S. Adaramola, and J. Morken, “A Review of Commercial Biogas Systems and Lessons for Africa,” *Energies*, vol. 11, no. 11, pp. 1–21, 2018.
- [113] E. C. Bensah, “Biogas: A clean waste treatment option for Ghana,” *GhanaWeb*, 2018. [Online]. Available:

<https://www.ghanaweb.com/GhanaHomePage/features/Biogas-A-clean-waste-treatment-option-for-Ghana-624872>. [Accessed: 20-May-2019].

- [114] M. Mohammed *et al.*, “Feasibility study for biogas integration into waste treatment plants in Ghana,” *Egypt. J. Pet.*, vol. 26, no. 3, pp. 695–703, 2017.
- [115] E. C. Bensah, M. Mensah, and E. Antwi, “Status and prospects for household biogas plants in Ghana – lessons, barriers, potential, and way forward,” *Int. J. Energy Environ.*, vol. 2, no. 5, pp. 887–898, 2011.
- [116] W. Ahiataku-Togobo and P. Y. Owusu-Obeng, “Biogas Technology - What works for Ghana?,” 2016. [Online]. Available: <http://energycom.gov.gh/files/Biogas - What works for Ghana.pdf>. [Accessed: 20-Dec-2020].
- [117] A. Kyaw, D. Digber, E. W. Mwangi, G. Adhikari, and G. Shegani, “Construction of Bio-gas Plants in Government Institutions in Accra Region Ghana-Africa.” The Weitz Center for Development Studies, pp. 1–20, 2015.
- [118] Energy Commission of Ghana, “National Energy Statistics 2008-2017,” Accra, 2018.
- [119] S. Asumadu-Sarkodie and P. A. Owusu, “A review of Ghana’s energy sector national energy statistics and policy framework,” *Cogent Eng.*, vol. 3, no. 1, 2016.
- [120] The World Bank, “Ghana: Agriculture Sector Policy Note,” Washington, DC, 2017.

- [121] ENDA, “Bioenergy for Rural Development in West Africa The case of Ghana , Mali and Senegal Final Report,” 2010.
- [122] F. Kemausuor, A. Addo, E. Ofori, L. Darkwah, S. Bolwig, and I. Nygaard, “Assessment of technical potential and selected sustainability impacts of second generation bioenergy in Ghana,” Kwame Nkrumah University of Science and Technology, 2015.
- [123] F. Präger, S. Paczkowski, G. Sailer, N. S. A. Derkyi, and S. Pelz, “Biomass sources for a sustainable energy supply in Ghana – A case study for Sunyani,” *Renew. Sustain. Energy Rev.*, vol. 107, pp. 413–424, 2019.
- [124] O. Domson and R. P. Vlosky, “A Strategic Overview of the Forest Sector in Ghana,” *LA*, 81, 2007.
- [125] Ghana Energy Commission, “Strategic National Energy Plan (2006 - 2020),” *Woodfuels and Renewables*, 2006. [Online]. Available: [http://energycom.gov.gh/files/snep/WOOD\\_FUEL\\_final\\_PD.pdf](http://energycom.gov.gh/files/snep/WOOD_FUEL_final_PD.pdf). [Accessed: 04-Jun-2019].
- [126] IRENA, “Ghana Renewables Readiness Assessment,” *International Renewable Energy Agency*, 2015. [Online]. Available: [https://www.irena.org/-/media/Files/IRENA/Agency/Publication/2015/IRENA\\_RRA\\_Ghana\\_Nov\\_2015.pdf](https://www.irena.org/-/media/Files/IRENA/Agency/Publication/2015/IRENA_RRA_Ghana_Nov_2015.pdf). [Accessed: 04-Jun-2019].
- [127] A. T. Kehbila, “Evaluation of primary wood processing residues for bioenergy in British Columbia,” The University of British Columbia, 2010.

- [128] J. Cai, R. Liu, and C. Deng, "An assessment of biomass resources availability in Shanghai: 2005 analysis," *Renew. Sustain. Energy Rev.*, vol. 12, no. 7, pp. 1997–2004, 2008.
- [129] FAOSTAT, "Crops and livestock products Ghana," *Food and Agriculture Organisation of the UN*, 2020. .
- [130] MBEP, "Clean Energy from Wood Residues in Michigan," 2006.
- [131] L. Wang, A. Shahbazi, and M. A. Hanna, "Characterization of corn stover, distiller grains and cattle manure for thermochemical conversion," *Biomass and Bioenergy*, vol. 35, no. 1, pp. 171–178, 2011.
- [132] C. E. M. Braza and P. M. Crnkovic, "Physical - Chemical characterization of biomass samples for application in pyrolysis process," *Chem. Eng. Trans.*, vol. 37, pp. 523–528, 2014.
- [133] Forest Research, "Effects of moisture content," 2022. [Online]. Available: <https://www.forestresearch.gov.uk/tools-and-resources/fthr/biomass-energy-resources/fuel/woodfuel-production-and-supply/woodfuel-processing/drying-biomass/effect-of-moisture-content/>. [Accessed: 08-Nov-2022].
- [134] Y. Xia, "An Experimental Research of Biomass Crushing System," *IOP Conf. Ser. Earth Environ. Sci.*, vol. 63, no. 1, 2017.
- [135] M. Gu, X. Chen, C. Wu, X. He, H. Chu, and F. Liu, "Effects of Particle Size Distribution and Oxygen Concentration on the Propagation Behavior of Pulverized Coal Flames in O<sub>2</sub>/CO<sub>2</sub> Atmospheres," *Energy and Fuels*, vol. 31, no. 5, pp. 5571–5580, 2017.

- [136] C. A. Forero-Nuñez, J. Jochum, and F. E. S. Vargas, “Effect of particle size and addition of cocoa pod husk on the properties of sawdust and coal pellets,” *Ing. e Investig.*, vol. 35, no. 1, pp. 17–23, 2015.
- [137] M. Shehab *et al.*, “Improved Metrological Methodology to Address the Challenges Associated with the Determination of Biofuels Calorific Value by Bomb Calorimeter,” *Chem. Eng. Trans.*, vol. 92, pp. 433–438, 2022.
- [138] L. J. R. Nunes, J. C. D. O. Matias, and J. P. D. S. Catalao, *Torrefaction of Biomass for Energy Applications*. Elsevier Inc., 2017.
- [139] K. M. Czajka, “Proximate analysis of coal by micro-TG method,” *J. Anal. Appl. Pyrolysis*, vol. 133, no. February, pp. 82–90, 2018.
- [140] TA Instruments, “Thermal Analysis Application Brief - Proximate Analysis of Coal and Coke,” *Therm. Anal. Rheol.*, no. TA-129, pp. 1–2, 2022.
- [141] J. F. Saldarriaga, R. Aguado, A. Pablos, M. Amutio, M. Olazar, and J. Bilbao, “Fast characterization of biomass fuels by thermogravimetric analysis (TGA),” *Fuel*, vol. 140, pp. 744–751, 2015.
- [142] Y. El may, M. Jeguirim, S. Dorge, G. Trouvé, and R. Said, “Study on the thermal behavior of different date palm residues: Characterization and devolatilization kinetics under inert and oxidative atmospheres,” *Energy*, vol. 44, no. 1, pp. 702–709, 2012.
- [143] P. Jha and B. Dass, “Analysis of biomasses for their thermochemical transformations to biofuels,” *Int. J. Energy Prod. Manag.*, vol. 5, no. 2,

pp. 115–124, 2020.

- [144] J. Parikh, S. A. Channiwala, and G. K. Ghosal, “A correlation for calculating HHV from proximate analysis of solid fuels,” *Fuel*, vol. 84, no. 5, pp. 487–494, 2005.
- [145] S. Jarungthammachote and A. Dutta, “Thermodynamic equilibrium model and second law analysis of a downdraft waste gasifier,” *Energy*, vol. 32, no. 9, pp. 1660–1669, 2007.
- [146] S. A. Channiwala and P. P. Parikh, “A unified correlation for estimating HHV of solid, liquid and gaseous fuels,” *Fuel*, vol. 81, no. 8, pp. 1051–1063, 2002.
- [147] J. O. Titiloye, M. S. Abu Bakar, and T. E. Odetoeye, “Thermochemical characterisation of agricultural wastes from West Africa,” *Ind. Crops Prod.*, vol. 47, pp. 199–203, 2013.
- [148] J. Szyszlak-Barglowicz, G. Zajac, and W. Piekarski, “Energy biomass characteristics of chosen plants,” *Int. Agrophysics*, pp. 175–179, 2012.
- [149] P. McKendry, “Energy production from biomass (part 1): Overview of biomass,” *Bioresour. Technol.*, vol. 83, no. 1, pp. 37–46, 2002.
- [150] A. Kaupp, *Small Scale Gas Producer-Engine Systems*. Springer Science & Business Media, 2013.
- [151] Y. D. Singh, P. Mahanta, and U. Bora, “Comprehensive characterization of lignocellulosic biomass through proximate, ultimate and compositional analysis for bioenergy production,” *Renew. Energy*, vol. 103, pp. 490–500, 2017.

- [152] B. Miller, “Fuel considerations and burner design for ultra-supercritical power plants,” *Ultra-Supercritical Coal Power Plants*, pp. 57–80, 2013.
- [153] C. Turare, *Biomass Gasification - Technology and Utilisation*. Germany: Artes Institute, University of Flensburg, 2002.
- [154] D. J. Martínez-Ángel, A. R. Villamizar-Gallardo, and O. O. Ortiz-Rodríguez, “CHARACTERIZATION AND EVALUATION OF COCOA (*Theobroma cacao* L.) POD HUSK AS A RENEWABLE ENERGY SOURCE,” *Agrociencia*, vol. 49, no. 3, pp. 329–345, 2015.
- [155] R. García, C. Pizarro, A. G. Lavín, and J. L. Bueno, “Spanish biofuels heating value estimation. Part I: Ultimate analysis data,” *Fuel*, vol. 117, pp. 1130–1138, 2014.
- [156] M. J. F. Llorente and J. E. C. Garcia, “Suitability of thermo-chemical corrections for determining gross calorific value in biomass,” *Thermochim. Acta*, vol. 468, pp. 101–107, 2008.
- [157] C. Sheng and J. L. T. Azevedo, “Estimating the higher heating value of biomass fuels from basic analysis data,” *Biomass and Bioenergy*, vol. 28, no. 5, pp. 499–507, 2005.
- [158] M. Puig-Arnavat, J. C. Bruno, and A. Coronas, “Modified thermodynamic equilibrium model for biomass gasification: A study of the influence of operating conditions,” *Energy and Fuels*, vol. 26, no. 2, pp. 1385–1394, 2012.
- [159] A. Ravikiran, T. Renganathan, S. Pushpavanam, R. K. Voolapalli, and Y. S. Cho, “Generalized analysis of gasifier performance using

- equilibrium modeling,” *Ind. Eng. Chem. Res.*, vol. 51, no. 4, pp. 1601–1611, 2012.
- [160] S. Jarunghammachote and A. Dutta, “Equilibrium modeling of gasification: Gibbs free energy minimization approach and its application to spouted bed and spout-fluid bed gasifiers,” *Energy Convers. Manag.*, vol. 49, no. 6, pp. 1345–1356, 2008.
- [161] M. Vaezi, M. Passandideh-Fard, M. Moghiman, and M. Charmchi, “Modeling Biomass Gasification: A New Approach To Utilize Renewable Sources of Energy,” in *Proceedings of IMECE2008 2008 ASME International Mechanical Engineering Congress and Exposition*, 2008, pp. 1–9.
- [162] S. A. Salaudeen, P. Arku, and A. Dutta, “Gasification of Plastic Solid Waste and Competitive Technologies,” in *Plastics to Energy: Fuel, chemicals, and sustainability implications*, Oxford, United Kingdom, 2019, pp. 269–293.
- [163] E. S. Aydin, O. Yucel, and H. Sadikoglu, “Development of a semi-empirical equilibrium model for downdraft gasification systems,” *Energy*, vol. 130, pp. 86–98, 2017.
- [164] N. S. Barman, S. Ghosh, and S. De, “Gasification of biomass in a fixed bed downdraft gasifier - A realistic model including tar,” *Bioresour. Technol.*, vol. 107, pp. 505–511, 2012.
- [165] Z. A. Zainal, R. Ali, C. H. Lean, and K. N. Seetharamu, “Prediction of performance of a downdraft gasifier using equilibrium modeling for different biomass materials,” *Energy Convers. Manag.*, vol. 42, no. 12,

pp. 1499–1515, 2001.

- [166] M. Mehrpooya, M. Khalili, and M. M. M. Sharifzadeh, “Model development and energy and exergy analysis of the biomass gasification process (Based on the various biomass sources),” *Renew. Sustain. Energy Rev.*, vol. 91, no. 2, pp. 869–887, 2018.
- [167] A. Z. Mendiburu, J. A. Carvalho, and C. J. R. Coronado, “Thermochemical equilibrium modeling of biomass downdraft gasifier: Stoichiometric models,” *Energy*, vol. 66, pp. 189–201, 2014.
- [168] H. Ghassemi and R. Shahsavan-Markadeh, “Effects of various operational parameters on biomass gasification process; A modified equilibrium model,” *Energy Convers. Manag.*, vol. 79, pp. 18–24, 2014.
- [169] T. H. Jayah, L. Aye, R. J. Fuller, and D. F. Stewart, “Computer simulation of a downdraft wood gasifier for tea drying,” *Biomass and Bioenergy*, vol. 25, no. 4, pp. 459–469, 2003.
- [170] V. R. Patel, D. Patel, N. S. Varia, and R. N. Patel, “Co-gasification of lignite and waste wood in a pilot-scale (10 kWe) downdraft gasifier,” *Energy*, vol. 119, pp. 834–844, 2017.
- [171] P. N. Sheth and B. V. Babu, “Experimental studies on producer gas generation from wood waste in a downdraft biomass gasifier,” *Bioresour. Technol.*, vol. 100, pp. 3127–3133, 2009.
- [172] C. Gai and Y. Dong, “Experimental study on non-woody biomass gasification in a downdraft gasifier,” *Int. J. Hydrogen Energy*, vol. 37, pp. 4935–4944, 2012.

- [173] S. Sharma and P. N. Sheth, “Air-steam biomass gasification: Experiments, modeling and simulation,” *Energy Convers. Manag.*, vol. 110, pp. 307–318, 2016.
- [174] K. Rabea, A. I. Bakry, A. Khalil, M. K. El-Fakharany, and M. Kadous, “Real-time performance investigation of a downdraft gasifier fueled by cotton stalks in a batch-mode operation,” *Fuel*, vol. 300, p. 120976, 2021.
- [175] E. Azzone, M. Morini, and M. Pinelli, “Development of an equilibrium model for the simulation of thermochemical gasification and application to agricultural residues,” *Renew. Energy*, vol. 46, pp. 248–254, 2012.
- [176] D. S. Upadhyay, A. K. Sakhiya, K. Panchal, A. H. Patel, and R. N. Patel, “Effect of equivalence ratio on the performance of the downdraft gasifier – An experimental and modelling approach,” *Energy*, vol. 168, pp. 833–846, 2019.

## APPENDICES

### Appendix 1: Excerpts of the gas composition calculation from the model spreadsheet.

			T=1100 K					
	<b>CPH A1</b>							
ER	0.3		0.4		0.5		0.6	
CO	0.643874	23.74531354	0.556053	18.6517 8	0.46703	14.3700 7	0.37669 8	10.7078
CO2	0.342043	12.6141384	0.433509	14.5412 7	0.52566 1	16.1740 8	0.61858 7	17.5836
CH4	0.014083	0.519361337	0.010438	0.35011 4	0.00731	0.22490 7	0.00471 6	0.13404 4
H2	0.630177	23.24019455	0.542524	18.1979 8	0.45400 6	13.9693 3	0.36465 9	10.3655 9
N2	1.081407	39.88099441	1.43871	48.2588 6	1.79601 2	55.2616 2	2.15331 5	61.2089 6
Total	2.711584		2.981234		3.25001 8		3.51797 4	
		LHV <sub>syn</sub> (MJ/m <sup>3</sup> )						
LHV <sub>syn</sub> (KJ/mol)	306.155	13.6676349	263.3299		220.168 3		176.686 9	
CGE %	70.78429		60.88294		50.9038 1		40.8507 4	

	<b>CPH A2</b>							
ER	0.3		0.4		0.5		0.6	
CO	0.674068	25.61623	0.58158	20.06172	0.488	15.41461	0.393224	11.45723
CO2	0.314223	11.94122	0.409758	14.13467	0.505946	15.98147	0.602879	17.56588
CH4	0.011709	0.44498	0.008662	0.298793	0.006053	0.191213	0.003897	0.113539
H2	0.57462	21.83696	0.494223	17.0483	0.413161	13.05064	0.331489	9.65848
N2	1.056791	40.16063	1.404732	48.45651	1.752673	55.36221	2.100615	61.20486
Total	2.631411		2.898955		3.165835		3.432104	
LHVsyn (KJ/mol)	281.751		242.1402		202.2737		162.1741	
CGE %	66.73496		57.35284		47.91014		38.41223	

	<b>CPH A3</b>							
ER	0.3		0.4		0.5		0.6	
CO	0.665777	24.79185	0.574698	19.43869	0.482461	14.9522	0.388958	11.12519
CO2	0.321206	11.96091	0.415663	14.05946	0.510795	15.83031	0.606696	17.35306
CH4	0.013017	0.484703	0.009639	0.326015	0.006743	0.208979	0.004346	0.124293
H2	0.605849	22.56027	0.521341	17.63392	0.436061	13.51417	0.350055	10.01248
N2	1.079619	40.20227	1.435125	48.54191	1.790631	55.49433	2.146137	61.38499
Total	2.685468		2.956466		3.226692		3.496192	
LHVsyn (KJ/mol)	295.7419		254.2719		212.5029		170.4555	
CGE %	68.61161		58.99065		49.30031		39.54539	

	<b>CPH A4</b>							
ER	0.3		0.4		0.5		0.6	
CO	0.632272	23.29127	0.546117	18.31225	0.458753	14.11992	0.370076	10.52894
CO2	0.353391	13.018	0.443254	14.86308	0.533801	16.42982	0.625118	17.78509
CH4	0.014338	0.528158	0.010629	0.356423	0.007446	0.229183	0.004805	0.136718
H2	0.635849	23.42304	0.547484	18.35808	0.458228	14.10375	0.368114	10.47312
N2	1.078781	39.73952	1.434765	48.11017	1.790748	55.11731	2.146732	61.07613
Total	2.71463		2.982248		3.248976		3.514846	
LHVsyn (KJ/mol)	308.3754		265.2726		221.8234		178.0426	
CGE %	71.18518		61.23536		51.20557		41.09923	

	<b>CPH B1</b>							
ER	0.3		0.4		0.5		0.6	
CO	0.627932	22.80103	0.542549	17.93994	0.455911	13.84246	0.367913	10.32897
CO2	0.356793	12.95561	0.44612	14.75141	0.536145	16.27854	0.626957	17.6015
CH4	0.015276	0.554674	0.011332	0.374698	0.007943	0.241178	0.00513	0.14402
H2	0.656318	23.83178	0.565283	18.69168	0.473281	14.36984	0.38034	10.67785
N2	1.097644	39.85689	1.458967	48.24227	1.82029	55.26797	2.181613	61.24766
Total	2.753962		3.02425		3.293571		3.561953	
LHVsyn (KJ/mol)	317.5953		273.2766		228.5811		183.5216	
CGE %	71.6866		61.68312		51.5946		41.42391	

	<b>CPH B2</b>							
ER	0.3		0.4		0.5		0.6	
CO	0.692474	26.89137	0.597101	21.02061	0.500712	16.12344	0.403207	11.96475
CO2	0.29736	11.54762	0.395389	13.91946	0.494047	15.90884	0.593424	17.60925
CH4	0.010166	0.394775	0.00751	0.264381	0.005241	0.168761	0.003369	0.099958
H2	0.53541	20.79198	0.460186	16.20058	0.38443	12.37904	0.308203	9.145598
N2	1.039669	40.37425	1.380364	48.59497	1.72106	55.41991	2.061755	61.18044
Total	2.575079		2.84055		3.10549		3.369958	

	<b>CPH B3</b>							
ER	0.3		0.4		0.5		0.6	
CO	0.606751	22.86829	0.523921	18.01299	0.439966	13.90933	0.354797	10.38367
CO2	0.380227	14.33065	0.466431	16.03642	0.553278	17.49163	0.640846	18.75536
CH4	0.013022	0.490787	0.009648	0.331723	0.006755	0.21356	0.004357	0.127518
H2	0.605971	22.83887	0.521608	17.93347	0.436448	13.7981	0.350523	10.2586
N2	1.047272	39.4714	1.386964	47.68538	1.726655	54.58737	2.066347	60.47485
Total	2.653243		2.908572		3.163104		3.41687	

	<b>CPH B4</b>							
ER	0.3		0.4		0.5		0.6	
CO	0.644193	23.73126938	0.556342	18.64041	0.467284	14.36121	0.376913	10.7012
CO2	0.341644	12.58572708	0.43316	14.51317	0.525363	16.14616	0.618343	17.55581
CH4	0.014164	0.521766176	0.010498	0.351737	0.007352	0.225954	0.004743	0.134671
H2	0.631978	23.28128573	0.544088	18.22983	0.455325	13.99365	0.365728	10.38363
N2	1.082554	39.87996222	1.440513	48.26484	1.798472	55.27302	2.15643	61.22469
Total	2.714532		2.984601		3.253797		3.522158	
LHVsyn (KJ/mol)	306.9881		264.0518		220.7765		177.1789	
CGE %	70.48082		60.62315		50.68766		40.67816	

	<b>CPH C1</b>							
ER	0.3		0.4		0.5		0.6	
CO	0.649831	23.91532	0.561149	18.7814	0.47127	14.46716	0.380085	10.7782
CO2	0.336245	12.37462	0.428533	14.3428	0.521506	16.00931	0.615255	17.44697
CH4	0.013924	0.512447	0.010318	0.345355	0.007225	0.221786	0.00466	0.132145
H2	0.626618	23.06103	0.539417	18.05403	0.451364	13.85609	0.362501	10.27955
N2	1.090597	40.13659	1.448374	48.47642	1.80615	55.44565	2.163926	61.36314
Total	2.717215		2.98779		3.257514		3.526427	
LHVsyn (KJ/mol)	304.7192		262.0762		219.1028		175.8165	
CGE %	69.91286		60.12912		50.26956		40.33823	

	<b>CPH C2</b>							
ER	0.3		0.4		0.5		0.6	
CO	0.687288	26.24382	0.592865	20.5285	0.497366	15.75671	0.400687	11.70061
CO2	0.301433	11.5101	0.398796	13.80868	0.496809	15.73907	0.595566	17.39136
CH4	0.011278	0.430662	0.008339	0.288761	0.005825	0.184547	0.003748	0.109444
H2	0.56395	21.5342	0.484937	16.79139	0.405299	12.84001	0.325095	9.493223
N2	1.054908	40.28121	1.403071	48.58266	1.751234	55.47967	2.099397	61.30537
Total	2.618858		2.888008		3.156533		3.424492	
LHVsyn (KJ/mol)	277.3062		238.2742		199.0023		159.5149	
CGE %	65.54764		56.32154		47.03873		37.70499	

	<b>CPH C3</b>							
ER	0.3		0.4		0.5		0.6	
CO	0.683766	24.99451	0.590271	19.5862	0.49558	15.05891	0.399578	11.20074
CO2	0.302682	11.0643	0.399692	13.26248	0.497397	15.11412	0.595896	16.70384
CH4	0.013552	0.495382	0.010037	0.333039	0.007023	0.213399	0.004526	0.12688
H2	0.618185	22.59724	0.532004	17.65279	0.445013	13.52236	0.357265	10.01466
N2	1.117479	40.84855	1.481704	49.1655	1.84593	56.09122	2.210155	61.95389
Total	2.735664		3.013708		3.290943		3.56742	
LHVsyn (KJ/mol)	301.9531		259.6302		216.9936		174.0657	
CGE %	68.40405		58.81626		49.15743		39.43261	

	<b>CPH C4</b>							
ER	0.3		0.4		0.5		0.6	
CO	0.670394	24.2874	0.578953	19.05149	0.486271	14.66164	0.392231	10.91498
CO2	0.315054	11.41394	0.410261	13.50038	0.506176	15.26178	0.602896	16.77736
CH4	0.014552	0.527184	0.010785	0.354914	0.007553	0.227729	0.004872	0.135587
H2	0.640579	23.20721	0.551487	18.14767	0.461502	13.91482	0.370668	10.31492
N2	1.119677	40.56425	1.4874	48.94554	1.855122	55.93405	2.222845	61.85717
Total	2.760256		3.038887		3.316624		3.593512	
LHVsyn (KJ/mol)	311.759		268.1505		224.1948		179.9112	
CGE%	70.34335		60.5038		50.58592		40.59404	

	<b>CPH D1</b>							
ER	0.3		0.4		0.5		0.6	
CO	0.676001	24.77577	0.583637	19.41916	0.490069	14.93368	0.395181	11.10991
CO2	0.310204	11.36913	0.406144	13.51348	0.502779	15.32098	0.600208	16.87392
CH4	0.013795	0.50559	0.010219	0.340017	0.007152	0.217947	0.004611	0.129633
H2	0.6237	22.85893	0.536813	17.86119	0.449094	13.68507	0.360592	10.1375
N2	1.104776	40.49059	1.468658	48.86616	1.832541	55.84231	2.196423	61.74905
Total	2.728476		3.005471		3.281635		3.557015	
LHVsyn (KJ/mol)	304.2245		261.6098		218.6728		175.4344	
CGE%	69.29093		59.58491		49.80546		39.95736	

	<b>CPH D2</b>							
ER	0.3		0.4		0.5		0.6	
CO	0.7022	27.16812	0.605487	21.22093	0.507747	16.26702	0.408876	12.0651
CO2	0.287516	11.12401	0.386916	13.56052	0.486952	15.6008	0.587716	17.34229
CH4	0.010284	0.397899	0.007597	0.266272	0.005302	0.169858	0.003408	0.10055
H2	0.538522	20.83542	0.462859	16.22216	0.386659	12.38767	0.309984	9.146981
N2	1.046124	40.47456	1.390394	48.73014	1.734665	55.57464	2.078935	61.34508
Total	2.584645		2.853253		3.121324		3.388919	
LHVsyn (KJ/mol)	266.1877		228.6319		190.8707		152.9304	
CGE%	63.8606		54.85067		45.79144		36.68924	

	<b>CPH D3</b>							
ER	0.3		0.4		0.5		0.6	
CO	0.67662	25.14235	0.583977	19.70247	0.490184	15.14759	0.395131	11.26552
CO2	0.310611	11.54194	0.40657	13.71703	0.503205	15.54993	0.60061	17.12391
CH4	0.012769	0.474476	0.009453	0.318913	0.006611	0.204291	0.004259	0.121425
H2	0.600057	22.29739	0.516286	17.41868	0.431766	13.34236	0.346549	9.880417
N2	1.091097	40.54383	1.447694	48.84289	1.80429	55.75583	2.160886	61.60872
Total	2.691155		2.96398		3.236056		3.507436	
LHVsyn (KJ/mol)	293.4444		252.2662		210.7984		169.0633	
CGE%	68.16681		58.60115		48.96823		39.27321	

	<b>CPH D4</b>							
ER	0.3		0.4		0.5		0.6	
CO	0.652056	24.10449	0.563028	18.92219	0.472812	14.57035	0.381299	10.85158
CO2	0.334211	12.35475	0.426797	14.34374	0.520065	16.02652	0.614107	17.47716
CH4	0.013733	0.507675	0.010175	0.341975	0.007123	0.219519	0.004594	0.13074
H2	0.622304	23.00468	0.535664	18.00255	0.448189	13.81158	0.359921	10.24317
N2	1.082817	40.0284	1.439827	48.38955	1.796837	55.37203	2.153847	61.29736
Total	2.705121		2.975491		3.245026		3.513768	
LHVsyn (KJ/mol)	302.8194		260.4259		217.7084		174.685	
CGE%	70.09873		60.28519		50.39665		40.4373	

	<b>CPH E1</b>							
ER	0.3		0.4		0.5		0.6	
CO	0.694409	25.6144	0.599358	20.04284	0.503124	15.39087	0.405591	11.43525
CO2	0.292396	10.78548	0.390873	13.07101	0.490043	14.99071	0.590007	16.63467
CH4	0.013195	0.486711	0.009769	0.326679	0.006833	0.209022	0.004402	0.124113
H2	0.609983	22.50021	0.524857	17.55149	0.438953	13.42784	0.352327	9.933531
N2	1.101028	40.61319	1.465526	49.00797	1.830024	55.98154	2.194521	61.87242
Total	2.711012		2.990383		3.268977		3.546849	
LHVsyn (KJ/mol)	298.5476	13.32802	256.6641		214.4799	9.574996	172.0189	7.679413
CGE%	67.89684		58.37153		48.77784		39.12118	

<b>CPH E2</b>								
0.3		0.4		0.5		0.6		
0.688187	25.59817	0.593908	20.03785	0.498478	15.39128	0.401783	11.43772	
0.299137	11.12685	0.396709	13.38458	0.494962	15.28272	0.593991	16.90939	
0.012677	0.471539	0.009383	0.316567	0.006561	0.202577	0.004226	0.120293	
0.597894	22.23958	0.514379	17.35463	0.430127	13.28086	0.345193	9.826754	
1.090528	40.56387	1.449551	48.90637	1.808574	55.84256	2.167597	61.70584	
2.688421		2.96393		3.238701		3.51279		
292.827	13.07263	251.7155		210.3192		168.6615		
67.21455		57.77796		48.27598		38.714		

	<b>CPH E3</b>							
ER	0.3		0.4		0.5		0.6	
CO	0.677101	25.95298	0.584069	20.3184	0.489977	15.60631	0.394723	11.59566
CO2	0.311801	11.95117	0.407725	14.18379	0.504291	16.06223	0.601589	17.6727
CH4	0.011098	0.425374	0.008206	0.285455	0.005732	0.182562	0.003688	0.108333
H2	0.559417	21.44217	0.48103	16.73391	0.402031	12.80514	0.322474	9.473225
N2	1.049538	40.22831	1.393554	48.47846	1.73757	55.34351	2.081585	61.15008
Total	2.608955		2.874584		3.139601		3.40406	
LHVsyn (KJ/mol)	274.9118	12.27285	236.2144		197.2814		158.1363	
CGE%	65.43588		56.22493		46.95791		37.6404	

	<b>CPH E4</b>							
ER	0.3		0.4		0.5		0.6	
CO	0.670313	24.71422	0.578691	19.37676	0.485882	14.90448	0.391775	11.09008
CO2	0.316183	11.65756	0.411307	13.77212	0.507118	15.5559	0.603713	17.08944
CH4	0.013504	0.497874	0.010002	0.334904	0.006999	0.214706	0.004512	0.12772
H2	0.61708	22.75153	0.531079	17.78255	0.444269	13.62799	0.356696	10.09707
N2	1.095178	40.37882	1.455442	48.73368	1.815705	55.69693	2.175969	61.59569
Total	2.712258		2.986521		3.259974		3.532665	
LHV <sub>syn</sub> (KJ/mol)	301.0176	13.43828	258.8379		216.3444		173.5576	
CGE%	69.01572		59.345		49.60231		39.79237	

	<b>CPH F1</b>							
ER	0.3		0.4		0.5		0.6	
CO	0.657239	24.49134	0.56738	19.21449	0.476361	14.78732	0.384073	11.00748
CO2	0.329605	12.28238	0.422876	14.32081	0.516821	16.04331	0.611532	17.5264
CH4	0.013156	0.490262	0.009744	0.329979	0.006818	0.211653	0.004395	0.125957
H2	0.609096	22.69736	0.524182	17.75158	0.438482	13.61147	0.352039	10.08938
N2	1.074459	40.03864	1.428695	48.38314	1.78293	55.34622	2.137165	61.25079
Total	2.683556		2.952877		3.221412		3.489204	
LHV <sub>syn</sub> (KJ/mol)	296.9515		255.3322		213.4081		171.1986	
CGE%	68.93366		59.27225		49.54008		39.74167	

	<b>CPH F2</b>							
ER	0.3		0.4		0.5		0.6	
CO	0.687107	26.77426	0.5925	20.93163	0.496875	16.05699	0.400135	11.91667
CO2	0.302662	11.79371	0.399941	14.12898	0.497849	16.08845	0.596473	17.76394
CH4	0.010231	0.398678	0.007559	0.267044	0.005276	0.170493	0.003391	0.101003
H2	0.537132	20.93023	0.46169	16.31044	0.38571	12.46458	0.30925	9.20996
N2	1.029165	40.10313	1.368952	48.36189	1.708739	55.2195	2.048526	61.00842
Total	2.566297		2.830643		3.094449		3.357776	
LHVsyn (KJ/mol)	265.0706		227.684		190.0914		152.3178	
CGE%	63.87197		54.86321		45.80483		36.70281	

	<b>CPH F3</b>							
ER	0.3		0.4		0.5		0.6	
CO	0.670877	25.5191	0.578822	19.9918	0.48568	15.3647	0.391349	11.42251
CO2	0.317486	12.07667	0.41257	14.24966	0.508304	16.08041	0.604778	17.65196
CH4	0.011637	0.442662	0.008608	0.297325	0.006016	0.19032	0.003873	0.113033
H2	0.572851	21.79034	0.492696	17.01711	0.411882	13.03005	0.330461	9.64533
N2	1.056069	40.17121	1.4026	48.44411	1.749132	55.33453	2.095663	61.16717
Total	2.62892		2.895296		3.161013		3.426124	
LHVsyn (KJ/mol)	280.8412		241.3566		201.6181		161.648	
CGE%	66.50968		57.15882		47.74781		38.28198	

--	--	--	--	--	--	--	--	--

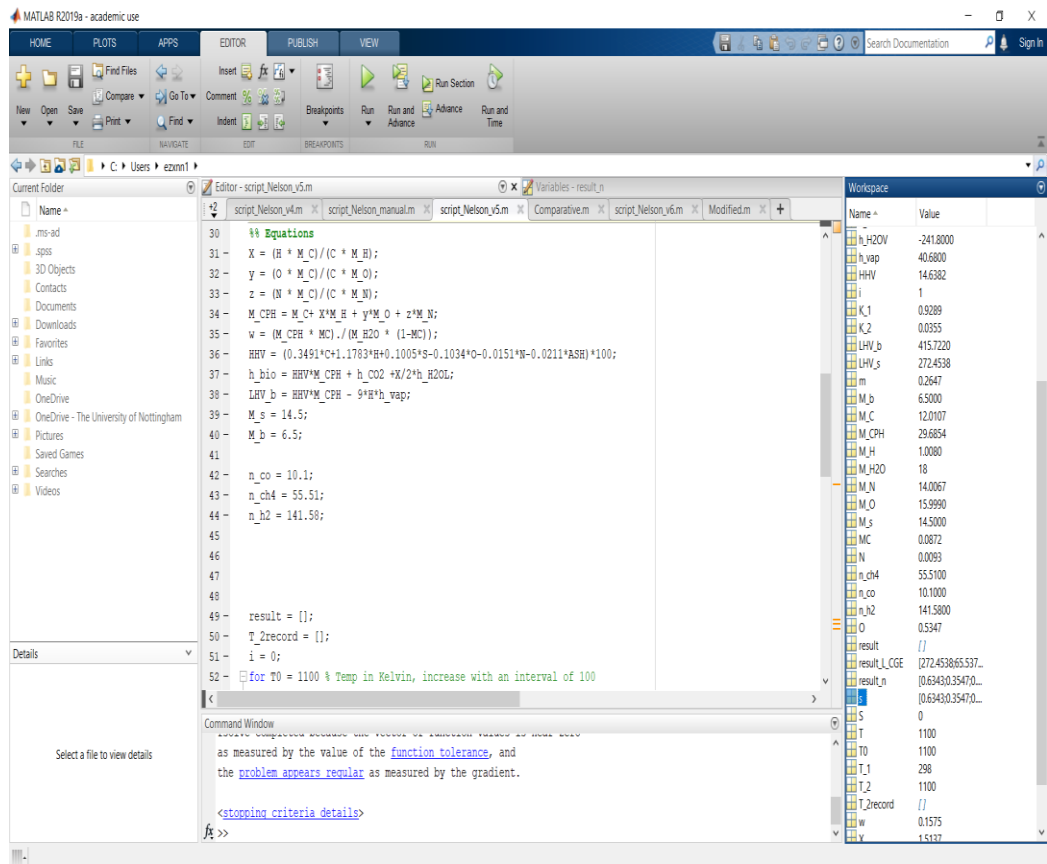
	<b>CPH F4</b>							
ER	0.3		0.4		0.5		0.6	
CO	0.670625	24.71272	0.57896	19.37582	0.486109	14.90393	0.391958	11.08977
CO2	0.315866	11.63974	0.411034	13.7559	0.506889	15.54106	0.603528	17.07578
CH4	0.013509	0.497821	0.010006	0.334873	0.007002	0.214689	0.004514	0.127711
H2	0.61721	22.74435	0.531191	17.77716	0.444362	13.624	0.356771	10.09421
N2	1.096474	40.40537	1.456863	48.75624	1.817251	55.71633	2.17764	61.61254
Total	2.713684		2.988054		3.261613		3.53441	
LHV <sub>syn</sub> (KJ/mol)	301.0867		258.8975		216.3942		173.5974	
CGE%	68.88428		59.23198		49.50784		39.71658	

## Appendix 2: Screenshots of samples of the model calculations in Matlab.

The screenshot displays the MATLAB R2019a software interface. The main window is the Editor, showing a script named 'script\_Nelson\_v5.m'. The code is organized into sections with comments:

```
1 %% constant parameters
2 % molecular weight
3 - M_C = 12.0107;
4 - M_H = 1.008;
5 - M_O = 15.999;
6 - M_N = 14.0067;
7 - M_H2O = 18;
8 % mass fractions
9 - C = 40.46*10^(-2);
10 - H = 5.14*10^(-2);
11 - O = 53.47*10^(-2);
12 - N = 0.93*10^(-2);
13 - MC = 8.72*10^(-2);
14 - S = 0.00*10^(-2);
15 - ASH = 0.00*10^(-2);
16 % heat of combustion in kJ/mol
17
18 % enthalpy of gaseous products
19 - h_CO = -110.5;
20 - h_CO2 = -393.5;
21 - h_H2OV = -241.8;
22 - h_H2OL = -285.8;
23 - h_CH4 = -74.8;
```

The Command Window at the bottom shows the prompt `>>`. The Workspace window on the right is empty. The status bar at the bottom indicates 'Ln 5 Col 14'.



<b>CPH A2</b>							
<b>0.3</b>		<b>0.4</b>		<b>0.5</b>		<b>0.6</b>	
0.674068	25.61623	0.58158	20.06172	0.488	15.41461	0.393224	11.45723
0.314223	11.94122	0.409758	14.13467	0.505946	15.98147	0.602879	17.56588
0.011709	0.44498	0.008662	0.298793	0.006053	0.191213	0.003897	0.113539
0.57462	21.83696	0.494223	17.0483	0.413161	13.05064	0.331489	9.65848
1.056791	40.16063	1.404732	48.45651	1.752673	55.36221	2.100615	61.20486
<b>2.631411</b>		<b>2.898955</b>		<b>3.165835</b>		<b>3.432104</b>	
281.751		242.1402		202.2737		162.1741	
66.73496		57.35284		47.91014		38.41223	